



**Modulation of oscillatory alpha activity
in the somatosensory system
by attention and hepatic encephalopathy**

Inaugural-Dissertation

zur Erlangung des Doktorgrades
der Mathematisch-Naturwissenschaftlichen Fakultät
der Heinrich-Heine-Universität Düsseldorf

vorgelegt von

Elisabeth Susanne May

aus Rheinbach

Düsseldorf, September 2012

Aus dem Institut für Klinische Neurowissenschaften
und Medizinische Psychologie
der Heinrich-Heine-Universität Düsseldorf

Gedruckt mit der Genehmigung der
Mathematisch-Naturwissenschaftlichen Fakultät der
Heinrich-Heine-Universität Düsseldorf

Referent: Prof. Dr. Alfons Schnitzler

Korreferent: Prof. Dr. Martin Heil

Tag der mündlichen Prüfung: 19.10.2012

Table of contents

Glossary	1
1 Abstract	2
2 Zusammenfassung	4
3 Introduction	6
3.1 Oscillatory alpha activity	7
3.1.1 The functional role of alpha activity: From idling to active inhibition	7
3.1.2 The alpha inhibition hypothesis	9
3.1.3 Alpha activity in the somatosensory system	11
3.1.4 Alpha activity associated with the processing of pain	13
3.1.5 Magnetoencephalography: Measuring oscillatory brain activity	15
3.1.6 Summary	16
3.2 Hepatic encephalopathy	17
3.2.1 Symptoms and clinical manifestations	17
3.2.2 Diagnosis and clinical grading	18
3.2.3 Pathophysiology	20
3.2.4 Somatosensory processing in HE	21
3.2.5 Summary	22
4 Aims and Hypotheses	23
5 Study 1: Pre- and post-stimulus alpha activity shows differential modulation with spatial attention during the processing of pain	24
5.1 Methods	24
5.2 Results	25
5.2.1 Pre-stimulus effects of spatial attention	25
5.2.2 Post-stimulus effects of spatial attention	26
5.2.3 Correlation between attention-modulated alpha activity and pain ratings	26
5.3 Discussion	26
5.4 Conclusions	28

Table of contents

6	Study 2: Hepatic encephalopathy slows and delays stimulus-associated somatosensory alpha activity	29
6.1	Methods	29
6.2	Results	30
6.2.1	Alpha peak frequencies	30
6.2.2	Time of maximal alpha rebound	30
6.3	Discussion	31
6.4	Conclusions	33
7	General conclusions	34
8	Outlook	36
9	References	39
10	Erklärung	52
11	Danksagung	53
12	Appendix	55

Glossary

BA	Brodmann area
CFF	critical flicker frequency
ECoG	electrocorticography
EEG	electroencephalography
fMRI	functional magnetic resonance tomography
HE	hepatic encephalopathy
HE0	patients with liver cirrhosis but no signs of HE
HE1	overt hepatic encephalopathy of grade 1
HE2	overt hepatic encephalopathy of grade 2
HE3	overt hepatic encephalopathy of grade 3
HE4	overt hepatic encephalopathy of grade 4
MEG	magnetoencephalography
mHE	minimal hepatic encephalopathy
S1	primary somatosensory cortex
S2	secondary somatosensory cortex
SEP	somatosensory evoked potential
SQUID	superconducting quantum interference device
tACS	transcranial alternating current stimulation
tDCS	transcranial direct current stimulation
TMS	transcranial magnetic stimulation
PET	positron emission tomography

1 Abstract

Oscillatory alpha activity at 8 to 12 Hz is the strongest electrophysiological signal measured from the surface of the awake human brain and was first described by Hans Berger in 1929. In spite of extensive research since then, the dynamics and the function of alpha activity are not yet fully understood. Using magnetoencephalography, this work investigated the modulation of alpha activity in the somatosensory system by attention and hepatic encephalopathy.

Recently, a sensory gating function of alpha activity was proposed by the so-called *alpha inhibition hypothesis*, which postulates that alpha activity routes information flow in the cortex by functionally inhibiting the processing of information in task-irrelevant regions. Evidence for this functional role stems from the visual, auditory and somatosensory modalities, but it has yet to be shown if it also applies to the processing of pain. In a first study, a spatial attention paradigm was employed, requiring healthy subjects to attend to painful stimuli on one hand while ignoring stimuli on the other. It could be shown that pain-associated alpha activity is differentially modulated by attention. In anticipation of a painful stimulus, pre-stimulus alpha activity displayed a lateralization across left and right primary somatosensory areas. In accordance with the alpha inhibition hypothesis, alpha activity was higher over primary somatosensory areas when the ipsilateral hand was attended compared to when the contralateral hand was attended. Indicating enhanced post-stimulus cortical activation, the stimulus-induced alpha suppression was intensified and prolonged if the stimulated hand was attended. Thus, pain-associated alpha activity was flexibly regulated according to current task demands, providing evidence that the functional role of alpha activity as a sensory gating mechanism includes pain processing.

Non-painful tactile stimuli induce a characteristic modulation of alpha activity in primary somatosensory areas in terms of an initial alpha suppression followed by a rebound to and above baseline levels. A slowing of oscillatory brain activity is thought to be a key mechanism in the development of hepatic encephalopathy (HE), a neuropsychiatric complication of liver diseases. This slowing was shown to be related to the so-called *critical flicker frequency* (CFF), a reliable indicator of HE disease severity. Previous studies furthermore indicated a delay of somatosensory processing in HE. However, oscillatory and

in particular alpha activity in this context has not yet been studied. In a second study, patients with liver cirrhosis and varying degrees of HE and healthy control subjects received electrical stimulation of sensory fibers of the right *median nerve*. The stimulus-induced rebound of alpha activity within the primary somatosensory cortex (S1) contralateral to the stimulated hand significantly differed between patients with manifest HE and controls. Increasing HE disease severity as quantified by the CFF was associated with a decreased peak frequency of S1 alpha activity and a delayed alpha rebound. The slowed frequency substantiates a global slowing of oscillatory brain activity as a key pathophysiological mechanism in HE. The delayed alpha rebound presumably indicates an impaired, slowed capability of the somatosensory system to adjust activation levels back to the default state.

In conclusion, this thesis extends the understanding of the functional role of oscillatory alpha activity in the healthy and pathologically impaired brain. By demonstrating its use as a sensory gating mechanism during the perception of pain, these findings might contribute to the development of new methods of pain relief and treatment. In addition, alterations of somatosensory alpha activity in association with HE as an example of pathologically impaired brain function were identified. These alterations broaden the understanding of the pathophysiological mechanisms of HE and might provide new parameters for an early diagnosis of the disease.

2 Zusammenfassung

Oszillatorische Alpha-Aktivität zwischen 8 und 12 Hz ist das stärkste im Wachzustand von der Oberfläche des menschlichen Gehirns messbare elektrophysiologische Signal und wurde erstmals 1929 von Hans Berger beschrieben. Trotz einer Vielzahl an seitdem durchgeführten Studien ist das Wissen bezüglich der Dynamik und Funktion von Alpha-Aktivität immer noch unvollständig. Im Rahmen der vorliegenden Arbeit wurde daher mit Hilfe der Magnetenzephalographie die Modulation von Alpha-Aktivität im somatosensorischen System durch Aufmerksamkeit und hepatische Enzephalopathie untersucht.

Die so genannte *Alpha-Inhibitions-Hypothese* postuliert für Alpha-Aktivität die Funktion eines sensorischen Filter-Mechanismus, mit dessen Hilfe der Informationsfluss im Kortex durch die Hemmung von Informationsverarbeitung in Aufgaben-irrelevanten Hirnarealen gesteuert wird. Diese Hypothese wird bereits durch Befunde aus dem visuellen, auditorischen und somatosensorischen System gestützt, aber bislang ist unklar, ob sie gleichermaßen auch für die Verarbeitung von Schmerz zutrifft. In einer ersten Studie wurden daher gesunde Probanden mit Hilfe eines räumlichen Aufmerksamkeitsparadigmas untersucht, in dem schmerzhaft Laserreize auf einer Hand beachtet und auf der anderen Hand ignoriert werden mussten. Es konnte eine differenzielle Modulation schmerz-assoziiierter Alpha-Aktivität durch Aufmerksamkeit gezeigt werden. Bereits während der Antizipation eines schmerzhaften Reizes zeigte sich eine Lateralisierung der Alpha-Aktivität über linke und rechte primäre somatosensorische Areale hinweg. In Einklang mit der Alpha-Inhibitions-Hypothese war die Alpha-Aktivität über primären somatosensorischen Arealen gemessen stärker bei Aufmerksamkeit auf der ipsilateralen im Vergleich zur Ausrichtung der Aufmerksamkeit auf die kontralaterale Hand. Im Sinne einer stärkeren kortikalen Aktivierung nach einem beachteten Reiz, wurde darüber hinaus die stimulus-induzierte Suppression von Alpha-Aktivität durch Aufmerksamkeit verstärkt. Diese Befunde zeigen, dass somatosensorische Alpha-Aktivität auch im Rahmen der Verarbeitung schmerzhafter Reize flexibel entsprechend der aktuellen Aufgabenstellung reguliert wird. Dies belegt eine Funktion als sensorischer Filter-Mechanismus auch für Schmerz.

Es ist gut bekannt, dass nicht-schmerzhaft, taktile Reize eine charakteristische Modulation von Alpha-Aktivität in primären somatosensorischen Arealen hervorrufen. Alpha-

Aktivität wird zunächst unterdrückt, erreicht anschließend wieder Basisniveau und steigt sogar darüber hinaus, was auch als *Rebound* bezeichnet wird. Eine Verlangsamung oszillatorischer Hirnaktivität wird als Schlüsselmechanismus in der Pathophysiologie der hepatischen Enzephalopathie (HE) angenommen, einer neuropsychiatrischen Komplikation von Lebererkrankungen. In diesem Kontext wurde ein Zusammenhang zwischen dieser Verlangsamung und der so genannten kritischen Flimmerfrequenz (*critical flicker frequency*, CFF) gezeigt, die ein reliabler Indikator des HE-Schweregrads ist. Die Ergebnisse vorheriger Studien deuten darüber hinaus auf eine verzögerte somatosensorische Verarbeitung bei HE-Patienten hin. Oszillatorische Hirnaktivität wurde in diesem Zusammenhang allerdings noch nicht untersucht. Zu diesem Zweck wurden in einer zweiten Studie die sensorischen Fasern des *Nervus medianus* der rechten Hand bei Patienten mit verschiedenen Schweregraden der HE und gesunden Kontrollprobanden elektrisch stimuliert. Dabei zeigte sich bei Patienten mit manifester HE im Vergleich zu gesunden Kontrollprobanden eine signifikante Veränderung des stimulus-induzierten Alpha-Rebounds im primären somatosensorischen Kortex (S1) kontralateral zur stimulierten Hand. Eine steigende HE-Schwere, quantifiziert durch die CFF, war mit einer verlangsamten Peak-Frequenz der S1-Alpha-Aktivität und einem verzögerten Alpha-Rebound verbunden. Die gefundene Frequenzverlangsamung untermauert die Hypothese einer globalen Verlangsamung oszillatorischer Hirnaktivität als einen grundlegenden pathophysiologischen Mechanismus der HE. Der verzögerte Alpha-Rebound deutet darüber hinaus auf eine eingeschränkte bzw. verlangsamte Fähigkeit des somatosensorischen Systems hin, die kortikale Aktivierung nach einem Reiz zurück auf das Basisniveau zu regulieren.

Insgesamt erweitert die vorliegende Arbeit das Verständnis der funktionalen Rolle oszillatorischer Alpha-Aktivität im gesunden und pathologisch veränderten Gehirn. Die Demonstration einer sensorischen Filter-Funktion auch im Rahmen der Verarbeitung von Schmerz könnte zu der Entwicklung neuer Methoden der Schmerzlinderung und Schmerzbehandlung beitragen. Darüber hinaus wurden pathologische Veränderungen somatosensorischer Alpha-Aktivität im Rahmen der HE als ein Beispiel pathologisch veränderter Hirnfunktion identifiziert. Diese Veränderungen tragen nicht nur zum Verständnis der pathophysiologischen Mechanismen dieser Erkrankung bei, sondern stellen möglicherweise neue Kennwerte für eine frühe Diagnose der HE dar.

3 Introduction

Our brain's activity is based upon the interaction of billions of neurons, which, if simultaneously active in large groups, generate signals that are measurable even from outside the skull. Rhythmic neuronal activity between 8 and 12 Hz, the so-called alpha activity, is the strongest electrophysiological signal measured from the surface of the awake human brain. The prominent posterior alpha rhythm was first described by Hans Berger (1873-1941) in 1929 and has the strongest amplitude in relaxed but awake subjects with eyes closed. Figure 1 illustrates one of the earliest measurements recorded from the back of the head of Berger's son Klaus. Berger was also the first to note a relation to attentional processes and reported a variation of the strength of alpha activity with the level of the subject's attention paid to the environment (Berger, 1929). Although almost a century of research has passed since these first recordings, the functional role of alpha activity in the brain is not yet fully understood.

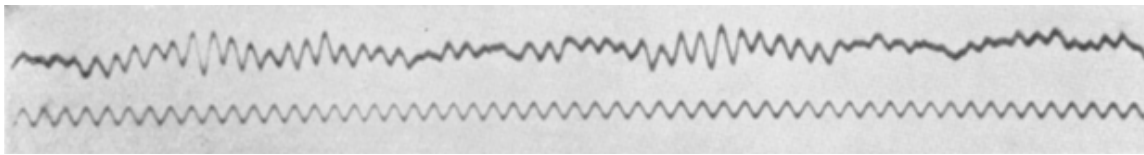


Figure 1: 5.5 s-recording of the alpha rhythm from Berger's son Klaus at the age of 15. The upper line represents the scalp recording from an electrode placed on the back of the head referenced to the forehead, the lower line the time in 1/10 seconds (from Berger, 1929).

This thesis examined the dynamics of alpha activity in the somatosensory cortex by investigating its modulation by attention and pathological impairment due to hepatic encephalopathy (HE). It aimed at extending the knowledge about the role of oscillatory somatosensory alpha activity in the healthy brain. Furthermore, it sought to identify potential alterations of somatosensory alpha activity in association with pathologically changed brain function.

A first study examined healthy subjects and investigated how somatosensory alpha activity associated with the perception of pain is modulated by spatial attention. Spatial attention paradigms are specifically useful for investigating a potential role of alpha activity as a sensory gating mechanism, which routes information flow in the cortex. In a second study, the processing of non-painful, electrical stimuli to the median nerve was scrutinized in hepatic encephalopathy (HE), a neuropsychiatric complication of liver disease.

HE is of particular interest in this context since it has been independently associated with a pathological slowing of oscillatory brain activity and delayed somatosensory processing. In both studies, brain activity was measured using magnetoencephalography (MEG) and analyzed with respect to modulations of the power and/or frequency of alpha activity in the somatosensory system.

This introduction will first give an overview of the current understanding of the functional role of alpha activity in the human brain and present the so-called alpha inhibition hypothesis. Then, evidence regarding the role of alpha activity specifically in the somatosensory system and in the context of the processing of pain will be summarized, before introducing MEG as the method used to measure brain activity in this thesis. Subsequently, the clinical picture and the pathophysiological mechanisms of HE will be described, since the second study examined patients with this disease. Following chapters will outline the aims and hypotheses of this thesis and describe the methods and results from both studies. In the last two chapters, general conclusions and important areas of future research, which can be deduced from this thesis, will be depicted.

3.1 Oscillatory alpha activity

Oscillatory brain activity is caused by rhythmic, synchronous activity of a large population of neurons (Box 1). Oscillatory alpha activity describes the frequency band between 8 and 12 Hz and thus has an approximate cycle duration of 100 ms. It can be found across the brain's different sub-systems and sensory modalities, i.e. in the visual, auditory and somatosensory system.

3.1.1 The functional role of alpha activity: From idling to active inhibition

Oscillatory alpha activity occurs spontaneously and continuously across the primary cortical areas of our different sensory modalities. In response to sensory stimuli, movements and even the imagination of movements, ongoing alpha activity is suppressed in the respective cortices, indicating that low levels of alpha activity represent a correlate of an activated or engaged cortical region (Neuper and Pfurtscheller, 2001; Pfurtscheller et al., 1996). With respect to spontaneous fluctuations of alpha activity, low levels of alpha activity were shown to precede good perceptual detection and discrimination ability (van Dijk et al., 2008; Ergenoglu et al., 2004; Hanslmayr et al., 2007). Furthermore, the excit-

ability of a cortical area is increased when the current level of alpha activity is low (Ergenoglu et al., 2004; Ploner et al., 2006a; Romei et al., 2008; Sauseng et al., 2009), providing additional evidence that low levels of alpha activity reflect cortical activation.

Box 1: Oscillatory brain activity

Neuronal oscillations are periodic variations in the amplitude of recorded neural activity. Such oscillatory brain activity is related to the firing and postsynaptic potentials of neuronal cells and arises from rhythmic variations in firing probabilities over time. Measured extracellularly by the local field potential and even outside of the skull using electro- and magnetoencephalography, oscillatory brain activity represents synchronized activity across a large population of neurons (for reviews see Buzsáki, 2006; Schnitzler and Gross, 2005).

Decomposing neuronal oscillatory signals into their frequency components, several functionally relevant frequency bands have been distinguished and associated with specific functional roles. Oscillatory activity in the alpha frequency band (8-12 Hz), the most prominent oscillatory brain activity and the focus of this thesis, is believed to be inversely related to the degree of activation or engagement of a cortical region (Pfurtscheller et al., 1996) and even to be used actively to inhibit brain areas (Fox and Snyder, 2011; Jensen and Mazaheri, 2010). In contrast, gamma band brain activity (30-100 Hz), for example, is strongly associated with active processing and stimulus selection and enhanced by attention (e.g. Fries, 2009; Kahlbrock et al., 2012b, Appendix 3+4).

High levels of alpha activity, in contrast, have been considered to be a correlate of an inactive or disengaged cortical area and were thought to merely reflect “cortical idling” (Pfurtscheller et al., 1996) for a long time. This interpretation was based on observations of increased alpha levels in brain areas not currently involved in a task. For example, the somatosensory alpha rhythm was shown to be stronger during tasks requiring visual processing (Koshino and Niedermeyer, 1975; Pfurtscheller and Klimesch, 1992) and increased in the cortical hand area when the foot was moved (Pfurtscheller et al., 1997). More recently, such results have been interpreted differently and alpha activity is discussed to have a more active role. In this view, alpha activity is employed by top-down, i.e. intentionally driven, processes like attention to actively inhibit areas currently not involved in a specific task (Foxe and Snyder, 2011; Jensen and Mazaheri, 2010).

3.1.2 The alpha inhibition hypothesis

According to the *alpha inhibition* or *gating by inhibition hypothesis*, oscillatory alpha activity represents a sensory gating mechanism used to actively route information flow in the cortex by functionally blocking off task-irrelevant pathways (Figure 2; Jensen and Mazaheri, 2010; Klimesch et al., 2007). In this view, alpha activity is actively increased in task-irrelevant brain regions to prevent interference from potentially distracting information. Consequently, low levels of alpha activity serve to facilitate processing in task-relevant regions, ultimately enabling us to preferentially process and retain information currently relevant for us.

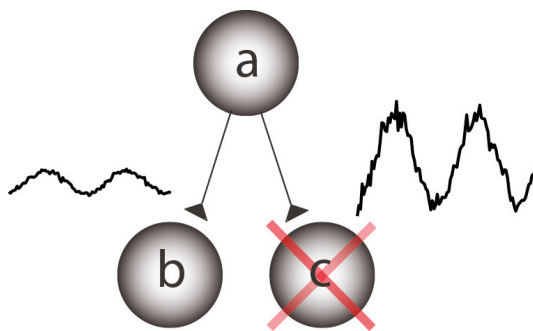


Figure 2: The principle of gating by inhibition. 3 nodes in a network are represented by a to c. Information flow from node b to a is gated through the active suppression of c by functional inhibition. The functional inhibition is reflected by increased alpha activity (from Jensen and Mazaheri, 2010).

Attention (Box 2) paradigms require the subject to attend to certain stimuli or features of stimuli while at the same time ignoring others. Thus, they provide a well-suited framework which has been repeatedly used for studying this presumed function of alpha activity as a sensory gating mechanism. In line with the alpha inhibition hypothesis, attention studies revealed specific modulations of alpha activity both across and within sensory modalities. It was shown that alpha activity is lower in cortical areas representing the current focus of attention compared to cortical areas representing stimuli or features of stimuli outside of the current attentional focus and thereby a potential source of distracting information (Foxe and Snyder, 2011). In visual spatial attention tasks, for example, anticipatory pre-stimulus alpha activity shows a lateralized pattern with decreased levels contralateral and/or increased levels ipsilateral to the attended visual hemifield (Händel et al., 2011; Kelly et al., 2006; Sauseng et al., 2005; Thut et al., 2006; Worden et al., 2000). The degree of this lateralization correlates with the behavioral performance (Händel et al., 2011; Thut et al., 2006). Similar anticipatory alpha modulation patterns were also found in the auditory system (Müller and Weisz, 2012; Thorpe et al., 2012).

Box 2: Attention

Attention is the cognitive process, which allows us to selectively concentrate on some aspects of our environment while ignoring others, and is closely related to the allocation of processing resources (Müller and Krummenacher, 2006). When a stimulus is selectively attended, it is preferentially processed at the expense of the processing other simultaneously incoming information and associated with enhanced stimulus induced neuronal responses. The degree of selective attention to a visual stimulus was, for example, shown to be closely related to the level of oscillatory gamma activity in primary visual areas (Kahlbrock et al., 2012b, Appendix 3+4).

Spatial attention involves the focusing of attention to a certain location in space. Spatial attention orienting can be performed covertly, i.e. without actually shifting the gaze (Posner, 1980) and is not restricted to the visual system. In a spatial attention study of the somatosensory system involving painful laser stimuli to the left and right hand, for example, the orienting of spatial attention to stimuli on one hand was shown to enhance stimulus-induced neuronal responses (Legrain et al., 2002). With respect to the behavioral consequences of such shifts in spatial attention, behavioral performance in a somatosensory discrimination task was, for instance, found to be worse and slower if the target stimulus occurred on the unattended instead of the attended hand (Haegens, 2011).

Recent studies further support an active role of alpha activity in suppressing distracting input by relating increases in alpha activity in task-irrelevant brain areas to behavioral performance (Haegens et al., 2010; Linkenkaer-Hansen et al., 2004; Meeuwissen et al., 2011). In a working memory task, for example, successful remembering of a somatosensory stimulus pattern on the right hand was associated with high alpha activity over posterior and right, i.e. ipsilateral, brain areas during the retention period (Haegens et al., 2010), presumably indicating a successful inhibition of interfering brain activity. Moreover, rhythmic transcranial magnetic stimulation (TMS) pulses at alpha frequency over the parietal and visual cortices selectively impair visual detection in the visual field opposite to the stimulated hemisphere by artificially inducing local alpha oscillations (Romei et al., 2010; Thut et al., 2011), providing evidence for a causal rather than correlative relation between alpha activity and behavior. Thus, behavioral performance seems to be impaired when functional inhibition of task-irrelevant areas fails or is induced in task-relevant brain areas.

Taken together, there is strong evidence that oscillatory alpha activity reflects a sensory gating mechanism. The current level of alpha activity seems to be differentially modulated across task-relevant and -irrelevant brain areas by top-down cognitive processes like memory and attention, affecting the subsequent behavioral performance.

3.1.3 Alpha activity in the somatosensory system

Most evidence regarding the functional significance of alpha activity described so far stems from studies of the visual system. However, it is hypothesized that oscillatory alpha activity serves a similar functional role across different modalities and cortical subsystems (Foxye and Snyder, 2011; Jensen and Mazaheri, 2010).

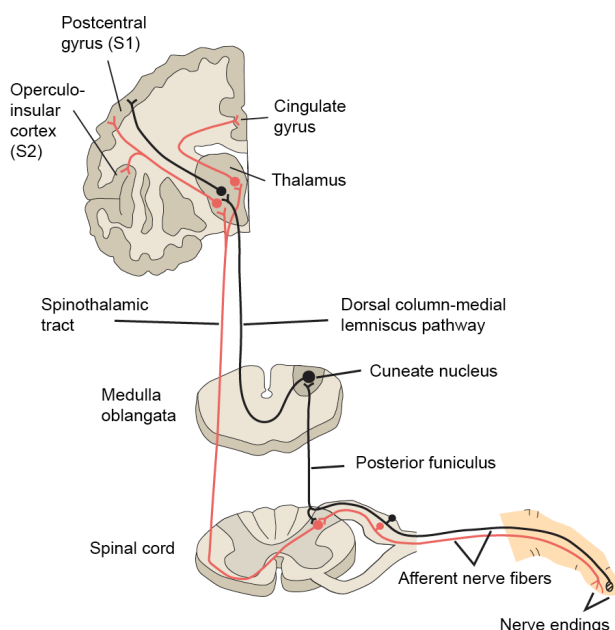
The somatosensory system mediates the perception of mechanic, thermal, and nociceptive, i.e. very intensive and potentially noxious and painful, stimuli (Box 3). Being less prominent than the posterior alpha rhythm, a corresponding alpha rhythm over rolandic, sensorimotor areas (also known as part of the mu rhythm) was first described by Gastaut in 1952. In spite of its reactivity to movements (Chatrian et al., 1959; Gastaut, 1952), rolandic alpha activity is assumed to mainly originate from somatosensory areas in the postcentral gyrus (Schnitzler et al., 2000) and will therefore be termed somatosensory alpha activity from now on.

The processing of tactile stimuli generally induces a characteristic modulation of alpha activity in early somatosensory cortices in terms of an initial suppression, interpreted as cortical activation, followed by a rebound to and above baseline levels (Bauer et al., 2006; Della Penna et al., 2004; Nikouline et al., 2000; Salenius et al., 1997). This rebound is reduced by concurrent motor tasks or tactile stimulation, which is again seen as evidence for a strong cortical activation indicated by a continuing level of low alpha activity (Salenius et al., 1997). Thus, from the time-course of alpha activity in response to simple somatosensory stimuli, inferences about the course of the associated cortical activation can be drawn.

Results regarding spontaneous fluctuations of somatosensory alpha activity and their consequences for behavior are inconsistent. Two studies found highest detection rates of near-threshold stimuli to be associated with medium levels of pre-stimulus somatosensory alpha power (Linkenkaer-Hansen et al., 2004; Zhang and Ding, 2010). Thus, these studies found a U-shaped relation between the current level of alpha activity level

Box 3: The somatosensory system

The somatosensory system is a diverse sensory system which, among other sensations, mediates the perception of mechanical, thermal, and nociceptive (i.e. potentially noxious and painful) stimuli of the skin. A range of specialized peripheral receptors transmits somatosensory sensations along differently wired neuronal pathways through the spinal cord to the thalamus contralateral to the stimulated body side. From there, information is passed on to the primary somatosensory cortex (S1) within the postcentral gyrus (Brodmann Area (BA) 1 to 3), which represents the complete contralateral body half in a somatotopic order. Here, body parts are represented proportionally to their receptor density. Thus, very sensitive areas like the fingers or the mouth cover relatively large parts of S1. S1 is responsible for the processing of basic properties of the somatosensory percept such as the localization of a stimulus and the identification of its strength and type. The secondary somatosensory cortex (S2) is situated within the parietal operculum (BA 43), receives bilateral input and is involved with the interpretation of stimuli processed in S1, including the identification of more complex stimuli like orientation and movement. Higher order areas like the insular cortex (BA 13) and the anterior cingulate gyrus (BA 24) are mainly associated with emotional and affective components of the somatosensory perception. Please note that this description is restricted to those aspects of the somatosensory system most relevant for this thesis. For detailed and comprehensive descriptions of the somatosensory system, see Meßlinger (2010) and Treede (2007). For a review of the neurophysiology and neuroanatomy of pain perception, see Schnitzler and Ploner (2000).



The pathways of the somatosensory system, exemplarily shown for the skin. Red: Spinothalamic system (thermal, visceral, and nociceptive perception). Black: Lemniscal system (mechanoreception and proprioception). Adapted from Treede, 2007.

and the associated behavioral outcome instead of a linear association as postulated by the alpha inhibition hypothesis. In contrast, another study demonstrated that a stimulus was resistant against subsequent masking if pre-stimulus somatosensory alpha activity was low (Schubert et al., 2009). Thus, this study did indicate better perceptual performance with low levels of alpha activity.

Attention studies of the somatosensory system have revealed clear evidence in favor of the alpha inhibition hypothesis. Jones and colleagues studied anticipatory pre-stimulus alpha activity within the hand area of the primary somatosensory cortex (S1) and found decreased alpha power after spatial attention was cued to the hand and increased power after attention was cued to the foot (Jones et al., 2010). Studies requiring subjects to spatially direct their attention to the left or right hand showed decreased anticipatory alpha activity in the primary somatosensory cortex contralateral to the attended hand, but increased alpha activity ipsilaterally (Anderson and Ding, 2011; Haegens et al., 2012, 2011). In line with a top-down control, this lateralization, quantified across hemispheres using a lateralization index, was employed in a graded manner according to current task demands (Haegens et al., 2011). In addition, it affected behavior. A strong overall lateralization, its single components (a contralateral alpha decrease and an ipsilateral alpha increase) and a posterior alpha increase were individually shown to contribute to a good behavioral discrimination performance of stimuli on the attended hand (Haegens et al., 2012, 2011).

All in all, evidence from research studying the somatosensory system suggests that oscillatory alpha activity serves a similar role for the processing of non-painful, tactile stimuli as for visual and auditory stimuli. In accordance with the alpha inhibition hypothesis, alpha activity seems to be employed as a sensory gating mechanism in the somatosensory system, which shapes perception and behavioral responses.

3.1.4 Alpha activity associated with the processing of pain

Somatosensory alpha activity in the context of the processing of pain is less well studied. In contrast to stimuli of other modalities, the suppression of spontaneous alpha activity in the brain by painful stimuli is not circumscribed to the respective sensory areas and regionally specific, but spreads globally across somatosensory, motor and visual areas (Ploner et al., 2006b). This finding has been interpreted as a special alerting function of pain, which is substantiated by an increased excitability of somatosensory cortices by

subsequent stimuli (Ploner et al., 2004). Thus, the processing of pain seems to be particularly intense and associated with a pronounced cortical activation. In addition, both the degree of excitability after a painful stimulus (Ploner et al., 2006a) and the response to a painful stimulus itself (Babiloni et al., 2008) are larger if the current level of somatosensory alpha activity is low. Again, this is in accordance with a facilitated processing by low levels of alpha activity.

The active gating function postulated by the alpha inhibition hypothesis was not yet directly tested for the processing of painful stimuli and studies investigating the modulation of pain-associated alpha activity by attention are scarce. In a study using subdural electrocorticographic recordings (ECoG) from epilepsy patients, Ohara et al. (2004) showed an intensified stimulus-induced suppression of somatosensory alpha activity compared to a pre-stimulus baseline if a painful laser stimulus was attended compared to when the subject was distracted by reading a magazine. Using MEG recordings from healthy subjects, Hauck et al. (2007), in contrast, did not observe a modulation of alpha activity associated with painful electrical stimulation by spatial attention to the middle or index finger. In both studies, pre-stimulus effects of attention were not examined.

Regarding pre-stimulus effects on pain-associated alpha activity, Babiloni and colleagues demonstrated in a series of studies that somatosensory alpha activity is already suppressed when a painful stimulus is expected and anticipated but not yet actually received (Babiloni et al., 2006, 2004, 2003; Del Percio et al., 2006). This anticipatory pre-stimulus alpha suppression is again stronger for a painful than for a non-painful stimulus (Babiloni et al., 2004, 2003). In addition, it is cancelled if the painful stimulus is immediately followed by a cognitive task and even replaced by an alpha increase if the painful stimulation is followed by a movement (Del Percio et al., 2006). These latter findings were interpreted as a transition from reduced cortical activation to cortical idling (Del Percio et al., 2006), but might also be indicative of sensory gating of the information flow by active modulations of alpha activity.

With respect to behavior, the current state of alpha activity appears to be related to the intensity of the subjective pain perception. A stronger pre-stimulus alpha suppression in anticipation of a painful stimulus was demonstrated to be associated with a higher perceived pain intensity across subjects (Babiloni et al., 2006). Within subjects, the stimulus-induced alpha suppression was also shown to inversely correlate with the level of the

perceived pain intensity across different trials (Schulz et al., 2011). Thus, a painful stimulus seems to be perceived more intensely, if alpha activity close to the time of stimulus onset is low.

In summary, the processing of pain is associated with pronounced modulations of the level of somatosensory alpha activity. These can already appear during anticipatory pre-stimulus periods, are influenced by attention and show an association with the subjectively perceived pain intensity. However, it is not yet clear if the sensory gating function of alpha activity proposed by the alpha inhibition hypothesis includes pain processing.

3.1.5 Magnetoencephalography: Measuring oscillatory brain activity

Oscillatory brain activity can be non-invasively measured using magnetoencephalography (MEG) (for a review see Hämäläinen et al., 1993, and Hari, 2005). From outside the skull, MEG records biomagnetic brain activity generated by electrical currents, provided that thousands of nearby neurons are simultaneously active. MEG is assumed to be most sensitive to postsynaptic potentials from pyramidal cells, which are oriented perpendicular to the surface of the cortex and lie within cortical fissures.

The strength of the brain's magnetic field is around 10^{-15} Tesla, which is several orders of magnitude smaller than surrounding magnetic fields. The earth's magnetic field, for example, has a strength of 10^{-5} Tesla, magnetic fields produced by electrical devices about 10^{-7} Tesla. To be able to measure the tiny magnetic field produced by the brain, recordings are performed within a magnetically shielded room using superconducting quantum interference devices (SQUIDS). These sensors need to be kept at a temperature of about -269 °C, which is achieved by an insulated dewar filled with liquid helium.

In contrast to methods like functional magnetic resonance imaging (fMRI) and positron emission tomography (PET), MEG measures neuronal activity instantaneously and with a high temporal resolution down to submillisecond time scales. Unlike the electrical currents measured by electroencephalography (EEG), the magnetic field measured with MEG is not distorted by the skull and surrounding tissue. This, in combination with a high number of sensors covering the entire skull, allows for a good spatial resolution of 2-3 mm on the cortical surface and good source reconstruction of the measured signals within the brain. Thus, MEG is able to measure biomagnetic activity from the brain with a very high temporal and a good spatial resolution.



Figure 3: 306-channel whole head MEG system (Elekta Oy, Helsinki, Finland) within a magnetically shielded room. Sensors measuring the brain's magnetic field are built into the helmet-shaped dewar, under which the subject can be comfortably seated.

For the two studies presented in this thesis, a 306-channel whole head MEG system (Elekta Oy, Helsinki, Finland) was used, comprising 102 sensor triplets consisting of one magnetometer and two orthogonal planar gradiometers each (Ahonen et al., 1993). Analyses were performed on signals recorded from gradiometers, which are most sensitive for directly underlying sources. Please see figure 3 for a depiction of the MEG system, which was used for this thesis and is situated at the University Hospital Düsseldorf.

3.1.6 Summary

External stimuli induce strong modulations of oscillatory alpha activity across different sensory modalities and types of stimuli. Evidence from cognitive studies suggests a functional role of alpha activity as a top-down controlled gating mechanism, which streamlines information flow in the cortex and shapes perception and behavioral responses. In line with the alpha inhibition hypothesis, evidence from the visual, auditory and somatosensory systems suggests that low levels of alpha activity are associated with cortical activation, while high levels of alpha activity reflect cortical disengagement and even active functional inhibition. Painful stimuli are associated with particularly strong modulations of somatosensory alpha activity, which are most likely related to the aversive nature and the alerting function of pain. However, the alpha inhibition hypothesis has not yet been directly tested for the processing of pain. Thus, it has yet to be shown, if the modulation of alpha activity by top-down processes like attention during the processing of pain is comparable to that during the processing of less salient stimuli. Generally, oscillatory brain activity can be measured with both high temporal and spatial resolution using MEG.

3.2 Hepatic encephalopathy

Hepatic encephalopathy (HE) is a potentially reversible, neuropsychiatric complication of acute and chronic liver disease associated with a variety of symptoms, including vigilance, cognitive and motor deficits (Häussinger and Blei, 2007). These symptoms vary strongly and gradually in severity from very mild forms not causing overt clinical symptoms (minimal HE) up to hepatic coma and death (Ferenci et al., 2002; Häussinger and Blei, 2007).

Estimates of the prevalence of HE are uncertain because of inconsistencies in the coding of the disease and difficulties in finding a reliable graduation scheme, particularly for low grades of HE (Bajaj et al., 2009; Häussinger et al., 2006a; Kircheis et al., 2007; Poordad, 2007). Estimates of the occurrence of overt HE in liver cirrhosis, for example, range from 30 to 45% (Poordad, 2007), those of minimal HE even from 20 to 80% (Kircheis et al., 2007). The true burden of HE in terms of its prevalence and resulting financial costs is assumed to be underestimated (Poordad, 2007).

3.2.1 Symptoms and clinical manifestations

HE is associated with a broad range of symptoms of varying severity, encompassing alterations in the state of awareness up to somnolence, gross disorientation and hepatic coma, impairments of cognitive and motor function, alterations of sleep patterns and personality changes (Butterworth, 2000; Ferenci et al., 2002; Häussinger and Blei, 2007; Prakash and Mullen, 2010). Typical motor symptoms are the tremor-like symptoms mini-asterixis and asterixis, but extrapyramidal abnormalities including bradykinesia, dysarthria, rigidity and tremor have also been described (Butz et al., 2010; Häussinger and Blei, 2007). In addition, higher degrees of HE are associated with abnormal reflexes (Häussinger and Blei, 2007). Deficits of attentional function exist at all HE stages, deteriorate as a function of disease severity and affect different attentional functions, including vigilance, attention orienting and higher executive processes (Amodio et al., 2005; Felipo et al., 2012; Pantiga et al., 2003; Weissenborn et al., 2005, 2001).

In this thesis, patients with chronic liver cirrhosis were studied. In association with liver cirrhosis, three types of HE are distinguished: Episodic, persistent (chronic) and minimal HE (Ferenci et al., 2002; Häussinger and Blei, 2007; Wettstein et al., 2003). The first two comprise overt clinical symptoms, which can be detected by clinical examination. Patients

with minimal HE, in contrast, do not show recognizable clinical symptoms of HE but exhibit slight cognitive and motor deficits, which are only revealed by detailed neuropsychometric testing.

Episodic HE is the most common presentation of HE and describes an alteration of the mental state of patients with chronic liver disease. It is usually the result of a precipitating factor like gastrointestinal bleeding, uraemia, the use of sedatives, an infection or an electrolyte disturbance, which also determines the main treatment actions. If no precipitating factor is discernable, the HE is classified as spontaneous (Ferenci et al., 2002; Häussinger and Blei, 2007).

Persistent HE comprises patients showing recurrent episodes of HE or a long-lasting, persisting alteration of the mental state. Persistent HE is often found in the context of pathophysiological or therapeutic, i.e. anatomically developed or surgically inserted, portal-systemic shunts (Häussinger and Blei, 2007).

Patients with *minimal HE* (mHE), which was previously also termed subclinical or latent HE, do not present with overt clinical symptoms of HE but show mild cognitive and motor impairment in neuropsychometric examinations (Amodio et al., 2004; Butterworth, 2000; Ferenci et al., 2002; Häussinger and Blei, 2007). Thus, it describes a syndrome in between normal brain function and clinically overt HE. In spite of its mild form, mHE impairs many aspects of daily life functioning (Groeneweg et al., 1998), including fitness to drive (Kircheis et al., 2009; Wein et al., 2004). In addition, mHE increases the probability of a clinically overt HE (Hartmann et al., 2000; Romero-Gómez et al., 2001).

3.2.2 Diagnosis and clinical grading

The diagnosis of HE comprises the exclusion of other causes of encephalopathy, the identification of potential precipitating causes and a trial of empiric treatment (Prakash and Mullen, 2010). Apart from that, different techniques and approaches have been tested and applied in the diagnosis of HE. These include neuropsychometric test batteries, electrophysiological assessments like EEG and the measurement of serum ammonia levels (Prakash and Mullen, 2010; Wettstein et al., 2003). Due to the variability of the clinical expression of HE, none of these tests supersedes a clinical assessment, which is usually sufficient for a diagnosis of overt HE in daily routine (Häussinger and Blei, 2007; Wettstein et al., 2003). A diagnosis of mHE, however, is per definition only possible using

neuropsychometric testing (Amodio et al., 2004; Butterworth, 2000; Ferenci et al., 2002; Häussinger and Blei, 2007).

A widely accepted scheme for the graduation of overt HE are the *West-Haven-Criteria*, a semiquantitative scale for a grading of the mental state (Ferenci et al., 2002). Based on a clinical assessment, these criteria classify patients with manifest HE into four groups, covering the range from mild symptoms like a shortened attention span and a trivial lack of awareness (grade 1 or HE1) up to the most severe form of a hepatic coma (grade 4 or HE4) (Table 1). When no overt clinical symptoms are discernable, the *Vienna test system* (Vienna test system, WINWTS, Version 4.50, 1999), a computerized test battery used for psychological diagnostics, can be applied to distinguish cirrhotics with no signs of HE (HE0) from those with mHE (Kircheis et al., 2002). Using selected subtests of the test battery, different aspects of attention, reaction times to optic and acoustic stimuli, fine motor skills and visual perceptual abilities are measured. Results are defined to indicate mHE if patients show impaired performance in at least two subtests compared to a large, age-matched control population (Kircheis et al., 2002).

Table 1: West-Haven-Criteria for the grading of overt hepatic encephalopathy
(adapted from Ferenci et al., 2002)

Grade 1 (HE1)	Trivial lack of awareness Euphoria or anxiety Shortened attention span Impaired performance of addition
Grade 2 (HE2)	Lethargy or apathy Minimal disorientation for time or place Subtle personality change Inappropriate behavior Impaired performance of subtraction
Grade 3 (HE3)	Somnolence to semistupor, but responsive to verbal stimuli Confusion Gross disorientation
Grade 4 (HE4)	Coma (unresponsive to verbal or noxious stimuli)

Thus, cirrhotic patients can overall be classified into one of six groups: *HE0*, *mHE*, and *HE1-4*. While *HE3* and *HE4* defined as somnolence and coma, respectively, are relatively easy to diagnose, the lower grades 1 and 2 and the pre-clinical *mHE* are more difficult to distinguish and are discussed to represent a continuum of deterioration of the mental state rather than distinct stages of the disease (Bajaj et al., 2009; Häussinger et al., 2006a).

The so-called *critical flicker frequency* (CFF) is a tool which is increasingly used to quantify and monitor HE and has been shown to provide a reliable and fine-graded assessment of HE disease severity (Biecker et al., 2011; Kircheis et al., 2002; Lauridsen et al., 2011; Prakash and Mullen, 2010; Romero-Gómez et al., 2007; Sharma et al., 2007). The CFF can be assessed using the Schuhfried Test System (Eberhardt, 1994). Light pulses are intrafoveally presented with decreasing frequency starting from 60 Hz. The CFF is determined as the frequency at which the subjective impression of a fused light switches to a flickering one, which is indicated by the subject with a button press (Kircheis et al., 2002). On average, healthy subjects and cirrhotics without any signs of HE (*HE0*) show a CFF around 42 Hz (Kircheis et al., 2002; Sharma et al., 2007). Increasing HE disease severity was repeatedly shown to be reflected by decreasing CFF values (Kircheis et al., 2002; Sharma et al., 2007). Using a cut-off value of 39 Hz, the CFF reliably distinguishes patients with overt HE from non-cirrhotic controls and cirrhotic *HE0* patients (Kircheis et al., 2002). Average values reported for patients with minimal HE are less consistent and vary between 36 and 39 Hz (Kircheis et al., 2002; Romero-Gómez et al., 2007; Sharma et al., 2007). The CFF is independent of training, education and the time of day and only slightly dependent on age (Kircheis et al., 2002).

3.2.3 Pathophysiology

The pathophysiology of HE is complex and not yet fully understood. A key factor in the pathogenesis of HE is ascribed to ammonia (Butterworth, 2000; Häussinger and Blei, 2007; Prakash and Mullen, 2010), which is mainly generated in the intestine and to a large extent metabolized by the liver. A strong impairment of liver function, as e.g. in liver cirrhosis, results in increased blood ammonia concentrations, which adversely affect the brain's metabolism. In the brain, astrocytes are the only cells that metabolize ammonia, by conversion to glutamine. Glutamine is an osmolyte, drawing water into the cell. If glutamine is synthesized excessively due to high ammonia concentrations, a low grade

cerebral edema due to astrocyte swelling develops, compromising the function of glial cells and glioneuronal communication and ultimately leading to HE (Häussinger and Blei, 2007; Prakash and Mullen, 2010). However, the pathogenesis of HE is much more complex and, among other factors, also involves additional neurotoxins like manganese, increased oxidative and nitrosative stress and altered gene expression (Häussinger, 2004; Häussinger and Blei, 2007; Prakash and Mullen, 2010). Regarding neurotransmission in the brain, multiple neurotransmitter systems are altered in HE, including GABAergic, glutamatergic, dopaminergic and serotonergic neurotransmission (Häussinger and Blei, 2007).

Of particular relevance for this thesis are *disturbances in oscillatory brain activity* associated with HE. A range of EEG studies measuring spontaneous oscillatory brain activity have demonstrated a progressive slowing of the mean peak frequency with increasing disease severity (Amodio and Gatta, 2005; Amodio et al., 2009; Kullmann et al., 2001; Montagnese et al., 2011, 2007). In line with these findings, thalamo-cortical-muscular coupling in the motor system was found to be slowed in patients with mini-asterixis (Timmermann et al., 2003, 2002). Most recently, a slowing of stimulus-induced oscillatory gamma activity in the visual system was demonstrated in HE, in combination with an impaired modulation of gamma power by attention (Kahlbrock et al., 2012a, Appendix 5). Interestingly, studies using the CFF for quantification of HE disease severity revealed correlations between the slowing of oscillatory activity within the studied frequency bands and the CFF (Kahlbrock et al., 2012a, Appendix 5; Timmermann et al., 2008), indicating a high sensitivity of the CFF for neurophysiological alterations in HE. Hence, slowed oscillatory activity in different cerebral subsystems of the brain is believed to be a key hallmark in HE and to represent a basic mechanism for its clinical manifestation (Timmermann et al., 2008, 2005).

3.2.4 Somatosensory processing in HE

Somatosensory processing in HE has been repeatedly studied using median nerve stimulation and the associated somatosensory evoked potentials (SEP) measured by EEG, mostly to evaluate their potential use as a diagnostic tool (Amodio and Gatta, 2005; Davies et al., 1991; Kullmann et al., 1995; van der Rijt and Schalm, 1992). As a function of HE disease severity, a sequential prolongation of peak and inter peak latencies in combination with a deformation or loss of SEP components was found (Blauenfeldt et al., 2010;

Chu and Yang, 1987; Chu et al., 1997; Davies et al., 1991; Kono et al., 1994; Yang et al., 1998, 1993, 1985), providing evidence for altered and delayed central processing of simple sensory stimuli. On a behavioral level, the quantitative sensory testing protocol (Rolke et al., 2006a, 2006b) did not show changes in tactile, mechanical detection thresholds in patients with HE up to grade 2, but did reveal impairments in the perception of cold temperatures and temperature changes (Brenner et al., 2010). Oscillatory brain activity, in particular oscillatory alpha activity as a prominent oscillatory feature of the somatosensory system with its characteristic stimulus-induced modulation (section 3.1.3), has not yet been studied in the context of somatosensory processing in HE.

3.2.5 Summary

HE is a neuropsychiatric complication of liver cirrhosis with a broad range of symptoms. HE disease severity can be quantified according to different clinical stages but also reliably and continuously assessed using the CFF. Regarding the pathophysiology of HE, a slowing of oscillatory brain activity is believed to be a key mechanism of the different symptoms. In addition, strong evidence suggests that somatosensory processing is altered in HE. However, this has not yet been examined with respect to oscillatory brain and in particular alpha activity. Thus, it still needs to be elucidated if the hypothesized global slowing of oscillatory brain activity in HE extends to the somatosensory system. In addition, it has yet to be examined if this type of pathologically changed brain function also affects other features of stimulus-associated alpha activity.

4 Aims and Hypotheses

The aim of this thesis was to investigate the modulation of oscillatory alpha activity in the somatosensory system by attention and hepatic encephalopathy, a disease associated with a progressive deterioration of brain function and pathologically slowed oscillatory brain activity.

Study 1 examined the modulation of pain-associated somatosensory alpha activity by attention. To this end, healthy subjects completed a spatial attention paradigm, while brain activity was measured using MEG. It was hypothesized that spatial attention differentially modulates both pre- and post-stimulus alpha activity. In anticipation of a lateralized painful stimulus, spatial attention was expected to lateralize pre-stimulus alpha activity across left and right primary somatosensory areas, in line with the alpha inhibition hypothesis. In response to the stimulus, attention was expected to be associated with decreased levels of post-stimulus alpha activity, in accordance with an enhanced cortical activation after an attended painful stimulus.

Study 2 investigated potential alterations of somatosensory alpha activity by hepatic encephalopathy. Cirrhotic patients with varying degrees of low-grade HE and healthy control subjects received electrical, non-painful stimulation of the right median nerve. Simultaneously, brain activity was recorded with MEG. In accordance with the suggested key role of slowed oscillatory brain activity in the pathophysiology of HE, stimulus-associated alpha activity in primary somatosensory areas was expected to be slowed in frequency as a function of HE disease severity. In line with delayed somatosensory processing, it was furthermore hypothesized that increasing levels of HE would be associated with a delayed stimulus-induced modulation of somatosensory alpha activity.

Overall, this thesis aimed at extending the knowledge about the dynamics of oscillatory alpha activity in the somatosensory system. The purpose was to extend the understanding of the role of alpha activity in the healthy brain, broaden the understanding of HE and identify alterations of somatosensory alpha activity associated with pathologically changed brain function.

5 Study 1: Pre- and post-stimulus alpha activity shows differential modulation with spatial attention during the processing of pain

In study 1 (Appendix 1), somatosensory alpha activity and its modulation by attention were investigated in the context of the processing of pain. The aim was to test if the functional role of alpha activity during pain processing is consistent with that during the processing of other sensory stimuli. A spatial attention paradigm required healthy subjects to attend to painful laser stimuli on the left or right hand and ignore stimuli on the other hand, while brain activity was simultaneously measured using MEG. Such a design is well-suited to test the alpha inhibition hypothesis, since the cortical representations of the attended and unattended spatial locations (i.e. the left and right hand) are clearly separable. At the same time, cognitive demands are not varied across the different attentional conditions, as done in many attention studies involving a distraction condition, which for example ask subjects to read or watch a movie to direct attention away from administered painful stimuli. Somatosensory alpha activity was analyzed both during pre- and post-stimulus time periods in order to disentangle effects of attention on somatosensory alpha activity in anticipation of and in response to painful stimuli. In addition, a possible relation between the level of attention-modulated alpha activity and the subjective pain perception was scrutinized.

5.1 Methods

15 healthy subjects completed a spatial attention paradigm, in which painful, cutaneous laser stimuli (Themis, Starmedtec, Starnberg, Germany) were randomly administered to the dorsum of their left or right hand. Such stimuli selectively activate nociceptive fibers without concomitant activation of tactile afferents (Treede, 2003). Spatial attention was manipulated in a block design, asking subjects either to focus on stimuli on the left hand while ignoring stimuli on the right hand or vice versa. Stimuli on the attended hand had to be rated as to their location in one of two target areas on the hand and with respect to the subjectively perceived pain intensity. No behavioral response was required for stimuli on the unattended hand. This design resulted in four types of trials: (i) left hand stimulated and attended, (ii) left hand stimulated, but unattended, (iii) right hand stimulated and

attended, (iv) and right hand stimulated, but unattended. Simultaneously, neuromagnetic brain activity was measured using MEG.

The recorded neurophysiological data were analyzed with respect to the time course and strength of oscillatory alpha activity during pre- and post-stimulus time periods with a focus on primary somatosensory areas. To examine a modulation of alpha activity by spatial attention, trials in which stimuli were attended were compared to those in which stimuli were unattended for both left and right hand stimulation trials. Furthermore, a lateralization index was computed, capturing the degree of anticipatory pre-stimulus alpha lateralization across left and right primary somatosensory areas in a single value. Lastly, correlation analyses examined a possible relation between the power of attention-modulated alpha activity and individual trial-by-trial pain ratings.

5.2 Results

Laser stimuli on the attended hand were consistently rated as slightly to moderately painful, pinprick-like sensations with an average rating of 3.3 out of 10 (with 10 equaling the worst imaginable pain). They were on average correctly localized to the stimulated target area in 85% of trials. While pain ratings did not differ between the left and right hand (3.2/10 vs. 3.3/10), the rate of correctly localized stimuli was significantly lower for left than right hand stimuli (80.0 vs. 88.9%).

Across attended and unattended trials, laser stimuli to both hands suppressed oscillatory alpha activity over bilateral somatosensory and parietal areas (Fig. 2a of Appendix 1). According to the strongest stimulus-induced response, two channel groups of interest over left and right primary somatosensory areas were selected as a basis for the analysis of attention effects (Fig. 2b of Appendix 1).

5.2.1 Pre-stimulus effects of spatial attention

Regarding the pre-stimulus period, spatial attention to one hand lateralized alpha activity in anticipation of a stimulus on that hand. Alpha activity over primary somatosensory areas was stronger when the ipsilateral hand was attended compared to when the contralateral hand was attended; indicating increased alpha activity over ipsilateral and/or decreased alpha activity over contralateral areas with respect to the attended hand. This pattern was revealed by comparison of attended and unattended trials over left and right

somatosensory areas separately (Fig. 3 of Appendix 1) and confirmed by the alpha lateralization index quantifying the modulation of alpha activity across hemispheres (Fig. 4 of Appendix 1). Generally, these attention effects appeared more consistently over left primary somatosensory areas.

5.2.2 Post-stimulus effects of spatial attention

During post-stimulus time periods in response to the painful laser stimuli, spatial attention was associated with decreased levels of alpha activity. A stimulus-induced suppression of alpha activity was seen in all conditions but was more intense and prolonged if a stimulus was attended. This attention effect started earlier in time and was more widely spread including ipsilateral somatosensory areas for left than right hand trials.

5.2.3 Correlation between attention-modulated alpha activity and pain ratings

Trends for an inverse correlation between attention-modulated post-stimulus alpha power and individual trial-by-trial pain ratings were found for trials in which the left hand was stimulated, indicating higher pain ratings if the level of post-stimulus alpha activity was low. Pre-stimulus alpha power in general as well as post-stimulus alpha power in right hand stimulation trials did not show evidence for a correlation with individual pain ratings.

5.3 Discussion

Study 1 aimed at investigating the modulation of pain-associated somatosensory alpha activity by attention to examine the role of alpha activity during pain processing. Results show that spatial attention to one hand differentially modulates alpha activity in anticipation of and in response to painful laser stimuli on that hand, indicating a pronounced role of attention for the processing of pain.

Anticipatory pre-stimulus alpha activity lateralized across the two hemispheres when spatial attention was directed to one hand; being lower in primary somatosensory areas when the contralateral hand was attended compared to when the ipsilateral hand was attended. This effect tallies previous findings showing a similar anticipatory lateralization in somatosensory (Anderson and Ding, 2011; Haegens et al., 2011), visual (Gould et al., 2011; Thut et al., 2006), and auditory (Müller and Weisz, 2012; Thorpe et al., 2012)

paradigms and is in line with effects expected according to the alpha inhibition hypothesis (Jensen and Mazaheri, 2010). Whether this pattern of results is caused by an alpha increase ipsilateral to the attended stimulus, an alpha decrease contralateral to the attended stimulus, or a combination of both cannot be deduced from the current data, since the study used a block design and lacked a neutral baseline without any anticipatory attentional orientation. Nevertheless, these results are in line with the notion that alpha activity reflects the degree of engagement/disengagement of the underlying cortical areas and is adjusted according to current goals and demands, already in anticipation of a stimulus.

Post-stimulus alpha activity was consistently decreased over primarily contralateral somatosensory areas when attention was placed on the stimulated hand, prolonging and intensifying the widespread alpha suppression induced by painful laser stimuli (Ploner et al., 2006b). This finding matches a previous study examining non-spatial attention effects on pain-associated alpha activity (Ohara et al., 2004), in which post-stimulus alpha levels were calculated relative to a pre-stimulus baseline, thereby intermixing pre- and post-stimulus attention effects. Here, the same results were found when pre- and post-stimulus effects were disentangled. Together, both studies thus strongly indicate an increased cortical activation and alerting function if a painful stimulus is attended.

In previous studies, an association between the amount of alpha activity close to the onset of a painful laser stimulus and subjective pain ratings was found (Babiloni et al., 2006; Schulz et al., 2011). Here, we only found a trend for such an effect for post-stimulus alpha activity in left hand stimulation trials. In these previous studies, correlation analyses were performed on selected electrodes of interest directly overlying the primary somatosensory cortex, in line with studies suggesting a prominent role for the contralateral primary somatosensory cortex in the perception of pain (Bushnell et al., 1999). Here, the focus was slightly different and alpha estimates for correlation analyses were averaged across all sensors and time points showing modulation of alpha activity with spatial attention. Possibly, this sensor selection based on the widespread attention effects led to an estimate of alpha activity too coarse to detect a significant relation to trial-by-trial pain ratings.

Interestingly, effects of attention on alpha activity were more consistently found for left than right hemispheric areas in this study, possibly indicating hemispheric differences in

the extent to which pain-associated alpha activity is affected by spatial attention. Behaviorally, subjects were more successful in correctly localizing stimuli on the attended hand for right than left hand trials, possibly hinting at a perceptual superiority of the dominant hand, since most subjects were right-handed. Thus, the attentional load might have been higher for left hand trials due to a higher difficulty of the localization task. Future studies equating performance levels between both hands need to examine to what extent handedness and attentional load contribute to the found hemispheric differences.

5.4 Conclusions

Study 1 complements the knowledge about the role of oscillatory alpha activity during the processing of pain by examining its modulation by attention. Spatial attention was shown to differentially modulate both pre- and post-stimulus pain-associated alpha activity. These results provide evidence for a pronounced role of attention during the processing of pain, which is at least partially mediated by the modulation of somatosensory alpha activity. In line with findings from other modalities, the anticipatory pre-stimulus alpha lateralization reconfirmed here strongly suggests that the presumed role of alpha activity as a top-down modulated gating mechanism includes pain processing. Thus, alpha activity seems to represent a general mechanism for resource allocation, which is used across different modalities and even in the context of a very salient painful stimulus. In addition, these findings confirm that attention also affects the widespread pain-induced suppression of alpha activity, leading to an increased and longer lasting post-stimulus cortical activation.

6 Study 2: Hepatic encephalopathy slows and delays stimulus-associated somatosensory alpha activity

Study 2 (Appendix 2) analyzed the modulation of somatosensory alpha activity associated with electrical, non-painful median nerve stimulation by hepatic encephalopathy. The aims were to broaden the understanding of the disease and investigate how pathologically altered brain function changes somatosensory alpha activity. HE provides the opportunity to examine alterations of oscillatory brain activity as a function of progressively deteriorating brain function, since the severity of HE varies gradually but can be reliably quantified using the CFF. Patients with liver cirrhosis and varying degrees of HE as well as healthy control subjects received electrical stimulation of the right median nerve, while brain activity was recorded with MEG. Neuronal activity within S1 contralateral to the stimulated hand was reconstructed. The frequency and the stimulus-induced modulation of S1 alpha activity were analyzed, compared between different patient groups and healthy control subjects and related to disease severity as quantified by the CFF.

6.1 Methods

21 patients with confirmed liver cirrhosis and 7 healthy control subjects participated in the study. To quantify the degree of HE, a clinical assessment, detailed neuropsychometric testing and measurement of the CFF were performed. Patients were classified into three groups according to the *West-Haven-Criteria* and neuropsychometric test results (Kircheis et al., 2002): (i) *HE0*, i.e. no signs of HE, (ii) minimal HE (*mHE*), i.e. no clinical signs of HE but pathological results in ≥ 2 psychometric tests, and (iii) *HE1*, i.e. manifest HE of grade 1 with clinically overt symptoms. The fourth group comprised healthy, age-matched control subjects: (iv) *controls*. Participant data is given in Table 1 of Appendix 2. Sensory neuropathy of the median and radial nerves was ruled out by bilateral sensory nerve conduction measures. To study alpha activity associated with somatosensory stimulation, all subjects received electrical stimulation of the right median nerve, while brain activity was measured using MEG.

From the recorded neurophysiological data, evoked responses to median nerve stimuli were individually localized in order to reconstruct brain activity within S1 contralateral to the stimulated hand. Oscillatory alpha activity within S1 was analyzed with respect to

its peak frequency and stimulus-induced modulation. The temporal evolution of alpha activity in individually-adjusted frequency bands was additionally quantified by determining the time point of the maximal stimulus-induced alpha rebound. To test for effects of HE, the overall stimulus-induced modulation of S1 alpha activity as well as its peak frequency and the time of maximal alpha rebound were compared between the different clinical groups. Furthermore, correlation analyses were performed to investigate relations between the individual alpha peak frequency, the time of maximal alpha rebound, and the CFF as a continuous measure of HE disease severity.

6.2 Results

Individual localizations of evoked responses in the brain were consistent with S1 contralateral to the stimulated hand (Fig. 1 of Appendix 2). All individual MEG-related data are given in Table 2 of Appendix 2. In all four groups under study, median nerve stimuli elicited the characteristic modulation of S1 alpha activity induced by somatosensory stimulation in terms of an initial suppression followed by a rebound to or above baseline levels (Fig. 2a of Appendix 2). Comparing the overall temporal evolution of alpha activity between the different groups revealed that S1 alpha activity during the rebound period was enhanced for HE1 patients compared to healthy controls, indicating a stronger and/or delayed alpha rebound (Fig. 2b of Appendix 2).

6.2.1 Alpha peak frequencies

Comparisons of the different subject groups revealed lower alpha peak frequencies for HE1 patients compared to healthy controls and a trend for lower alpha peak frequencies for mHE patients, again in comparison to the healthy control subjects (Fig. 3a of Appendix 2, left panel). Accordingly, correlation analyses showed an association of lower alpha peak frequencies with lower CFF values, when all subjects were considered (Fig. 3a of Appendix 2, middle panel) and for patients only (Fig. 3a of Appendix 2, right panel).

6.2.2 Time of maximal alpha rebound

Comparisons of the subject groups did not show differences in the time of maximal alpha rebound (Fig. 3b of Appendix 2, left panel). However, correlation analysis indicated a later time of alpha rebound with increasing disease severity as quantified by the CFF. When all

subjects were considered, a significant relation showing a later time of alpha rebound with lower CFF values was revealed (Fig. 3b of Appendix 2, middle panel). For patients only, a corresponding trend was found (Fig. 3b of Appendix 2, right panel).

6.3 Discussion

The aim of study 2 was to investigate a potential pathological alteration of stimulus-associated somatosensory alpha activity in HE. A slowing of the peak frequency of S1 alpha activity along with a delay of its stimulus-induced modulation could be shown, even in earliest stages of the disease.

The observed slowing of the S1 alpha peak frequency is in accordance with previous studies demonstrating a slowing of spontaneous oscillatory activity (Amodio and Gatta, 2005; Amodio et al., 2009; Kullmann et al., 2001; Montagnese et al., 2011, 2007) and of oscillatory activity associated with the motor and attentional deficits apparent in HE (Kahlbrock et al., 2012a, Appendix 5; Timmermann et al., 2003, 2002). In the present work, oscillatory activity was for the first time studied in the context of somatosensory processing. Importantly, no previous study examined a slowing of oscillatory activity directly within a primary sensory area. These results extend previous findings to the somatosensory system and further substantiate the notion that slowed oscillatory activity represents a key mechanism in the pathophysiology of HE (Timmermann et al., 2008, 2005).

A delayed time of maximal alpha rebound associated with increasing HE disease severity also matches previous studies showing delayed somatosensory processing in HE using SEPs (Blauenfeldt et al., 2010; Chu and Yang, 1987; Chu et al., 1997; Davies et al., 1991; Kono et al., 1994; Yang et al., 1998, 1993, 1985). Here, somatosensory processing was studied on a larger time scale than in previous studies, examining the time course of the cortical activation of S1 rather than immediate stimulus processing. No evidence was found for an alteration of the initial suppression of alpha activity by somatosensory stimuli, which reflects stimulus-induced cortical activation (Bauer et al., 2006; Della Penna et al., 2004; Nikouline et al., 2000; Salenius et al., 1997). Instead, this study demonstrated a delay specifically of the alpha rebound. This finding indicates a specific impairment of S1 to return to the pre-stimulus or baseline state of cortical activation after activation by an external stimulus. Such a decreased capability to flexibly adjust activation levels back to baseline levels is in line with a previous study demonstrating an impaired ability of

cirrhotic patients to disengage visual attention previously focused on a location (Amodio et al., 2005). Future studies need to combine neurophysiological parameters of somatosensory dysfunction with behavioral measures to investigate the consequences of altered somatosensory oscillatory activity for behavioral performance.

Notably, differences in alpha activity between the clinical groups were only found when comparing the most extreme disease stages, i.e. control subjects vs. mHE/HE1 patients. It was expected, for example, that HE0 patients, who did not show any HE symptoms, would be equally distinguishable from mHE/HE1 patients using the neurophysiological results, which was not the case. Of course, the relatively small size of this carefully selected patient sample might have been a factor, which contributed to the missing group effects. However, these results might also indicate that impairments of somatosensory processing appear even before deficits of motor and attentional abilities can be revealed by neuropsychometric testing. Also, the grading into distinct clinical stages might not be optimal to capture the diversity of HE. Noteworthy, the CFF was more sensitive in quantifying the pathological alterations of S1 alpha activity as a function of disease severity. This is in line with previous work (Kahlbrock et al., 2012a, Appendix 5) and ongoing discussions about the usefulness of the common classification scheme with distinct clinical groups such as *West-Haven-Criteria* (Ferenci et al., 2002). Instead, it has been suggested to approach the neurocognitive changes in HE as a continuum (Bajaj et al., 2009; Häussinger et al., 2006b; Kircheis et al., 2007). By the present data, the use of the CFF as a measure to determine and monitor HE disease severity is further encouraged, even in early stages of HE. Importantly, relations between the CFF and neurophysiological parameters of alpha activity were also found when considering patients only, indicating that correlations were not primarily caused by differences between patients and healthy control subjects. Instead, both the frequency and the time of alpha rebound seem to gradually depend on disease severity, even in the low grades of HE studied here.

Last but not least, this study demonstrated how the study of HE provides an opportunity to examine alterations of oscillatory brain activity as a function of gradually increasing levels of deteriorating brain function. This is possible because of the CFF, which permits to reliably and fine-gradedly quantify increasing levels of HE severity. By examining how these increasing pathological changes of brain function affect different features of oscillatory brain activity, inferences can also be drawn about healthy brain function.

6.4 Conclusions

Study 2 extends previous findings of slowed oscillatory activity in HE to the somatosensory system. Thereby, the hypothesis of a general slowing of oscillatory brain activity as a key hallmark in the pathophysiology of HE was substantiated, broadening the understanding of the disease. In addition, a specific delay of the stimulus-induced alpha activity rebound was found in association with HE, hinting at an impaired capability of the somatosensory system to flexibly adjust cortical activation levels back to the default state. Regarding the general modulation of alpha activity by disease, the results show that different features of somatosensory alpha activity can be gradually affected by pathological alterations of brain function as shown by an effect of HE on both the peak frequency of alpha activity and its modulation by external stimulation.

7 General conclusions

This thesis investigated the dynamics of oscillatory alpha activity in the somatosensory system in the context of spatial attention and hepatic encephalopathy in order to broaden the understanding of the functional role of alpha activity in the healthy brain and identify potential alterations caused by pathologically changed brain function. Results confirm that alpha activity constitutes a sensitive measure of the degree of activation of a cortical area. Across different sensory modalities including the processing of pain, alpha activity reacts to incoming stimuli, but is also closely regulated by top-down processes like attention according to current goals and needs. If brain function deteriorates, somatosensory alpha activity can be pathologically altered.

As hypothesized, spatial attention modulated both pre- and post-stimulus alpha activity associated with pain. The post-stimulus attention effects shown by study 1 demonstrate that a top-down driven, cognitive modulation of the attentional orientation influences the degree and time course of cortical activation evoked by a painful stimulus. If a painful stimulus is attended, it leads to a stronger cortical activation. In addition, the pre-stimulus effects show that spatial attention already affects alpha activity in anticipation of pain, in line with an engagement of task-relevant and/or disengagement of task-irrelevant regions as proposed by the alpha inhibition hypothesis. Together, these results demonstrate a pronounced modulation of pain-associated somatosensory alpha activity with attention. This tight relation with the orienting of attention strongly suggests that the functional role of alpha as a sensory gating mechanism includes pain processing. Thus, across different sensory modalities and types of stimuli, alpha activity seems to consistently route the information flow in the healthy brain by a precise and task-adapted engagement and disengagement of cortical areas, also in the context of a very salient painful stimulus. Future studies need to investigate if subjects can learn to intentionally apply such a sensory gating to the processing of pain, out of the context of experimental paradigms like the one used here. If so, this function of oscillatory activity might be used therapeutically, for example in the context of chronic pain conditions.

Study 2 demonstrated alterations of somatosensory alpha activity as a function of HE severity in line with the hypothesized effects. The observed delayed modulation of somatosensory alpha activity revealed a delayed time course of the underlying cortical activation, indicating an impaired capability of the somatosensory system to return to the

default level of cortical activation. In addition, a slowing of oscillatory brain activity was for the first time demonstrated in the somatosensory system and within a primary sensory area, extending previous findings of slowed oscillatory activity in HE. Hence, the hypothesis that slowed oscillatory activity in different cerebral subsystems represents a key mechanism in the pathophysiology of HE (Timmermann et al., 2008, 2005) is substantiated. Importantly, the CFF as a continuous measure was most sensitive in quantifying the pathological alterations of somatosensory alpha activity as a function of disease severity. This finding agrees with proposals to approach the neurocognitive changes induced by HE as a continuum rather than a stage-like disease (Bajaj et al., 2009; Häussinger et al., 2006b; Kircheis et al., 2007) and further encourages the use of the CFF as a measure to determine and monitor HE disease severity. Moreover, alterations of alpha activity associated with median nerve stimulation might themselves be a promising diagnostic tool. Even in the low grades of hepatic encephalopathy studied here, gradual changes of oscillatory alpha activity as a function of disease severity were observed and might provide a useful addition to standard clinical assessments.

HE affected two features of somatosensory alpha activity: the alpha peak frequency and its stimulus-induced power modulation. This tallies previous studies, which also reported associations of declining brain function with alterations of the power as well as the frequency of oscillatory brain activity. Like HE, Parkinson's disease, for example, has been related to both pathologically synchronized (Hammond et al., 2007) and slowed (Stoffers et al., 2007) oscillatory brain activity. In addition, evidence suggests an inverse relation between the frequency of oscillatory brain activity and age (Dustman et al., 1999; Muthukumaraswamy et al., 2010). Healthy cognitive processes like attention and memory, however, are particularly related to modulations of the power of oscillatory brain activity, as also shown in this thesis. Thus, alterations of the frequency of oscillatory brain activity seem particularly indicative of potentially declining brain function. Hence, the frequency and power changes found here in association with increasing levels of HE might represent markers of different pathophysiological processes.

Overall, results from this thesis confirm that MEG and the measurement of oscillatory brain activity are useful tools for the study of healthy brain function as well as the detection and monitoring of pathological brain states.

8 Outlook

This thesis extends our knowledge about the dynamics of oscillatory alpha activity in the somatosensory system. However, open questions and interesting lines of further research remain, a few of which will be outlined in the following.

The present work shows that the functional role of alpha activity as a sensory gating mechanism includes pain processing. Importantly, painful stimuli are associated with particularly strong suppressions of oscillatory alpha activity, both in response to (Ploner et al., 2006b) but also in expectation of an upcoming painful event (Babiloni et al., 2006, 2004, 2003; Del Percio et al., 2006). These findings are most likely related to the aversive nature of pain and indicate that painful stimuli could be used as very efficient distractors. It is conceivable that the need to ignore and inhibit the perception of an upcoming distracting painful stimulus evokes a particularly strong anticipatory alpha modulation, for example in terms of a stronger alpha lateralization in spatial attention paradigms like the one used in study 1. This would further substantiate the alpha inhibition hypothesis with its proposal that active alpha activity modulations are especially involved in the inhibition of distracting information. In this context, the association of oscillatory alpha activity with oscillations in other frequency bands is a further appealing topic for future studies. Particularly interesting is the coupling to oscillatory gamma activity, which has been found in the somatosensory system in response to both non-painful and painful somatosensory stimuli (for example (Bauer et al., 2006; Gross et al., 2007)). Gamma activity is associated with active processing and enhanced by attention ((Fries, 2009; Kahlbrock et al., 2012b, Appendix 3+4), and thus seems to represent a mechanism complementary to that assumed for alpha activity.

Studies investigating the role of oscillatory alpha activity during cognitive processes are usually correlative in nature, for example showing parallel modulations of alpha activity and the behavioral performance within a specific task. Neurostimulation methods such as TMS or transcranial direct/alternating current stimulation (tDCS/tACS) provide the unique opportunity to actively modulate oscillatory brain activity from outside the skull. If such modulations changed the behavioral outcome in a task, this would allow for causal rather than correlative inferences about the functional role of oscillatory brain activity. Accordingly, TMS-induced boosts of oscillatory alpha activity in different brain areas were already shown to differentially modulate associated behavioral responses in visual

attention tasks (Romei et al., 2012, 2010; Thut et al., 2011). Similar experimental paradigms could also be used to provide evidence for a causal role of oscillatory alpha activity for somatosensory processing. An intriguing possibility is to potentially reduce the subjectively perceived intensity of a painful stimulus by boosting alpha activity in S1. Again, this could pave the way towards new ways of pain relief and treatment.

This thesis investigated modulations of the power and frequency of alpha activity. Another very interesting area of recent research focuses on a different feature and investigates effects of its phase on perception and behavior. According to the *pulsed inhibition hypothesis*, a single alpha cycle reflects changes of the level of cortical activation and cortical excitability at a much faster time scale than that of slower alpha power modulations, representing an even more fine-graded mechanism underlying perception and stimulus processing (Mathewson et al., 2011). The phase of oscillatory alpha activity is even hypothesized to provide a mechanism for prioritizing and ordering input according to its relevance (Jensen et al., 2012). Recent studies support this view, for example by showing that the phase of ongoing alpha oscillations biases visual (Busch et al., 2009; Dugué et al., 2011; Mathewson et al., 2009) as well as somatosensory perception (Palva et al., 2005). Thus, the association between the phase of ongoing somatosensory alpha activity, somatosensory perception and associated behavior is a promising area of future research. Again, it has for example not yet been investigated how the subjectively perceived intensity of a painful stimulus is influenced by the phase of somatosensory alpha activity.

Results from this thesis revealed that hepatic encephalopathy affects different features of oscillatory alpha activity in the somatosensory system. Very likely, the slowing of somatosensory alpha activity along with its delayed rebound affects associated behavioral responses or impairs the processing of immediately following stimuli. Such potential behavioral consequences of the observed alpha activity alterations are an important area of further investigations and might reveal yet unknown sensory impairments in HE. In addition, studies of attentional modulations of pre- and post-stimulus oscillatory alpha activity with paradigms similar to the one employed in study 1 could advance our understanding of the neural mechanisms of the attentional deficits apparent in HE, bringing together findings from both studies of this thesis.

Lastly, going beyond the disease studied here, future studies should examine if chronic pain conditions, which can involve an attentional bias towards pain (Crombez et al., 2005;

McCracken, 1997), are associated with corresponding maladaptive alterations of oscillatory alpha activity. If so, neurofeedback training, which enables subjects to actively modulate cortical alpha activity levels (Zoefel et al., 2011), would be a promising tool to test in such patient populations. Thus, studies of somatosensory alpha activity in the context of different pain syndromes could potentially broaden our understanding of the involved neural mechanisms and possibly uncover new treatment options.

9 References

- Ahonen, A.I., Hämäläinen, M.S., Kajola, M.J., Knuutila, J.E.T., Laine, P.P., Lounasmaa, O.V., Parkkonen, L.T., Simola, J.T., Tesche, C.D., 1993. 122-channel squid instrument for investigating the magnetic signals from the human brain. *Physica Scripta T49A*, 198–205.
- Amodio, P., Orsato, R., Marchetti, P., Schiff, S., Poci, C., Angeli, P., Gatta, A., Sparacino, G., Toffolo, G.M., 2009. Electroencephalographic analysis for the assessment of hepatic encephalopathy: comparison of non-parametric and parametric spectral estimation techniques. *Neurophysiol Clin* 39 (2), 107–115.
- Amodio, P., Schiff, S., Del Piccolo, F., Mapelli, D., Gatta, A., Umiltà, C., 2005. Attention dysfunction in cirrhotic patients: an inquiry on the role of executive control, attention orienting and focusing. *Metab Brain Dis* 20 (2), 115–127.
- Amodio, P., Gatta, A., 2005. Neurophysiological investigation of hepatic encephalopathy. *Metab Brain Dis* 20 (4), 369–379.
- Amodio, P., Montagnese, S., Gatta, A., Morgan, M.Y., 2004. Characteristics of minimal hepatic encephalopathy. *Metab Brain Dis* 19 (3-4), 253–267.
- Anderson, K.L., Ding, M., 2011. Attentional modulation of the somatosensory mu rhythm. *Neuroscience* 180, 165–180.
- Babiloni, C., Del Percio, C., Brancucci, A., Capotosto, P., Le Pera, D., Marzano, N., Valeriani, M., Romani, G.L., Arendt-Nielsen, L., Rossini, P.M., 2008. Pre-stimulus alpha power affects vertex N2-P2 potentials evoked by noxious stimuli. *Brain Res Bull* 75 (5), 581–590.
- Babiloni, C., Brancucci, A., Del Percio, C., Capotosto, P., Arendt-Nielsen, L., Chen, A.C.N., Rossini, P.M., 2006. Anticipatory electroencephalography alpha rhythm predicts subjective perception of pain intensity. *J Pain* 7 (10), 709–717.
- Babiloni, C., Brancucci, A., Arendt-Nielsen, L., Babiloni, F., Capotosto, P., Carducci, F., Cincotti, F., Del Percio, C., Petrini, L., Rossini, P.M., Chen, A.C.N., 2004. Attentional processes and cognitive performance during expectancy of painful galvanic stimulations: a high-resolution EEG study. *Behav Brain Res* 152 (1), 137–147.

- Babiloni, C., Brancucci, A., Babiloni, F., Capotosto, P., Carducci, F., Cincotti, F., Arendt-Nielsen, L., Chen, A.C.N., Rossini, P.M., 2003. Anticipatory cortical responses during the expectancy of a predictable painful stimulation. A high-resolution electroencephalography study. *Eur J Neurosci* 18 (6), 1692–1700.
- Bajaj, J.S., Wade, J.B., Sanyal, A.J., 2009. Spectrum of neurocognitive impairment in cirrhosis: Implications for the assessment of hepatic encephalopathy. *Hepatology* 50 (6), 2014–2021.
- Bauer, M., Oostenveld, R., Peeters, M., Fries, P., 2006. Tactile spatial attention enhances gamma-band activity in somatosensory cortex and reduces low-frequency activity in parieto-occipital areas. *J Neurosci* 26 (2), 490–501.
- Berger, H., 1929. Über das Elektrenkephalogramm des Menschen. *Arch Psychiatr Nervenkr* 87, 527–570.
- Biecker, E., Hausdörfer, I., Grünhage, F., Strunk, H., Sauerbruch, T., 2011. Critical flicker frequency as a marker of hepatic encephalopathy in patients before and after transjugular intrahepatic portosystemic shunt. *Digestion* 83 (1-2), 24–31.
- Blauenfeldt, R.A., Olesen, S.S., Hansen, J.B., Graversen, C., Drewes, A.M., 2010. Abnormal brain processing in hepatic encephalopathy: evidence of cerebral reorganization? *Eur J Gastroenterol Hepatol* 22 (11), 1323–1330.
- Brenner, M., Butz, M., May, E.S., Kahlbrock, N., Kircheis, G., Häussinger, D., Schnitzler, A., 2010. Verminderte Wahrnehmung von Kälte und Temperaturänderungen bei Patienten mit Hepatischer Enzephalopathie. 83. Jahrestagung der Deutschen Gesellschaft für Neurologie, Mannheim, Germany.
- Busch, N.A., Dubois, J., VanRullen, R., 2009. The phase of ongoing EEG oscillations predicts visual perception. *J Neurosci* 29 (24), 7869–7876.
- Bushnell, M.C., Duncan, G.H., Hofbauer, R.K., Ha, B., Chen, J.I., Carrier, B., 1999. Pain perception: is there a role for primary somatosensory cortex? *Proc Natl Acad Sci U S A* 96 (14), 7705–7709.
- Butterworth, R.F., 2000. Complications of cirrhosis III. Hepatic encephalopathy. *J Hepatol* 32 (1 Suppl), 171–180.

- Butz, M., Timmermann, L., Braun, M., Groiss, S.J., Wojtecki, L., Ostrowski, S., Krause, H., Pollok, B., Gross, J., Südmeyer, M., Kircheis, G., Häussinger, D., Schnitzler, A., 2010. Motor impairment in liver cirrhosis without and with minimal hepatic encephalopathy. *Acta Neurol Scand* 122 (1), 27–35.
- Buzsáki, G., 2006. *Rhythms of the Brain*, 1st ed. Oxford University Press, New York, USA.
- Chatrian, G.E., Petersen, M.C., Lazarte, J.A., 1959. The blocking of the rolandic wicket rhythm and some central changes related to movement. *Electroencephalogr Clin Neurophysiol* 11 (3), 497–510.
- Chu, N.S., Yang, S.S., Liaw, Y.F., 1997. Evoked potentials in liver diseases. *J Gastroenterol Hepatol* 12 (9-10), S288–293.
- Chu, N.S., Yang, S.S., 1987. Somatosensory and brainstem auditory evoked potentials in alcoholic liver disease with and without encephalopathy. *Alcohol* 4 (4), 225–230.
- Crombez, G., Van Damme, S., Eccleston, C., 2005. Hypervigilance to pain: an experimental and clinical analysis. *Pain* 116 (1-2), 4–7.
- Davies, M.G., Rowan, M.J., Feely, J., 1991. EEG and event related potentials in hepatic encephalopathy. *Metab Brain Dis* 6 (4), 175–186.
- Della Penna, S., Torquati, K., Pizzella, V., Babiloni, C., Franciotti, R., Rossini, P.M., Romani, G.L., 2004. Temporal dynamics of alpha and beta rhythms in human SI and SII after galvanic median nerve stimulation. A MEG study. *NeuroImage* 22 (4), 1438–1446.
- van Dijk, H., Schoffelen, J.-M., Oostenveld, R., Jensen, O., 2008. Prestimulus oscillatory activity in the alpha band predicts visual discrimination ability. *J Neurosci* 28 (8), 1816–1823.
- Dugué, L., Marque, P., VanRullen, R., 2011. The phase of ongoing oscillations mediates the causal relation between brain excitation and visual perception. *J Neurosci* 31 (33), 11889–11893.
- Dustman, R.E., Shearer, D.E., Emmerson, R.Y., 1999. Life-span changes in EEG spectral amplitude, amplitude variability and mean frequency. *Clin Neurophysiol* 110 (8), 1399–1409.
- Eberhardt, G., 1994. *Flimmerfrequenz-Analysator. Automatische Messmethode. Version 3.00*. Dr. G. Schuhfried GmbH, Mödling, Austria.

- Ergenoglu, T., Demiralp, T., Bayraktaroglu, Z., Ergen, M., Beydagi, H., Uresin, Y., 2004. Alpha rhythm of the EEG modulates visual detection performance in humans. *Brain Res Cogn Brain Res* 20 (3), 376–383.
- Felipo, V., Ordoño, J.F., Urios, A., El Mili, N., Giménez-Garzó, C., Aguado, C., González-Lopez, O., Giner-Duran, R., Serra, M.A., Wassel, A., Rodrigo, J.M., Salazar, J., Montoliu, C., 2012. Patients with minimal hepatic encephalopathy show impaired mismatch negativity correlating with reduced performance in attention tests. *Hepatology* 55 (2), 530–539.
- Ferenci, P., Lockwood, A., Mullen, K., Tarter, R., Weissenborn, K., Blei, A.T., 2002. Hepatic encephalopathy--definition, nomenclature, diagnosis, and quantification: final report of the working party at the 11th World Congresses of Gastroenterology, Vienna, 1998. *Hepatology* 35 (3), 716–721.
- Foxe, J.J., Snyder, A.C., 2011. The role of alpha-band brain oscillations as a sensory suppression mechanism during selective attention. *Front Psychol* 2, 154.
- Fries, P., 2009. Neuronal gamma-band synchronization as a fundamental process in cortical computation. *Annu Rev Neurosci* 32, 209–224.
- Gastaut, H., 1952. Electrographic study of the reactivity of rolandic rhythm. *Rev Neurol (Paris)* 87 (2), 176–182.
- Gould, I.C., Rushworth, M.F., Nobre, A.C., 2011. Indexing the graded allocation of visuospatial attention using anticipatory alpha oscillations. *J Neurophysiol* 105 (3), 1318–1326.
- Groeneweg, M., Quero, J.C., De Bruijn, I., Hartmann, I.J., Essink-bot, M.L., Hop, W.C., Schalm, S.W., 1998. Subclinical hepatic encephalopathy impairs daily functioning. *Hepatology* 28 (1), 45–49.
- Gross, J., Schnitzler, A., Timmermann, L., Ploner, M., 2007. Gamma oscillations in human primary somatosensory cortex reflect pain perception. *PLoS Biol* 5 (5), e133.
- Haegens, S., Luther, L., Jensen, O., 2012. Somatosensory anticipatory alpha activity increases to suppress distracting input. *J Cogn Neurosci* 24 (3), 677–685.

- Haegens, S., Händel, B.F., Jensen, O., 2011. Top-down controlled alpha band activity in somatosensory areas determines behavioral performance in a discrimination task. *J Neurosci* 31 (14), 5197–5204.
- Haegens, S., Osipova, D., Oostenveld, R., Jensen, O., 2010. Somatosensory working memory performance in humans depends on both engagement and disengagement of regions in a distributed network. *Hum Brain Mapp* 31 (1), 26–35.
- Hämäläinen, M., Hari, R., Ilmoniemi, R.J., Knuutila, J., Lounasmaa, O.V., 1993. Magnetoencephalography—theory, instrumentation, and applications to noninvasive studies of the working human brain. *Rev Mod Phys* 65 (2), 413–497.
- Hammond, C., Bergman, H., Brown, P., 2007. Pathological synchronization in Parkinson's disease: networks, models and treatments. *Trends Neurosci* 30 (7), 357–364.
- Händel, B.F., Haarmeier, T., Jensen, O., 2011. Alpha oscillations correlate with the successful inhibition of unattended stimuli. *J Cogn Neurosci* 23 (9), 2494–2502.
- Hanslmayr, S., Aslan, A., Staudigl, T., Klimesch, W., Herrmann, C.S., Bäuml, K.-H., 2007. Prestimulus oscillations predict visual perception performance between and within subjects. *NeuroImage* 37 (4), 1465–1473.
- Hari, R., 2005. Magnetoencephalography in clinical neurophysiological assessment of human cortical functions, in: Niedermeyer, E., Lopes da Silva, F. (Eds.), *Electroencephalography - Basic principles, clinical applications and related fields*. Lippincott Williams & Wilkins, Philadelphia, USA, pp. 1165–97.
- Hartmann, I.J., Groeneweg, M., Quero, J.C., Beijeman, S.J., de Man, R.A., Hop, W.C., Schalm, S.W., 2000. The prognostic significance of subclinical hepatic encephalopathy. *Am J Gastroenterol* 95 (8), 2029–2034.
- Häussinger, D., Blei, A.T., 2007. Hepatic encephalopathy, in: Benhamou, J.-P., Rodes, J., Rizzetto, M. (Eds.), *The textbook of hepatology: From basic science to clinical practice*. Blackwell Publ, Oxford, UK, pp. 728–760.
- Häussinger, D., Córdoba, J., Kircheis, G., Vilstrup, H., Fleig, W.E., Jones, E.A., Schliess, F., Blei, A.T., 2006a. Definition and assessment of low-grade hepatic encephalopathy, in: Häussinger, D., Kircheis, G., Schliess, F. (Eds.), *Hepatic encephalopathy and nitrogen metabolism*, 1st ed. Springer, Dordrecht, The Netherlands, pp. 423–432.

- Häussinger, D., Kircheis, G., Schliess, F., 2006b. Hepatic encephalopathy and nitrogen metabolism, 1st ed. Springer, Dordrecht, The Netherlands.
- Häussinger, D., 2004. Hepatic encephalopathy: clinical aspects and pathogenesis. *Dtsch Med Wochenschr* 129 Suppl 2, S66–67.
- Jensen, O., Bonnefond, M., VanRullen, R., 2012. An oscillatory mechanism for prioritizing salient unattended stimuli. *Trends Cogn Sci* 16 (4), 200–206.
- Jensen, O., Mazaheri, A., 2010. Shaping functional architecture by oscillatory alpha activity: gating by inhibition. *Front Hum Neurosci* 4, 186.
- Jones, S.R., Kerr, C.E., Wan, Q., Pritchett, D.L., Hämäläinen, M., Moore, C.I., 2010. Cued spatial attention drives functionally relevant modulation of the mu rhythm in primary somatosensory cortex. *J Neurosci* 30 (41), 13760–13765.
- Kahlbrock, N., Butz, M., May, E.S., Brenner, M., Kircheis, G., Häussinger, D., Schnitzler, A., 2012a. Lowered frequency and impaired modulation of gamma band oscillations in a bimodal attention task are associated with reduced critical flicker frequency. *NeuroImage* 61 (1), 216–227.
- Kahlbrock, N., Butz, M., May, E.S., Schnitzler, A., 2012b. Sustained gamma band synchronization in early visual areas reflects the level of selective attention. *NeuroImage* 59 (1), 673–681.
- Kelly, S.P., Lalor, E.C., Reilly, R.B., Foxe, J.J., 2006. Increases in alpha oscillatory power reflect an active retinotopic mechanism for distracter suppression during sustained visuospatial attention. *J Neurophysiol* 95 (6), 3844–3851.
- Kircheis, G., Knoche, A., Hilger, N., Manhart, F., Schnitzler, A., Schulze, H., Häussinger, D., 2009. Hepatic encephalopathy and fitness to drive. *Gastroenterology* 137 (5), 1706–1715.e1–9.
- Kircheis, G., Fleig, W.E., Görtelmeyer, R., Grafe, S., Häussinger, D., 2007. Assessment of low-grade hepatic encephalopathy: a critical analysis. *J Hepatol* 47 (5), 642–650.
- Kircheis, G., Wettstein, M., Timmermann, L., Schnitzler, A., Häussinger, D., 2002. Critical flicker frequency for quantification of low-grade hepatic encephalopathy. *Hepatology* 35 (2), 357–366.

- Klimesch, W., Sauseng, P., Hanslmayr, S., 2007. EEG alpha oscillations: the inhibition-timing hypothesis. *Brain Res Rev* 53 (1), 63–88.
- Kono, I., Ueda, Y., Nakajima, K., Araki, K., Kagawa, K., Kashima, K., 1994. Subcortical impairment in subclinical hepatic encephalopathy. *J Neurol Sci* 126 (2), 162–167.
- Koshino, Y., Niedermeyer, E., 1975. Enhancement of Rolandic mu-rhythm by pattern vision. *Electroencephalogr Clin Neurophysiol* 38 (5), 535–538.
- Kullmann, F., Hollerbach, S., Lock, G., Holstege, A., Dierks, T., Schölmerich, J., 2001. Brain electrical activity mapping of EEG for the diagnosis of (sub)clinical hepatic encephalopathy in chronic liver disease. *Eur J Gastroenterol Hepatol* 13 (5), 513–522.
- Kullmann, F., Hollerbach, S., Holstege, A., Schölmerich, J., 1995. Subclinical hepatic encephalopathy: the diagnostic value of evoked potentials. *J Hepatol* 22 (1), 101–110.
- Lauridsen, M.M., Jepsen, P., Vilstrup, H., 2011. Critical flicker frequency and continuous reaction times for the diagnosis of minimal hepatic encephalopathy: a comparative study of 154 patients with liver disease. *Metab Brain Dis* 26 (2), 135–139.
- Legrain, V., Guérit, J.-M., Bruyer, R., Plaghki, L., 2002. Attentional modulation of the nociceptive processing into the human brain: selective spatial attention, probability of stimulus occurrence, and target detection effects on laser evoked potentials. *Pain* 99 (1-2), 21–39.
- Linkenkaer-Hansen, K., Nikulin, V.V., Palva, S., Ilmoniemi, R.J., Palva, J.M., 2004. Prestimulus oscillations enhance psychophysical performance in humans. *J Neurosci* 24 (45), 10186–10190.
- Mathewson, K.E., Lleras, A., Beck, D.M., Fabiani, M., Ro, T., Gratton, G., 2011. Pulsed out of awareness: EEG alpha oscillations represent a pulsed-inhibition of ongoing cortical processing. *Front Psychol* 2, 99.
- Mathewson, K.E., Gratton, G., Fabiani, M., Beck, D.M., Ro, T., 2009. To see or not to see: prestimulus alpha phase predicts visual awareness. *J Neurosci* 29 (9), 2725–2732.
- McCracken, L.M., 1997. “Attention” to pain in persons with chronic pain: A behavioral approach. *Behavior Therapy* 28 (2), 271–284.

- Meeuwissen, E.B., Takashima, A., Fernández, G., Jensen, O., 2011. Increase in posterior alpha activity during rehearsal predicts successful long-term memory formation of word sequences. *Hum Brain Mapp* 32 (12), 2045–2053.
- Meßlinger, K., 2010. Somatoviszzerale Sensibilität, in: Klinke, R., Pape, H.-C., Kurtz, A., Silbernegel, S. (Eds.), *Physiologie*. Georg Thieme Verlag KG, Stuttgart, Germany, pp. 643–673.
- Montagnese, S., Biancardi, A., Schiff, S., Carraro, P., Carlà, V., Mannaioni, G., Moroni, F., Tonno, N., Angeli, P., Gatta, A., Amodio, P., 2011. Different biochemical correlates for different neuropsychiatric abnormalities in patients with cirrhosis. *Hepatology* 53 (2), 558–566.
- Montagnese, S., Jackson, C., Morgan, M.Y., 2007. Spatio-temporal decomposition of the electroencephalogram in patients with cirrhosis. *J Hepatol* 46 (3), 447–458.
- Müller, H., Krummenacher, J., 2006. Funktionen und Modelle der selektiven Aufmerksamkeit, in: Karnath, H.-O., Thier, P. (Eds.), *Neuropsychologie*. Springer Medizin Verlag, Heidelberg, Germany, pp. 239–271.
- Müller, N., Weisz, N., 2012. Lateralized auditory cortical alpha band activity and interregional connectivity pattern reflect anticipation of target sounds. *Cereb Cortex* 22 (7), 1604–1613.
- Muthukumaraswamy, S.D., Singh, K.D., Swettenham, J.B., Jones, D.K., 2010. Visual gamma oscillations and evoked responses: variability, repeatability and structural MRI correlates. *NeuroImage* 49 (4), 3349–3357.
- Neuper, C., Pfurtscheller, G., 2001. Event-related dynamics of cortical rhythms: frequency-specific features and functional correlates. *Int J Psychophysiol* 43 (1), 41–58.
- Nikouline, V.V., Linkenkaer-Hansen, K., Wikström, H., Kesäniemi, M., Antonova, E.V., Ilmoniemi, R.J., Huttunen, J., 2000. Dynamics of mu-rhythm suppression caused by median nerve stimulation: a magnetoencephalographic study in human subjects. *Neurosci Lett* 294 (3), 163–166.
- Ohara, S., Crone, N.E., Weiss, N., Lenz, F.A., 2004. Attention to a painful cutaneous laser stimulus modulates electrocorticographic event-related desynchronization in humans. *Clin Neurophysiol* 115 (7), 1641–1652.

- Palva, S., Linkenkaer-Hansen, K., Näätänen, R., Palva, J.M., 2005. Early neural correlates of conscious somatosensory perception. *J Neurosci* 25 (21), 5248–5258.
- Pantiga, C., Rodrigo, L.R., Cuesta, M., Lopez, L., Arias, J.L., 2003. Cognitive deficits in patients with hepatic cirrhosis and in liver transplant recipients. *J Neuropsychiatry Clin Neurosci* 15 (1), 84–89.
- Del Percio, C., Le Pera, D., Arendt-Nielsen, L., Babiloni, C., Brancucci, A., Chen, A.C.N., De Armas, L., Miliucci, R., Restuccia, D., Valeriani, M., Rossini, P.M., 2006. Distraction affects frontal alpha rhythms related to expectancy of pain: an EEG study. *NeuroImage* 31 (3), 1268–1277.
- Pfurtscheller, G., Neuper, C., Andrew, C., Edlinger, G., 1997. Foot and hand area mu rhythms. *Int J Psychophysiol* 26 (1–3), 121–135.
- Pfurtscheller, G., Stancák, A., Jr, Neuper, C., 1996. Event-related synchronization (ERS) in the alpha band--an electrophysiological correlate of cortical idling: a review. *Int J Psychophysiol* 24 (1-2), 39–46.
- Pfurtscheller, G., Klimesch, W., 1992. Functional topography during a visuo-verbal judgment task studied with event-related desynchronization mapping. *J Clin Neurophysiol* 9 (1), 120–131.
- Ploner, M., Gross, J., Timmermann, L., Pollok, B., Schnitzler, A., 2006a. Oscillatory activity reflects the excitability of the human somatosensory system. *NeuroImage* 32 (3), 1231–1236.
- Ploner, M., Gross, J., Timmermann, L., Pollok, B., Schnitzler, A., 2006b. Pain suppresses spontaneous brain rhythms. *Cereb Cortex* 16 (4), 537–540.
- Ploner, M., Pollok, B., Schnitzler, A., 2004. Pain facilitates tactile processing in human somatosensory cortices. *J Neurophysiol* 92 (3), 1825–1829.
- Poordad, F.F., 2007. Review article: the burden of hepatic encephalopathy. *Aliment Pharmacol Ther* 25 Suppl 1, 3–9.
- Posner, M.I., 1980. Orienting of attention. *Q J Exp Psychol* 32 (1), 3–25.
- Prakash, R., Mullen, K.D., 2010. Mechanisms, diagnosis and management of hepatic encephalopathy. *Nat Rev Gastroenterol Hepatol* 7 (9), 515–525.

- van der Rijt, C.C., Schalm, S.W., 1992. Quantitative EEG analysis and evoked potentials to measure (latent) hepatic encephalopathy. *J Hepatol* 14 (2-3), 141–142.
- Rolke, R., Magerl, W., Campbell, K.A., Schalber, C., Caspari, S., Birklein, F., Treede, R.-D., 2006a. Quantitative sensory testing: a comprehensive protocol for clinical trials. *Eur J Pain* 10 (1), 77–88.
- Rolke, R., Baron, R., Maier, C., Tölle, T.R., Treede, R.-D., Beyer, A., Binder, A., Birbaumer, N., Birklein, F., Bötefür, I.C., Braune, S., Flor, H., Hüge, V., Klug, R., Landwehrmeyer, G.B., Magerl, W., Maihöfner, C., Rolko, C., Schaub, C., Scherens, A., Sprenger, T., Valet, M., Wasserka, B., 2006b. Quantitative sensory testing in the German Research Network on Neuropathic Pain (DFNS): standardized protocol and reference values. *Pain* 123 (3), 231–243.
- Romei, V., Thut, G., Mok, R.M., Schyns, P.G., Driver, J., 2012. Causal implication by rhythmic transcranial magnetic stimulation of alpha frequency in feature-based local vs. global attention. *Eur J Neurosci* 35 (6), 968–974.
- Romei, V., Gross, J., Thut, G., 2010. On the Role of Prestimulus Alpha Rhythms over Occipito-Parietal Areas in Visual Input Regulation: Correlation or Causation? *J Neurosci* 30 (25), 8692–8697.
- Romei, V., Brodbeck, V., Michel, C., Amedi, A., Pascual-Leone, A., Thut, G., 2008. Spontaneous fluctuations in posterior alpha-band EEG activity reflect variability in excitability of human visual areas. *Cereb Cortex* 18 (9), 2010–2018.
- Romero-Gómez, M., Córdoba, J., Jover, R., del Olmo, J.A., Ramírez, M., Rey, R., de Madaria, E., Montoliu, C., Nuñez, D., Flavia, M., Compañy, L., Rodrigo, J.M., Felipo, V., 2007. Value of the critical flicker frequency in patients with minimal hepatic encephalopathy. *Hepatology* 45 (4), 879–885.
- Romero-Gómez, M., Boza, F., García-Valdecasas, M.S., García, E., Aguilar-Reina, J., 2001. Subclinical hepatic encephalopathy predicts the development of overt hepatic encephalopathy. *Am J Gastroenterol* 96 (9), 2718–2723.
- Salenius, S., Schnitzler, A., Salmelin, R., Jousmäki, V., Hari, R., 1997. Modulation of human cortical rolandic rhythms during natural sensorimotor tasks. *NeuroImage* 5 (3), 221–228.

- Sauseng, P., Klimesch, W., Gerloff, C., Hummel, F.C., 2009. Spontaneous locally restricted EEG alpha activity determines cortical excitability in the motor cortex. *Neuropsychologia* 47 (1), 284–288.
- Sauseng, P., Klimesch, W., Stadler, W., Schabus, M., Doppelmayr, M., Hanslmayr, S., Gruber, W.R., Birbaumer, N., 2005. A shift of visual spatial attention is selectively associated with human EEG alpha activity. *Eur J Neurosci* 22 (11), 2917–2926.
- Schnitzler, A., Gross, J., 2005. Normal and pathological oscillatory communication in the brain. *Nat Rev Neurosci* 6 (4), 285–296.
- Schnitzler, A., Gross, J., Timmermann, L., 2000. Synchronised oscillations of the human sensorimotor cortex. *Acta Neurobiol Exp (Wars)* 60 (2), 271–287.
- Schnitzler, A., Ploner, M., 2000. Neurophysiology and functional neuroanatomy of pain perception. *J Clin Neurophysiol* 17 (6), 592–603.
- Schubert, R., Haufe, S., Blankenburg, F., Villringer, A., Curio, G., 2009. Now you'll feel it, now you won't: EEG rhythms predict the effectiveness of perceptual masking. *J Cogn Neurosci* 21 (12), 2407–2419.
- Schulz, E., Tiemann, L., Schuster, T., Gross, J., Ploner, M., 2011. Neurophysiological coding of traits and states in the perception of pain. *Cereb Cortex* 21 (10), 2408–2414.
- Sharma, P., Sharma, B.C., Puri, V., Sarin, S.K., 2007. Critical flicker frequency: diagnostic tool for minimal hepatic encephalopathy. *J Hepatol* 47 (1), 67–73.
- Stoffers, D., Bosboom, J.L.W., Deijen, J.B., Wolters, E.C., Berendse, H.W., Stam, C.J., 2007. Slowing of oscillatory brain activity is a stable characteristic of Parkinson's disease without dementia. *Brain* 130 (7), 1847–1860.
- Thorpe, S., D'Zmura, M., Srinivasan, R., 2012. Lateralization of frequency-specific networks for covert spatial attention to auditory stimuli. *Brain Topogr* 25 (1), 39–54.
- Thut, G., Veniero, D., Romei, V., Miniussi, C., Schyns, P., Gross, J., 2011. Rhythmic TMS Causes Local Entrainment of Natural Oscillatory Signatures. *Curr Biol* 21 (14), 1176–1185.
- Thut, G., Nietzel, A., Brandt, S.A., Pascual-Leone, A., 2006. Alpha-band electroencephalographic activity over occipital cortex indexes visuospatial attention bias and predicts visual target detection. *J Neurosci* 26 (37), 9494–9502.

- Timmermann, L., Butz, M., Gross, J., Ploner, M., Südmeyer, M., Kircheis, G., Häussinger, D., Schnitzler, A., 2008. Impaired cerebral oscillatory processing in hepatic encephalopathy. *Clin Neurophysiol* 119 (2), 265–272.
- Timmermann, L., Butz, M., Gross, J., Kircheis, G., Häussinger, D., Schnitzler, A., 2005. Neural synchronization in hepatic encephalopathy. *Metab Brain Dis* 20 (4), 337–346.
- Timmermann, L., Gross, J., Butz, M., Kircheis, G., Häussinger, D., Schnitzler, A., 2003. Mini-asterixis in hepatic encephalopathy induced by pathologic thalamo-motor-cortical coupling. *Neurology* 61 (5), 689–692.
- Timmermann, L., Gross, J., Kircheis, G., Häussinger, D., Schnitzler, A., 2002. Cortical origin of mini-asterixis in hepatic encephalopathy. *Neurology* 58 (2), 295–298.
- Treede, R.-D., 2007. Das somatosensorische System, in: Schmidt, R., Lang, F. (Eds.), *Physiologie des Menschen*. Springer, Berlin Heidelberg New York Tokio, pp. 295–323.
- Treede, R.-D., 2003. Neurophysiological studies of pain pathways in peripheral and central nervous system disorders. *J Neurol* 250 (10), 1152–1161.
- Vienna test system, WINWTS, Version 4.50, 1999. Dr. G. Schuhfried GmbH, Mödling, Austria.
- Wein, C., Koch, H., Popp, B., Oehler, G., Schauder, P., 2004. Minimal hepatic encephalopathy impairs fitness to drive. *Hepatology* 39 (3), 739–745.
- Weissenborn, K., Giewekemeyer, K., Heidenreich, S., Bokemeyer, M., Berding, G., Ahl, B., 2005. Attention, memory, and cognitive function in hepatic encephalopathy. *Metab Brain Dis* 20 (4), 359–367.
- Weissenborn, K., Heidenreich, S., Ennen, J., Rückert, N., Hecker, H., 2001. Attention deficits in minimal hepatic encephalopathy. *Metab Brain Dis* 16 (1-2), 13–19.
- Wettstein, M., Kircheis, G., Häussinger, D., 2003. Hepatic encephalopathy--diagnostics. *Dtsch Med Wochenschr* 128 (50), 2654–2657.
- Worden, M.S., Foxe, J.J., Wang, N., Simpson, G.V., 2000. Anticipatory biasing of visuospatial attention indexed by retinotopically specific alpha-band electroencephalography increases over occipital cortex. *J Neurosci* 20 (6), RC63.

- Yang, S.S., Wu, C.H., Chiang, T.R., Chen, D.S., 1998. Somatosensory evoked potentials in subclinical portosystemic encephalopathy: a comparison with psychometric tests. *Hepatology* 27 (2), 357–361.
- Yang, S.S., Chu, N.H., Wu, C.H., 1993. Subcortical somatosensory evoked potentials in patients with hepatic encephalopathy caused by severe acute hepatitis. *J Gastroenterol Hepatol* 8 (6), 545–549.
- Yang, S.S., Chu, N.S., Liaw, Y.F., 1985. Somatosensory evoked potentials in hepatic encephalopathy. *Gastroenterology* 89 (3), 625–630.
- Zhang, Y., Ding, M., 2010. Detection of a weak somatosensory stimulus: role of the pres-timulus mu rhythm and its top-down modulation. *J Cogn Neurosci* 22 (2), 307–322.
- Zoefel, B., Huster, R.J., Herrmann, C.S., 2011. Neurofeedback training of the upper alpha frequency band in EEG improves cognitive performance. *NeuroImage* 54 (2), 1427–1431.

10 Erklärung

Hiermit erkläre ich, dass ich die vorgelegte Dissertation eigenständig und ohne unerlaubte Hilfe angefertigt habe. Die Dissertation wurde in der vorliegenden oder in ähnlicher Form noch bei keiner anderen Institution eingereicht. Ich habe bisher keine erfolglosen Promotionsversuche unternommen.

Düsseldorf, den 04.09.2012

Elisabeth May

11 Danksagung

An dieser Stelle möchte ich mich ganz herzlich bei all denen bedanken, die mich während der Zeit meiner Promotion begleitet haben und ohne die das Entstehen dieser Arbeit nicht möglich gewesen wäre.

Zunächst möchte ich mich bei meinem Doktorvater Prof. Dr. Alfons Schnitzler bedanken. Alfons, vielen Dank für die Möglichkeit, meine Arbeit an deinem Institut durchzuführen, meine ersten wissenschaftlichen Schritte unter deiner Anleitung zu gehen und dabei von deiner fundierten wissenschaftlichen Erfahrung zu profitieren. Danke für viele fachliche Diskussionen, wichtige Anregungen und stetige Unterstützung.

Prof. Dr. Martin Heil danke ich für die Übernahme des Zweitgutachtens, wertvolle fachliche Diskussionen und Ratschläge.

Mein ganz besonderer Dank gilt Dr. Markus Butz. Markus, vielen Dank für deine immerwährende und tatkräftige Unterstützung, deinen unerschütterlichen Optimismus, deinen Glauben an mich und die viele Zeit, die du dir immer und oft auch kurzfristig für mich genommen hast, auch wenn du in London schon längst neue Aufgaben hattest. Ich habe sehr viel von dir gelernt und danke dir dafür.

Vielen Dank an meine Doppelkopfmädels Dr. Nina Kahlbrock, Meike Brenner und Dr. Jennifer Finis. Ihr habt die Zeit meiner Doktorarbeit sehr bereichert. Auch euch danke ich für die Unterstützung bei allen Belangen der Doktorarbeit, aber auch für viele schöne Abende mit und ohne Doppelkopf und immer offene Ohren.

Auch meinen restlichen Kollegen und Kolleginnen danke ich ganz herzlich für fachlichen Austausch, Inspiration, das gute Arbeitsklima und das ein oder andere Matlab-Skript. Allen voran gilt mein Dank Dr. Nienke Hoogenboom, Dr. Holger Krause, Dr. Joachim Lange, Jan Hirschmann, Dr. Hanneke von Dijk und Dr. Tolga Özkurt.

Weiterer Dank gilt meinen Kollegen aus der Gastroenterologie für die gute Zusammenarbeit. Besonders zu erwähnen sind hier Diethelm Plate und Dr. Gerald Kircheis, die eine überaus große Hilfe in allen Patientenangelegenheiten waren und maßgeblich zum Gelingen dieser Arbeit beigetragen haben.

Ein herzliches Dankeschön möchte ich weiterhin allen Probandinnen und Probanden aussprechen, die viel Zeit, Mühe und Geduld aufgebracht haben und diese Doktorarbeit durch ihre Teilnahme an meinen Experimenten erst möglich gemacht haben.

Danksagung

Mein großer Dank gilt auch meiner Familie, die mich in all den Jahren immer unterstützt hat. Ich bin froh, dass ich euch alle habe! Heiner, dir danke ich für das kurzfristige Korrekturlesen meiner Doktorarbeit und deine hilfreichen Anregungen.

Am allermeisten möchte ich dir danken, Daniel. Du hast dich nicht nur für mich in das Thema meiner Arbeit eingedacht, mir bei meinen ersten Programmierversuchen geholfen und vieles Korrektur gelesen, sondern bist seit vielen Jahren immer für mich da und unterstützt mich bedingungslos. Danke für viele tausende Kilometer, die du für mich quer durch Deutschland gereist bist. Ich freue mich auf unsere gemeinsame Zukunft!

12 Appendix

This work is based on:

Publication 1 (Appendix 1):

May, E.S., Butz, M., Kahlbrock, N., Hoogenboom, N., Brenner, M. & Schnitzler, A. (2012). Pre- and post-stimulus alpha activity shows differential modulation with spatial attention during the processing of pain. *NeuroImage*, 62 (1), 1965-1974.

Impact factor (2011): 5.895

Personal contribution: 80%

Publication 2 (Appendix 2):

May, E.S., Butz, M., Kahlbrock, N., Hoogenboom, N., Brenner, M., Kircheis, G., Häussinger, D. & Schnitzler, A. (submitted). Hepatic encephalopathy slows and delays stimulus-associated somatosensory alpha activity.

Personal contribution: 80%

Other aspects are taken from:

Publication 3 (Appendix 3 + 4):

Kahlbrock, N., Butz, M., May, E.S. & Schnitzler, A. (2012). Sustained gamma band synchronization in early visual areas reflects the level of selective attention. *NeuroImage*, 59 (1), 673-681.

Impact factor (2011): 5.895

Kahlbrock, N., Butz, M., May, E.S. & Schnitzler, A. (2012). Gammaband-Oszillationen hängen mit dem Grad selektiv visueller Aufmerksamkeit zusammen. *Klinische Neurophysiologie*, online publication, DOI: [dx.doi.org/10.1055/s-0032-1312628](https://doi.org/10.1055/s-0032-1312628).

Impact factor (2011): 0.140

Personal contribution: 20%

Publication 4 (Appendix 5):

Kahlbrock, N., Butz, M., May, E.S., Brenner, M., Kircheis, G., Häussinger, D. & Schnitzler, A. (2012). Lowered frequency and impaired modulation of gamma band oscillations in a bimodal attention task are associated with reduced critical flicker frequency. *NeuroImage*, 61(1), 216-227.

Impact factor (2011): 5.895

Personal contribution: 20%



Pre- and post-stimulus alpha activity shows differential modulation with spatial attention during the processing of pain

Elisabeth S. May^{a,1}, Markus Butz^{a,b,*}, Nina Kahlbrock^a, Nienke Hoogenboom^a,
Meike Brenner^a, Alfons Schnitzler^a

^a Heinrich-Heine-University Düsseldorf, Medical Faculty, Institute of Clinical Neuroscience and Medical Psychology, Universitätsstrasse 1, D-40225 Düsseldorf, Germany

^b Sobell Department of Motor Neuroscience and Movement Disorders, UCL Institute of Neurology, Queen Square, London, WC1N 3BG, United Kingdom

ARTICLE INFO

Article history:

Accepted 27 May 2012

Available online 1 June 2012

Keywords:

MEG
Oscillations
Lateralization
Gating
Inhibition
Top-down

ABSTRACT

Extensive work using magneto- and electroencephalography (M/EEG) suggests that cortical alpha activity represents a top-down controlled gating mechanism employed by processes like attention across different modalities. However, it is not yet clear to what extent this presumed gating function of alpha activity also applies to the processing of pain.

In the current study, a spatial attention paradigm was employed requiring subjects to attend to painful laser stimuli on one hand while ignoring stimuli on the other hand. Simultaneously, brain activity was recorded with MEG. In order to disentangle pre- and post-stimulus effects of attention, alpha activity was analyzed during time windows in anticipation of and in response to painful laser stimulation.

Painful laser stimuli led to a suppression of alpha activity over both ipsi- and contralateral primary somatosensory areas irrespective if they were attended or ignored. Spatial attention was associated with a lateralization of anticipatory pre-stimulus alpha activity. Alpha activity was lower over primary somatosensory areas when the contralateral hand was attended compared to when the ipsilateral hand was attended, in line with the notion that oscillatory alpha activity regulates the flow of incoming information by engaging and/or disengaging early sensory areas. On the contrary, post-stimulus alpha activity, for stimuli on either hand, was consistently decreased with attention over contralateral areas. Most likely, this finding reflects an increased cortical activation and enhanced alerting if a painful stimulus is attended.

The present results show that spatial attention results in a modulation of both pre- and post-stimulus alpha activity associated with pain. This flexible regulation of alpha activity matches findings from other modalities. We conclude that the assumed functional role of alpha activity as a top-down controlled gating mechanism includes pain processing and most likely represents a unified mechanism used throughout the brain.

© 2012 Elsevier Inc. All rights reserved.

Introduction

Rhythmic neuronal alpha oscillations between 8 and 12 Hz are the strongest electrophysiological signal measured from the awake human brain (Berger, 1929; Niedermeyer and Lopes da Silva, 2005). For a long time, alpha activity was thought to merely reflect “cortical idling” (Pfurtscheller et al., 1996). Recently, alpha activity has been assumed to have a more active role in terms of a graded functional inhibition of brain areas not directly involved in a specific task (Jensen and Mazaheri, 2010). In this context, alpha activity has been closely related to selective attention and is understood to actively gate the incoming flow of information (Foxe and Snyder, 2011), enabling us to favor and more efficiently process those of the many incoming stimuli in our

environment that are behaviorally relevant. Across different modalities, attention affects oscillatory alpha activity already during anticipatory pre-stimulus periods, i.e. when a stimulus is expected but not yet actually received and processed (Del Percio et al., 2006; Jones et al., 2010; Thorpe et al., 2012; Thut et al., 2006). In the somatosensory system, for example, spatial attention to one hand lateralizes alpha activity in anticipation of a tactile stimulus. Specifically, alpha activity is decreased in the primary somatosensory cortex contralateral to the attended hand, but increased ipsilaterally (Anderson and Ding, 2011; Haegens et al., 2011). Moreover, it has been shown that the degree of pre-stimulus alpha lateralization determines the subsequent behavioral response (Haegens et al., 2011). These findings tally the notion that an increase of alpha activity reflects an active inhibition or disengagement of a cortical area (Foxe and Snyder, 2011; Jensen and Mazaheri, 2010) whereas a decrease of alpha activity is a correlate of an activated or engaged cortical region (Pfurtscheller et al., 1996).

Painful stimuli have been demonstrated to affect oscillatory activity across a range of frequency bands (Hauck et al., 2007, 2008; Schulz et

* Corresponding author at: Sobell Department of Motor Neuroscience and Movement Disorders, UCL Institute of Neurology, Queen Square, London, WC1N 3BG, United Kingdom.

E-mail address: m.butz@ucl.ac.uk (M. Butz).

¹ These two authors contributed equally to this work.

al., 2012). With respect to lower frequencies, previous work showed that painful laser stimuli, in contrast to stimuli of other modalities (Hari and Salmelin, 1997), globally suppress spontaneous alpha and beta oscillations in somatosensory, motor and visual areas (Ploner et al., 2006a). This finding has been interpreted as a specific alerting function of pain, which is also reflected by an increased excitability of somatosensory cortices to subsequent tactile stimuli (Ploner et al., 2006b). Interestingly, seeing an image of a limb in a painful situation also induces stronger alpha suppression in sensorimotor areas than seeing an image of a non-painful situation (Whitmarsh et al., 2011). Together, these results suggest that the processing of pain and pain-associated stimuli in somatosensory cortices is particularly intense and associated with a strong modulation of oscillatory activity.

The relationship between pain-associated oscillatory alpha activity and attention is not yet fully understood. In a study using subdural electrocorticographic recordings (ECoG) from epilepsy patients, Ohara et al. (2004) found that alpha suppression in response to an attended compared to a non-attended painful laser stimulus is more intense and widespread over primary somatosensory and parasyllian cortices. In contrast, using an oddball paradigm and painful intracutaneous electrical stimulation in healthy subjects, Hauck et al. (2007) did not observe any modulation of pain-associated alpha activity with attention. Both studies, however, did not investigate possible pre-stimulus effects of attention. Previous work addressing pre-stimulus effects showed that anticipation of a painful stimulus already results in a suppression of alpha activity (Babiloni et al., 2003, 2004, 2006; Del Percio et al., 2006). This anticipatory suppression is again stronger for a painful compared to a non-painful stimulus (Babiloni et al., 2003) and less prominent, if the subject is distracted by mentally performing an arithmetical task (Del Percio et al., 2006).

Linking the attentional modulation of pain processing to behavior, previous studies have consistently shown that a stimulus is perceived as less painful if attention is directed away from it (Bushnell et al., 1999; Miron et al., 1989; Petrovic et al., 2000; Schlereth et al., 2003). Yet, even under constant experimental conditions, the pain experience varies substantially both across and within subjects (Babiloni et al., 2006; Gross et al., 2007; Schulz et al., 2011, 2012). These variations covary with alpha activity. For example, the strength of anticipatory pre-stimulus alpha suppression in expectation of a painful stimulus correlates with the intensity of the individual pain perception across subjects (Babiloni et al., 2006). Within subjects, pain ratings across different trials with stimuli of constant intensity vary in close relation to the post-stimulus pain-induced alpha suppression (Schulz et al., 2011). Therefore, the pain sensation seems to be related to the current state of alpha activity. More specifically, pain appears to be perceived more intensely, if alpha activity close to the moment of stimulus onset is low.

The current study intended to shed further light on the role of alpha activity in relation to pain processing. Previous studies indicate both a modulation of pain-related alpha activity by attention and an association between alpha activity and the subjective pain experience. However, concurrent effects of attention on both pre- and post-stimulus pain-associated alpha activity have not yet been addressed. We aimed to test the hypothesis that alpha activity has a similar function for pain processing as for other modalities, representing a gating mechanism employed by top-down processes to streamline information flow in the brain. To this end, we used a spatial attention paradigm requiring subjects to attend to painful laser stimuli on the dorsum of one hand, while at the same time ignoring stimuli on the other hand. Simultaneously, brain activity was recorded using magnetoencephalography (MEG). To disentangle pre- and post-stimulus attention effects, we analyzed alpha activity both in anticipation of and in response to painful laser stimuli. For the anticipatory pre-stimulus period, spatial attention was hypothesized to lateralize alpha activity across left and right somatosensory cortices. In line with an active regulation of the incoming information flow, alpha activity was expected to be lower in primary somatosensory areas when

the contralateral hand was attended compared to when the ipsilateral hand was attended. For the post-stimulus period, attention was assumed to decrease alpha activity primarily over contralateral somatosensory areas, in accordance with an increased cortical activation. Lastly, we expected attention-related alpha activity to be predictive of the individual pain perception.

Materials and methods

Subjects

Fifteen healthy subjects (7 female, 14 right-handed, mean age \pm standard deviation: 48.33 ± 17.67 years, range: 24–74 years) participated in the study after giving written informed consent. The study was approved by the local ethics committee (study no. 2895) and conducted in conformity with the Declaration of Helsinki.

Experimental paradigm

Subjects performed a spatial attention paradigm as depicted in Fig. 1. Before the experiment, two adjacent rectangles were marked as target areas on the dorsum of each hand within the area innervated by the radial nerve. Each rectangle had a size of $1.5 \text{ cm} \times 4 \text{ cm}$. Both rectangles adjoined along the longer flank with the border between the two following the prolonged course of the index finger. During the experiment, painful laser stimuli of constant intensity were applied to the 4 target areas. In a block design, subjects were instructed to either attend to stimuli on the left hand and rate their localization and intensity while ignoring stimuli on the right hand (left hand attended) or vice versa (right hand attended).

Each trial began with the onset of a visual fixation cross, on which participants were instructed to remain fixated. After a random time interval between 2 and 6 s, a painful laser stimulus was applied to the left or right hand to one of the two designated target areas. In trials where the painful laser stimulus was delivered to the attended hand, a question mark replaced the fixation cross 5 s after the stimulus for 10 s. This cued the subject to verbally rate the last stimulus regarding location on the attended hand (left or right target area) and intensity (from 0 = “not painful” to 10 = “worst imaginable pain”). After the screen turned black for 1 s, the next trial began. In trials where the stimulus was applied to the unattended hand, a black screen appeared instead of the question mark lasting 11 s until the next trial. In these trials, the subject was not asked to give any response to ensure that maximal attention remained on the attended hand. Altogether, interstimulus intervals between two subsequent laser stimuli randomly varied between 18 and 22 s.

Each block (left hand attended or right hand attended) consisted of 40 trials. The combination of the two factors *stimulated hand* (left or right) and *attended hand* (left or right) resulted in four conditions: (i) left hand stimulated and attended; (ii) left hand stimulated, but unattended; (iii) right hand stimulated and attended; and (iv) right hand stimulated, but unattended. In each block, both the respective attended and unattended condition contained 20 trials of which 10 were applied to the left and 10 to the right target area. Within each block, the order of stimulation was randomized. Thus, the probability of a stimulus to occur on a given hand in any given trial was 50%. Each block lasted for about 14 min with a few minutes break in between. The order of blocks was counterbalanced.

The first nine subjects performed one run of each block type (left hand attended/right hand attended) resulting in a total number of 20 trials of each of the four conditions. Six additional subjects underwent a second run of each block type, increasing the total number of trials to 40 trials per condition. The number of trials was aimed to be kept minimal to reduce the risk of potential skin damage associated with laser stimulation at painful intensities, but high enough to obtain a good signal-to-noise ratio.

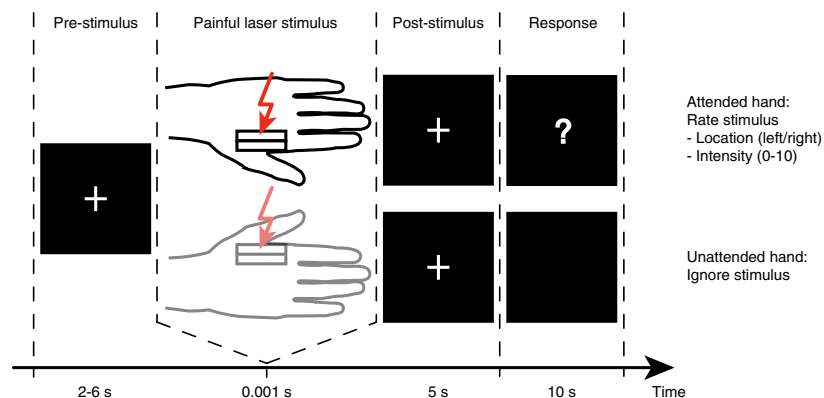


Fig. 1. Experimental paradigm. Subjects performed a spatial attention paradigm where painful laser stimuli were randomly applied to their left or right hand. In a block design, subjects attended to stimuli on the left hand while ignoring stimuli on the right hand or vice versa (left hand attended block shown). Each trial began with the onset of a visual fixation cross. After a random period between 2 and 6 s, a painful laser stimulus was applied to one of the two hands. If the stimulus was delivered to the attended hand, subjects were visually cued by a question mark to rate the stimulus with respect to its location and intensity 5 s after the laser stimulus. The question mark remained on for 10 s followed by 1 s of black screen after which the next trial started (not shown in figure for simplicity). If the stimulus was delivered to the unattended hand, a black screen appeared instead of the question mark and subjects were not asked to give any response but to ignore the stimulus. This black screen was displayed for a total of 11 s after which the next trial began (again, last second not shown in figure for simplicity). The design resulted in four types of trials: (i) left hand stimulated and attended; (ii) left hand stimulated, but unattended; (iii) right hand stimulated and attended; and (iv) right hand stimulated, but unattended.

Stimuli and experimental setup

The administered painful stimuli were cutaneous laser stimuli that selectively activate nociceptive afferents without concomitant activation of tactile afferents (Treede, 2003). Two Tm:YAG-laser devices (Themis, Starmedtec, Starnberg, Germany) with a wavelength of 1960 nm, a pulse duration of 1 ms and a spot diameter of approximately 5 mm were used. Stimulus energy was kept constant at 540 mJ, which evoked slightly to moderately painful, pinprick-like sensations.

Two assistants sat to the left and right of the subject during recordings. Before the experiment, all assistants involved in the data acquisition received detailed instructions on how to perform the stimulation to standardize stimulus application across hands and subjects. Throughout the experiment, each assistant held one laser handle constantly above the subject's left or right hand, respectively, while the actual laser devices were placed outside the MEG room. The assistants were instructed about the target area for the next trial via earphones. Within the marked target areas, stimulation sites were slightly changed after each stimulus. To avoid differences in the exact energy output between the two laser devices leading to unequal stimulation intensities between the hands, assistants exchanged laser handles between subject's left and right hand after half of each block. This ensured that the average stimulation intensity was similar across hands and attentional conditions. For the six subjects who received one additional experimental run of both left and right hand attended blocks, assistants relocated to the other side of the subject after two blocks and performed the stimulation of the other hand for the rest of the experiment.

To prevent subjects from looking at their hands and using visual information rather than the actual somatosensory perception to solve the localization task on the attended hand, their hands were taken as far out of the visual field as possible. Two laser devices were used, of which the two assistants kept the handles constantly above the subject's hands, so that only minimal movements were necessary to target the requested location on each hand. These movements were not detectable by the subject without directly looking at the laser handles. Subjects were instructed to keep central fixation throughout the experiment, which was controlled by the recording of horizontal electrooculograms. Since the probability to receive a stimulus to either hand was 50%, participants could not predict the upcoming hand of stimulation.

Verbal responses of the subjects (left or right target area and pain rating) were collected by the experimenter outside the shielded room, recoded into trigger values and recorded simultaneously with the MEG data. The paradigm was implemented using Presentation (version 13.1, Neurobehavioral Systems, Albany, NY, USA).

MEG recording

Neuromagnetic activity was continuously measured within a magnetically and acoustically shielded room with a 306-channel whole head MEG system (Elekta Oy, Helsinki, Finland) comprising 102 sensor triplets consisting of one magnetometer and two orthogonal planar gradiometers each. Bipolar vertical and horizontal electrooculograms were recorded to later identify epochs containing eye blinks and movements. All data were band-pass filtered by an online filter (0.03 to 330 Hz), digitized at 1000 Hz and stored for offline analysis.

Analysis of behavioral data

Behavioral data were analyzed by means of percentage of correct responses in the localization task and trial-by-trial pain ratings using IBM SPSS Statistics 19 (IBM Corporation, Somers, USA). Results are reported as mean \pm standard deviation. Dependent sample *t*-tests were used to compare both the percentage of correct responses and the average pain ratings between the left and right hand.

MEG data analysis

MEG data were analyzed using Matlab 7.1 (Mathworks, Natick, MA, USA) and FieldTrip, an open-source Matlab toolbox (Oostenveld et al., 2011). Unless otherwise stated, all trials of the different conditions were analyzed. Statistical tests were one-tailed.

Preprocessing

MEG data were divided into epochs of interest, starting 2 s before and ending 4 s after the laser stimulus in each trial. Only data recorded by the 204 planar gradiometers were analyzed. For each epoch, power line noise was removed by estimating and subtracting the 50, 100 and 150 Hz components in the MEG data, using a discrete Fourier transform. After visual inspection, epochs and sensors with high variance (containing,

e.g., muscle artifacts or MEG sensor jumps) were removed from the data. This resulted in an average of 19.08 trials \pm 0.83 standard deviation (range: 17 to 20 trials) across subjects and conditions for those subjects who completed 20 trials per condition and 38.83 trials \pm 1.04 standard deviation (range: 37 to 40 trials) for those who completed 40 trials per condition. Data from all measurement blocks of each subject were then combined. Independent component analysis (ICA) (Jung et al., 2000) was used to identify eye and heart artifacts. The ICA components were visually inspected and those representing eye and heart artifacts were projected out of the data.

Time–frequency analysis

Time–frequency representations (TFRs) of power were estimated using the fast Fourier transform (FFT) for each trial and all channels. An adaptive time window of 7 cycles length was shifted in 50 ms time-steps between -2 and 4 s. After applying a Hanning taper, power was estimated for frequencies between 2 and 30 Hz in steps of 1 Hz. In this type of frequency analysis, alpha power estimates are calculated on the basis of several hundred milliseconds and overlap. This approach allows illustrating and examining the temporal evolution of alpha activity in the different conditions across the complete trial. Since the planar gradiometers of each sensor triplet consist of a horizontal and vertical component, time–frequency analyses were performed separately on each component and afterwards summed to obtain one combined value.

Channel selection

For a selection of channels for further analysis, the obtained TFRs were averaged across subjects and power changes relative to a pre-stimulus baseline interval were computed (percent change relative to a baseline of -1 to 0 s). This was done separately for trials with stimulation of the left and right hand while averaging across attended and unattended trials of each hand. Similar to previous studies investigating the effects of spatial attention on somatosensory alpha activity associated with non-painful tactile stimuli (Haegens et al., 2011; van Ede et al., 2011), channels of interest for the examination of attention effects were chosen according to the strongest stimulus-induced response. Two groups of four adjacent combined sensors, each overlying left and right primary somatosensory areas, were selected according to the strongest post-stimulus alpha and beta suppression to a stimulus on the contralateral hand. For the sake of clarity, these two regions of interest will in the following be termed left and right primary somatosensory (S1) channels with respect to the hemisphere or ipsi- and contralateral S1 channels with respect to the stimulated hand (see highlighted sensors in Fig. 2A). The two groups of channels were symmetrically distributed with respect to the midline of the sensor array.

Individually adjusted alpha activity

For the analysis of pain-associated alpha activity, alpha band power was individually estimated for each subject by averaging power from TFRs across a 4 Hz frequency band comprising each subject's alpha peak frequency \pm 2 Hz. To determine the individual peak frequency, segments of data from -1 to 0 s with respect to stimulus onset were extracted and multiplied with a Hanning taper prior to applying an FFT. Power spectra were computed between 2 and 30 Hz, combined for horizontal and vertical gradiometers and averaged across all trials and sensors. Then, the individual peak frequency between 7 and 15 Hz was determined for each subject.

Statistical analysis of attention effects

To analyze attention effects on pain-associated alpha activity, we performed analyses as follows. For each region of interest (left and right S1 channels), individual alpha activity was averaged separately for the 4 conditions (attended left hand stimulation, unattended left hand stimulation, attended right hand stimulation, unattended right hand stimulation). For both attended conditions, only trials in which stimuli were correctly localized were used. To disentangle attention

effects in anticipation and in response to painful laser stimuli, the analysis focused on selected pre- (-1 to 0 s) and post-stimulus (0 to 2 s) time windows. The pre-stimulus interval was chosen regarding earlier findings showing that anticipatory attention effects are deployed with temporal specificity and are strongest just before an expected event (Rohenkohl and Nobre, 2011; van Ede et al., 2011). Therefore, in the current experiment, attention effects were expected to build up over the course of the anticipation period and be strongest immediately before each laser pulse. The post-stimulus interval was selected in accordance with earlier work demonstrating that the alpha suppression induced by painful laser stimuli is strongest within this time window (Ploner et al., 2006a).

Each statistical, time-resolved comparison between attended and unattended trials was performed in line with a two-step statistical approach used previously elsewhere (Hoogenboom et al., 2010; Lange et al., 2011). In a first step, individual alpha power was compared between attended and unattended trials by computing t -values for each subject and time point. Since t -values consist of the difference in mean power between the two attention conditions relative to the variance in power across trials, this step normalizes for inter-individual differences. The outcome was a subject-wise comparison of attended and unattended trials in the form of a t -value time course. For a further distributional normalization, all t -values were transformed to z -values (Mazaheri et al., 2009; van Dijk et al., 2008). In a second step, a group-level statistic used these single-subject z -value time courses and determined their consistency across subjects. The statistical significance of the difference between the two conditions was evaluated using a cluster-based randomization test (Maris and Oostenveld, 2007). Pooled z -values across subjects were computed for all time points. Neighboring time-bins exceeding an a priori threshold (uncorrected $p < .05$) were combined to clusters. Within every cluster, z -values were summed and the maximum of these sums was used as a cluster-level test statistic. Under the hypothesis of no difference between the two conditions, the difference between attended and unattended trials should not significantly differ from zero; i.e. the computed z -values should be interchangeable with zero. By randomly interchanging data across the two conditions within each subject (i.e. the individual z -scores and 0) and recalculating the cluster-level test statistic 1000 times, a reference distribution of maximum cluster z -value sums was obtained. This was then used to evaluate the statistical significance of the observed maximum cluster-level test statistic of the actual data. By clustering neighboring time points showing the same effect and selecting the maximum cluster-level statistic from each randomization for the reference distribution, this method deals with the multiple comparison problem and is not affected by partial dependence in the data (Lange et al., 2011; Maris and Oostenveld, 2007). Using this two-step statistical approach, 4 comparisons of attended vs. unattended trials were performed per hand: left S1 channels, pre-stimulus interval; left S1 channels, post-stimulus interval; right S1 channels, pre-stimulus interval; and right S1 channels, post-stimulus interval. Thereby, time periods showing significant modulation with attention were identified.

A further statistical analysis focused on the time periods with significant attentional modulation and examined the topographical distribution of attention effects beyond the preselected channels of interest. To this end, the same two-step procedure was applied without making an a priori channel selection. Single subject z -values were now computed for power averages of individual alpha activity over those time windows that had previously shown significant attentional differences. Clusters showing differences between attended and unattended trials were now formed along the channel instead of the time dimension and then tested for significance.

Pre-stimulus alpha lateralization index

To capture the hypothesized pre-stimulus alpha lateralization over both hemispheres in one value, a lateralization index of alpha power was calculated for each subject, in line with indices used by Haegens et al. (2011) and Thut et al. (2006) in similar spatial attention paradigms.

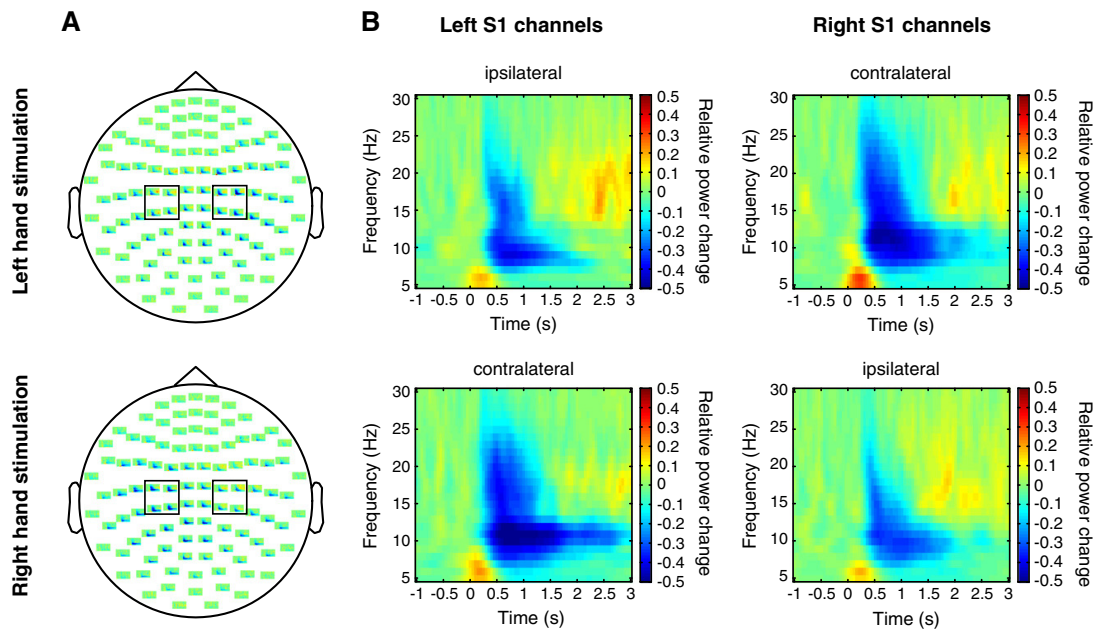


Fig. 2. Stimulus-induced effects used for channel selection. **A.** Grand average time–frequency representations (TFRs) of all combined MEG sensors across all trials with stimulation of the left (upper row) and right hands (lower row). TFRs were averaged across attended and unattended trials of the respective hand. 2 groups of 4 combined sensors each showing the strongest alpha and beta suppression in response to a laser stimulus on the contralateral hand were chosen for further analysis and denoted as left and right S1 channels. Both sensor groups are highlighted for both left and right hand stimulation trials, respectively. Scale as in **B.** **B.** Grand average TFRs across channels marked in **A** for left (upper row) and right (lower row) hand stimulation trials with time-point 0 representing the onset of the laser stimulus. Power changes relative to a pre-stimulus baseline (–1 to 0 s) are color-coded.

Again, this analysis focused on the last second immediately preceding laser stimulation. Using the previously identified left and right hemispheric S1 channel groups as regions of interest (ROIs), the index was calculated using the following formula:

$$\text{Alpha lateralization index} = \frac{(\text{Alpha ROI}_{\text{ipsilateral}} - \text{Alpha ROI}_{\text{contralateral}})}{(\text{Alpha ROI}_{\text{ipsilateral}} + \text{Alpha ROI}_{\text{contralateral}})}$$

Ipsi- and contralateral refers to the hemisphere with respect to the alleged spatial attentional orientation to the left or right hand. The calculation was based on the same FFT computation used for determination of the individual alpha peak frequency described in [Individually adjusted alpha activity](#) section. This approach was chosen to capture pure pre-stimulus effects and avoid a possible intermixture of pre- and post-stimulus effects close to the time point of laser stimulation caused by the sliding time window approach used for the calculation of TFRs. Power values were averaged across individually adjusted alpha frequency bands and the predefined sensors of interest before the alpha lateralization index were computed. This index gives a positive value when alpha power is lower over contralateral channels and/or higher over ipsilateral channels with respect to the attentional orientation and a negative value for the opposite scenario. The distribution of alpha lateralization indices across subjects was tested against the null hypothesis of zero mean, using a *t*-test. This analysis was performed for both left and right hand stimulation trials.

Trial-by-trial correlation of alpha power and pain ratings

In order to examine the functional relevance of attention-modulated alpha activity for behavior, the relationship between alpha power and pain ratings was investigated in a trial-by-trial analysis. For each trial, alpha power was averaged across those time periods and channels that were significantly modulated with attention in the previous analyses

and subsequently log-transformed. Spearman correlation coefficients were calculated between the log-transformed power values and pain ratings for each subject. This analysis was restricted to attended trials since pain ratings were only obtained for trials in which the attended hand was stimulated. Again, the distribution of correlation coefficients across subjects was tested against the null hypothesis of zero mean, using a *t*-test. Bonferroni–Holm correction ([Holm, 1979](#)) was applied to all alpha levels to correct for multiple comparisons.

Results

Behavioral results

Laser stimuli on the attended hand were consistently rated as painful, pinprick-like sensations with an average rating of 3.26 ± 1.42 across both hands. Mean pain ratings did not differ between the left and right hand (3.20 ± 1.37 vs. 3.31 ± 1.51 , $p > 0.1$). Stimuli on the attended hand were on average correctly localized to the stimulated target area in $84.44\% \pm 9.83$ of the trials. This rate was significantly lower for the left than the right hand ($79.96\% \pm 10.13$ vs. $88.93\% \pm 7.37$, $p = 0.005$).

Stimulus effects

Grand average time–frequency analysis across all left and right hand stimulation trials is illustrated in [Fig. 2](#). Painful laser stimuli to either hand elicited a well-known sequence of a pain-induced power increase between 4 and 8 Hz reflecting the pain-evoked field followed by a pronounced alpha and beta suppression ([Ploner et al., 2006a; Schulz et al., 2011](#)). Alpha and beta suppression was widely distributed across bilateral somatosensory and parietal areas. Two groups of channels were selected for further analysis according to the strongest stimulus-induced response, which are supposed to overlay primary sensory cortices ([Fig. 2A](#)). Stimulus-induced suppression effects appeared slightly

enhanced over contralateral S1 sensors compared to ipsilateral S1 sensors (Fig. 2B).

Modulation of alpha activity with spatial attention

Across subjects, individual alpha peak frequencies varied between 8 and 11 Hz (mean \pm standard deviation: 10.07 ± 0.88 Hz). For one subject, no individual alpha peak frequency could be detected. Instead, a standard value of 10 Hz corresponding to the average peak frequency across subjects was used for subsequent analyses. To reveal time windows during which attention affects pain-associated alpha activity, effects of spatial attention on individual alpha activity were analyzed for both hands on left and right S1 channels and during pre- and post-stimulus time intervals. In Fig. 3A, grand averages of alpha power illustrate the temporal evolution of alpha activity in the different conditions for left and right hand stimuli. Gray boxes mark time windows showing significant differences between attended and unattended trials. Please note that, while raw alpha power is displayed in Fig. 3A, group level statistics were performed on individual z-values, quantifying power differences between conditions relative to the variance across trials for each subject. In line with the general stimulus-induced response, alpha power was suppressed on both left and right S1 channels in response to painful laser stimuli, irrespective of whether they were attended or not. Differential attention effects were observed for pre- and post-stimulus time periods.

Pre-stimulus attention effects

For trials with stimulation of the left hand (Fig. 3A, upper row), significant pre-stimulus clusters were found for both ipsi- and contralateral S1 channels. Over ipsilateral S1 channels, a cluster extended from -0.65 to -0.4 s before the laser stimulus and showed increased

alpha activity in attended compared to unattended trials (left hand cluster C1: $p = 0.020$). Over contralateral S1 channels, a cluster spanned the time period between -0.2 and 0 s and displayed the opposite pattern showing decreased alpha activity when the left hand was attended compared to when it was unattended (left hand cluster C3: $p = 0.034$). For trials with stimulation of the right hand (Fig. 3A, lower row), a trend for a cluster was observed on contralateral channels. This cluster extended from -0.15 to 0 s and showed decreased alpha activity for attended compared to unattended trials (right hand cluster C5: $p = 0.069$).

After having identified time windows during which attention significantly affects pre-stimulus pain-associated alpha activity, a further statistical analysis examined the topographical distribution of these attention effects over the complete sensor array. Individual alpha activity was averaged over those time windows showing significant differences in the time-resolved analysis and compared between attended and unattended trials for each hand. This analysis resulted in three topographies corresponding to the three time clusters found in the previous analysis (Fig. 3B, left column). The pre-stimulus effects indicated a lateralization of anticipatory alpha activity across hemispheres. For left hand stimulation trials, the topographies showed increased alpha activity over left/ipsilateral primary somatosensory areas (left hand cluster C1: $p = 0.040$) and decreased alpha activity over right/contralateral primary somatosensory areas when the left hand was attended (left hand cluster C3: $p = 0.009$). For right hand stimulation trials, the pre-stimulus cluster showed the corresponding mirroring effect displaying a trend for decreased alpha activity over left/contralateral S1 channels when the right hand was attended (right hand cluster C5: $p = 0.078$).

To capture this anticipatory alpha lateralization over both hemispheres in a single value, pre-stimulus attention effects from -1 to 0 s with respect to the stimulation were additionally quantified by calculating a subject-wise alpha lateralization index. As depicted in Fig. 4,

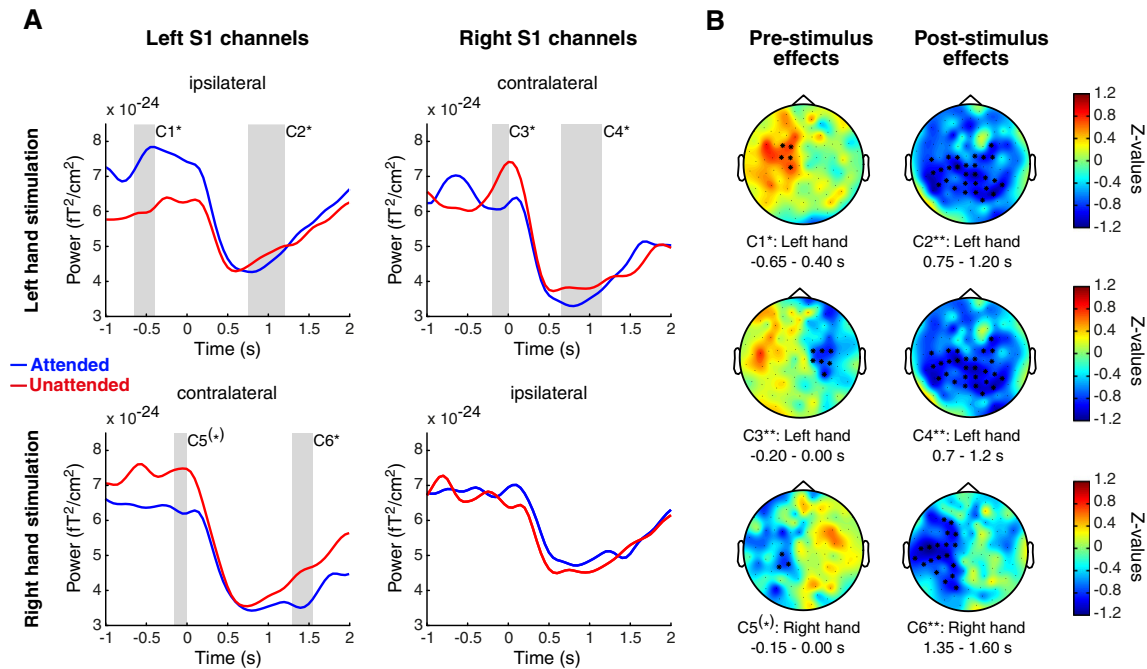


Fig. 3. Attention effects. A. Grand average temporal evolution of individual alpha activity on left and right S1 channels in attended and unattended trials of left (upper row) and right hand (lower row) stimulation trials (please see Fig. 2A for channel selection). Time-point 0 represents the onset of the laser stimulus. Gray boxes mark six time clusters (C1–C6) showing differences between attended and unattended trials ($(^*)p < 0.1$, $(^*)p < 0.05$). B. Topographical distribution of attention effects on alpha activity during time windows showing differences in A (topographical clusters C1–C6 correspond to time clusters C1–C6 in A). Z-values representing the statistical comparison between attended and unattended trials are color-coded. Positive values indicate increased, negative values decreased alpha power with attention. Sensor clusters showing modulation associated with attention are marked ($(^*)p < 0.1$, $(^*)p < 0.05$, $(^{**})p < 0.01$).

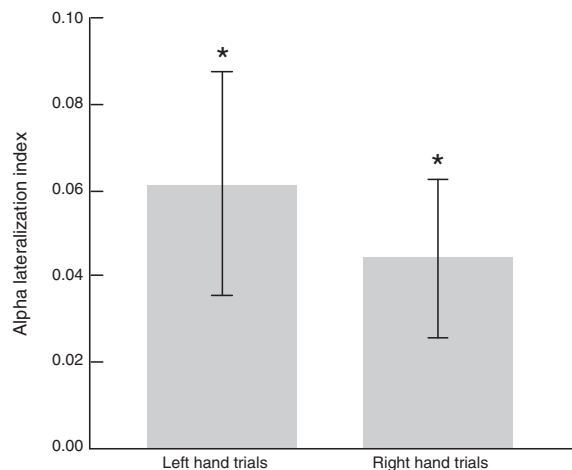


Fig. 4. Pre-stimulus alpha lateralization index. Mean values of alpha lateralization indices across subjects quantifying anticipatory pre-stimulus alpha modulation across both hemispheres. Error bars indicate the standard error of mean. The distribution of alpha lateralization indices across subjects was tested against the hypothesis of zero mean for both left and right hand stimulation trials separately. For both trial types, alpha lateralization indices were significantly higher than zero, indicating decreased contralateral and/or increased ipsilateral alpha power with respect to the attentional orientation to the left or right hand (* $p < 0.05$).

pre-stimulus alpha lateralization was significantly higher than zero across subjects for both left and right hand stimulation trials (left hand: $p = 0.016$, right hand: $p = 0.016$), indicating lower alpha power over contralateral S1 channels and/or higher alpha power over ipsilateral S1 channels during the anticipation of a lateralized painful stimulus.

In summary, these pre-stimulus results indicate a lateralization of alpha activity in anticipation of a painful stimulus to the left or right hand. More specifically, alpha activity in primary somatosensory areas seems to be stronger when the ipsilateral hand is attended compared to when the contralateral hand is attended, indicating increased alpha activity over ipsilateral and/or decreased alpha activity over contralateral channels with respect to the attended hand.

Post-stimulus attention effects

The subsequent post-stimulus period was marked by significant decreases of alpha activity with attention (Fig. 3A). For trials with stimulation of the left hand, significant clusters emerged over both ipsi- (left hand cluster C2: $p = 0.018$) and contralateral (left hand cluster C4: $p = 0.011$) S1 channels. The significant cluster on ipsilateral S1 channels (C2) covered a time window from 0.75 to 1.2 s, whereas the cluster on contralateral S1 channels (C4) covered a time window from 0.7 to 1.2 s. For trials with stimulation of the right hand, a significant post-stimulus attention effect was found on contralateral S1 channels only (right hand cluster C6: $p = 0.045$). This significant time cluster started later and extended from 1.35 to 1.6 s after stimulus onset. Again, alpha activity was decreased in attended trials. Overall, the post-stimulus effects indicate that alpha suppression in response to a painful laser stimulus is stronger and/or prolonged when the stimulated hand is attended.

In accordance with the analysis of pre-stimulus attention effects, a further analysis examined the topographical distribution of post-stimulus attention effects beyond the pre-selected channels of interest (Fig. 3B, right column). For both hands, significant clusters of reduced alpha activity with attention included channels over somatosensory and parietal areas contralaterally to the stimulated hand (left hand cluster C2: $p = 0.002$, left hand cluster C4: $p = 0.001$, right hand cluster C6:

$p = 0.002$). For left hand trials, the topographic clusters (C2 and C4) additionally covered ipsilateral somatosensory channels.

To summarize, post-stimulus attention effects of decreased alpha activity with attention were found for both left and right hand stimulation trials covering primarily contralateral somatosensory and parietal areas. The corresponding left hand stimulation post-stimulus clusters appeared both earlier in time and more widely spread including ipsilateral channels.

Correlation between early post-stimulus alpha activity and pain perception

To investigate the functional relevance of attention-related alpha activity for individual pain ratings, single trial correlation analyses were performed. Alpha power was averaged over time windows and channels that had shown modulation associated with attention in the previous analyses (Fig. 3). For each subject and on a trial-by-trial basis, the average alpha power was correlated with individual pain ratings during attended trials.

Trends for inverse correlations between individual pain ratings and alpha power averaged over the two post-stimulus clusters in trials with stimulation of the left hand were found (left hand cluster C2: mean $r = -0.13$; $p = 0.027$, uncorrected; left hand cluster C4: mean $r = -0.15$; $p = 0.018$, uncorrected). However, these correlations were no longer significant when p -values were corrected for a total of 6 comparisons between alpha power and pain ratings. Pre-stimulus alpha power and post-stimulus alpha power in trials with stimulation of the right hand did not show a correlation or a trend for a correlation with individual pain ratings.

Discussion

The aim of the current study was to investigate pre- and post-stimulus effects of attention on oscillatory alpha activity associated with painful laser stimuli to shed further light on the role of alpha activity during pain processing. We found that spatial attention to one hand differentially modulates alpha activity in anticipation of and in response to a painful stimulus on that hand. As hypothesized, alpha activity during the pre-stimulus period lateralized across the two hemispheres, being lower over primary somatosensory areas when the contralateral hand is attended compared to when the ipsilateral hand is attended. Post-stimulus alpha activity was consistently decreased over contralateral areas when attention was placed on the stimulated hand.

Pre- and post-stimulus alpha activity is differentially modulated with attention

On average, subjects correctly localized attended stimuli to the stimulated target area in 84% of the trials. Thus, performance was well above chance level but below ceiling effects, indicating an appropriate difficulty for a task intended to demand attention. Differential effects of attention on pain-associated alpha activity were observed, supporting a pronounced role of attention for the processing of pain.

Pre-stimulus attention effects

Spatial attention to the left or right hand was associated with a lateralization of pre-stimulus alpha activity. Alpha activity was lower over primary somatosensory areas when the contralateral hand was attended compared to when the ipsilateral hand was attended. This pattern was shown by comparisons of alpha activity in attended and unattended trials over left and right somatosensory areas separately and was additionally confirmed by the calculation of the alpha lateralization index across hemispheres. Interestingly, the alpha lateralization index seems to be most sensitive in detecting this effect. While the alpha lateralization index did reveal significant alpha lateralization for right hand stimulation trials, separate comparisons of alpha activity over left and right S1 channels only displayed a trend for an attention effect over left S1

channels. Together, these pre-stimulus attention effects support previous findings showing a similar anticipatory lateralization of alpha activity in somatosensory (Anderson and Ding, 2011; Haegens et al., 2011), visual (Gould et al., 2011; Thut et al., 2006) and auditory (Müller and Weisz, 2011; Thorpe et al., 2012) tasks. The present study extends these findings to the perception of pain. Our results thereby further substantiate the notion that the level of alpha activity reflects the degree of engagement/disengagement of a cortical region and is actively regulated by top-down processes like attention (Foxy and Snyder, 2011; Jensen and Mazaheri, 2010; Pfurtscheller et al., 1996). Interestingly, pre-stimulus attention effects in the present study appeared more consistently over left primary somatosensory areas, indicating possible hemispheric differences in the strength of modulation of ongoing oscillatory alpha activity in anticipation of a lateralized painful stimulus.

Whether the lateralization of anticipatory alpha activity found here is caused by an ipsilateral increase of alpha activity, a contralateral decrease, or a combination of both cannot be deduced from the current data, since the study used a block design lacking a baseline without an attentional orientation to the left or right hand. Studying anticipatory alpha modulation in the somatosensory system in a similar paradigm using non-painful tactile stimuli, Haegens et al. (2011) found that anticipatory alpha lateralization is mainly driven by a decrease of alpha activity contralateral to the attended hand in combination with a slight ipsilateral increase when the right hand is attended. However, the authors also concluded that the overall lateralization best reflects the attentional bias.

An active inhibition of cortical areas by increased alpha activity has particularly been discussed in the context of inhibiting distracting input presented simultaneously to task-relevant target stimuli (Fu et al., 2001; Haegens et al., 2012; Händel et al., 2011; Kelly et al., 2006). In the present study, painful stimuli were never presented simultaneously to both hands. Our aim was to investigate both pre- and post-stimulus effects of attention on pain-associated alpha activity. A concurrent stimulation of both hands, however, would have caused overlapping neuronal responses to both stimuli in the post-stimulus period. To be able to examine the attentional modulation of a single stimulus, painful stimuli were applied either to the attended or the unattended hand. Previous work showing both stronger anticipatory and stimulus-induced alpha suppression for painful compared to non-painful stimuli already suggested a particularly intense processing of pain and pain-associated stimuli (Babiloni et al., 2003; Ploner et al., 2006a; Whitmarsh et al., 2011). Therefore, one might assume that the inhibition of a distracting painful stimulus by anticipatory alpha modulation requires more resources than the inhibition of a non-painful distracting stimulus. Future studies should examine if anticipatory pre-stimulus alpha lateralization in the context of distracting painful stimuli is also particularly pronounced.

Lastly, anticipatory alpha modulation has been shown to be reduced in older compared to younger subjects in a visual paradigm requiring subjects to anticipate an upcoming target stimulus in time (Zanto et al., 2011). Since the age of subjects in the current study spanned a broad range between 24 and 74 years, age might have had an influence on the size of the effects reported here. However, a correlation analysis between pre-stimulus alpha lateralization as measured by the alpha lateralization index and age did not reveal a significant relation between the two measures (data not reported). Since Zanto et al. (2011) studied temporal attention effects in the visual system, these different results might indicate that age affects attentional processes differently in different modalities and/or regarding different types of attention, which again is a very interesting area of future research.

Post-stimulus attention effects

Attention consistently reduced post-stimulus alpha activity in line with an increased cortical activation following an attended painful stimulus. Since we expected attention to affect both pre- and post-stimulus alpha activity, absolute alpha power values rather than relative power changes with respect to baseline were statistically compared. If

attention affects pre-stimulus activity, performing a baseline correction relative to this activity can artificially induce post-stimulus attention effects that in fact originate from baseline differences. Controlling for such a mixture of effects, our data demonstrate that attention can independently influence both pre- and post-stimulus activity. The time courses of alpha activity in the different attention conditions shown in Fig. 3A suggest that spatial attention intensifies and prolongs the stimulus-induced suppression of alpha activity. These findings are consistent with a previous report of increased alpha suppression in response to painful laser stimuli with attention (Ohara et al., 2004). This study analyzed data with respect to a pre-stimulus baseline, which might have biased the size of the attention effect. However, our data revealed a similar effect with an analysis controlling for pre-stimulus effects. Taken together, these results strongly suggest that the widespread pain-induced alpha suppression reflecting the alerting function of pain is increased with attention. Interestingly, attention reduced post-stimulus alpha activity for left hand stimulation trials even on channels overlying ipsilateral somatosensory areas. Thus, the enhancement of the widespread alerting effect of painful stimuli by attention affects large parts of the brain. Again, this hints at the interesting possibility that the left hemisphere is more easily modulated than the right hemisphere during processing of a lateralized painful stimulus.

Relation between attention-modulated alpha activity and individual pain ratings

Under the assumption that the present attention effects are functionally relevant, pain-associated alpha activity should also affect behavioral responses. In the current study, we found trends for an inverse relation between post-stimulus alpha activity and individual pain rating for trials with stimulation of the left hand. In principle, this pattern tallies with previous studies that showed higher pain ratings when alpha activity close the moment of stimulus onset was low (Babiloni et al., 2006; Schulz et al., 2011). In these studies, correlation analyses were performed using selected electrodes of interest, representative of primary somatosensory areas contralateral to the stimulated hand. In the current analysis, alpha activity estimates for the correlation analysis were averaged across all sensors showing significant modulation with spatial attention, which were distributed across broad areas of the brain. Possibly, the level of alpha activity in primary somatosensory areas contralateral to the stimulated hand is most relevant for the actual pain perception while attention affects pain-associated alpha activity in much broader areas. This would have led to relatively small and more variable correlation coefficients between alpha activity and individual pain ratings in the current study.

Regarding pre-stimulus alpha activity, there was no indication of a relation to individual pain ratings. Previously, it has been demonstrated for the visual system that pre-stimulus alpha lateralization across subjects correlates with motion detection performance in the unattended but not in the attended visual hemifield (Händel et al., 2011). The pre-stimulus modulation of alpha might therefore be more related to the successful inhibition of unattended than of the processing of attended stimuli. However, this hypothesis could not be tested in the current study since there was no pain rating given for stimuli applied to the unattended side.

Higher localization rate for right hand than left hand stimuli

As shown by the behavioral results, subjects were more successful in localizing attended stimuli on the right than on the left hand although the subjectively perceived pain intensity did not differ between the two. This finding is unexpected since a previous study by Schlereth et al. (2001) reported no differences in spatial discrimination thresholds for laser stimuli between both hands in a similar task. As the majority of subjects (14 out of 15 subjects) in the current study were right-handed, this might reflect a perceptual superiority of the dominant hand in the specific

task used here. As a consequence, the attentional load due to the localization task might have been higher when the left hand was attended compared to when the right hand was attended, leading to stronger attention effects.

Importantly, such hand differences could not differentially influence pre-stimulus effects for left and right hand stimulation trials since the number of trials where the left hand was attended and the number of trials where the right hand was attended was equal for both, i.e. 50% each. Regarding post-stimulus effects, however, a higher attentional load when the left hand was attended might have contributed to a topographically more widespread reduction of alpha activity with attention for a left hand stimulus. For right hand stimuli, in contrast, the attention effect was confined to the left, i.e. contralateral, hemisphere and we did not find a post-stimulus attention effect over right primary somatosensory areas. Future studies equating performance levels between the two hands are needed to further examine potential effects of attentional load and handedness on the degree of modulation of pain-associated alpha activity with attention.

Conclusions

The present study demonstrated that both pre- and post-stimulus oscillatory alpha activity is modulated, if attention is spatially shifted to one hand during anticipation of a painful laser stimulus to that hand. These effects indicate a pronounced role of attention during the processing of pain, which is at least partially mediated by modulation of alpha activity. Spatial attention was associated with a lateralization of pre-stimulus alpha activity, i.e. alpha activity was decreased over primary somatosensory areas when the contralateral hand was attended compared to when the ipsilateral hand was attended. This modulation of ongoing alpha activity presumably subserves the overall facilitation of processing of stimuli on the attended hand. Post-stimulus alpha activity, in contrast, was reduced with attention over widespread areas, most likely reflecting an increased cortical activation and intensified alerting function of pain. This flexible regulation of alpha activity is in accordance with previous findings in other modalities. Thus, our results further strengthen the notion that oscillatory alpha activity reflects a top-down controlled gating mechanism employed throughout the brain.

Role of the funding source

This study was supported by the German Research Foundation (SFB 575, project C4). M.Bu. was supported by a Marie Curie Fellowship of the EU (FP7-PEOPLE-2009-IEF-253965), N.K. by the German National Academic Foundation and M.Br. by the Integrated Graduate School 575. E.M. and N.K. were supported by travel grants from the Integrated Graduate School 575 and the Boehringer Ingelheim Foundation (B.I.F.).

Acknowledgments

We thank Ms. Alla Solotuchin and Mr. Ulf M. Zierhut for help with the MEG data collection. Furthermore, we are grateful to our colleagues from the University of Düsseldorf Dr. Joachim Lange, Dr. Tolga Özkurt, Dr. Holger Krause, Dr. Hanneke van Dijk and Jan Hirschmann for support with data analysis and for helpful discussions and comments.

References

Anderson, K.L., Ding, M., 2011. Attentional modulation of the somatosensory mu rhythm. *Neuroscience* 180, 165–180.

Babiloni, C., Brancucci, A., Babiloni, F., Capotosto, P., Carducci, F., Cincotti, F., Arendt-Nielsen, L., Chen, A.C.N., Rossini, P.M., 2003. Anticipatory cortical responses during the expectancy of a predictable painful stimulation. A high-resolution electroencephalography study. *Eur. J. Neurosci.* 18 (6), 1692–1700.

Babiloni, C., Brancucci, A., Arendt-Nielsen, L., Babiloni, F., Capotosto, P., Carducci, F., Cincotti, F., Del Percio, C., Petrin, L., Rossini, P.M., Chen, A.C.N., 2004. Attentional processes and cognitive performance during expectancy of painful galvanic stimulations: a high-resolution EEG study. *Behav. Brain Res.* 152 (1), 137–147.

Babiloni, C., Brancucci, A., Del Percio, C., Capotosto, P., Arendt-Nielsen, L., Chen, A.C.N., Rossini, P.M., 2006. Anticipatory electroencephalography alpha rhythm predicts subjective perception of pain intensity. *J. Pain* 7 (10), 709–717.

Berger, H., 1929. Über das Elektroencephalogramm des Menschen. *Arch. Psychiatr. Nervenkr.* 87, 527–570.

Bushnell, M.C., Duncan, G.H., Hofbauer, R.K., Ha, B., Chen, J.L., Carrier, B., 1999. Pain perception: is there a role for primary somatosensory cortex? *Proc. Natl. Acad. Sci. U. S. A.* 96 (14), 7705–7709.

Del Percio, C., Le Pera, D., Arendt-Nielsen, L., Babiloni, C., Brancucci, A., Chen, A.C.N., De Armas, L., Miliucci, R., Restuccia, D., Valeriani, M., Rossini, P.M., 2006. Distraction affects frontal alpha rhythms related to expectancy of pain: an EEG study. *Neuroimage* 31 (3), 1268–1277.

Foxe, J.J., Snyder, A.C., 2011. The role of alpha-band brain oscillations as a sensory suppression mechanism during selective attention. *Front. Psychol.* 2, 154.

Fu, K.M., Foxe, J.J., Murray, M.M., Higgins, B.A., Javitt, D.C., Schroeder, C.E., 2001. Attention-dependent suppression of distracter visual input can be cross-modally cued as indexed by anticipatory parieto-occipital alpha-band oscillations. *Brain Res. Cogn. Brain Res.* 12 (1), 145–152.

Gould, I.C., Rushworth, M.F., Nobre, A.C., 2011. Indexing the graded allocation of visuo-spatial attention using anticipatory alpha oscillations. *J. Neurophysiol.* 105 (3), 1318–1326.

Gross, J., Schnitzler, A., Timmermann, L., Ploner, M., 2007. Gamma oscillations in human primary somatosensory cortex reflect pain perception. *PLoS Biol.* 5 (5), e133.

Haegens, S., Händel, B.F., Jensen, O., 2011. Top-down controlled alpha band activity in somatosensory areas determines behavioral performance in a discrimination task. *J. Neurosci.* 31 (14), 5197–5204.

Haegens, S., Luther, L., Jensen, O., 2012. Somatosensory anticipatory alpha activity increases to suppress distracting input. *J. Cogn. Neurosci.* 24 (3), 677–685.

Händel, B.F., Haarmeier, T., Jensen, O., 2011. Alpha oscillations correlate with the successful inhibition of unattended stimuli. *J. Cogn. Neurosci.* 23 (9), 2494–2502.

Hari, R., Salmelin, R., 1997. Human cortical oscillations: a neuromagnetic view through the skull. *Trends Neurosci.* 20 (1), 44–49.

Hauck, M., Lorenz, J., Engel, A.K., 2007. Attention to painful stimulation enhances gamma-band activity and synchronization in human sensorimotor cortex. *J. Neurosci.* 27 (35), 9270–9277.

Hauck, M., Lorenz, J., Engel, A.K., 2008. Role of synchronized oscillatory brain activity for human pain perception. *Rev. Neurosci.* 19 (6), 441–450.

Holm, S., 1979. A simple sequentially rejective multiple test procedure. *Scand. J. Stat.* 6 (2), 65–70.

Hoogenboom, N., Schoffelen, J.-M., Oostenveld, R., Fries, P., 2010. Visually induced gamma-band activity predicts speed of change detection in humans. *Neuroimage* 51 (3), 1162–1167.

Jensen, O., Mazaheri, A., 2010. Shaping functional architecture by oscillatory alpha activity: gating by inhibition. *Front. Hum. Neurosci.* 4, 186.

Jones, S.R., Kerr, C.E., Wan, Q., Pritchett, D.L., Hämäläinen, M., Moore, C.I., 2010. Cued spatial attention drives functionally relevant modulation of the mu rhythm in primary somatosensory cortex. *J. Neurosci.* 30 (41), 13760–13765.

Jung, T.P., Makeig, S., Humphries, C., Lee, T.W., McKeown, M.J., Iragui, V., Sejnowski, T.J., 2000. Removing electroencephalographic artifacts by blind source separation. *Psychophysiology* 37 (2), 163–178.

Kelly, S.P., Lalor, E.C., Reilly, R.B., Foxe, J.J., 2006. Increases in alpha oscillatory power reflect an active retinotopic mechanism for distracter suppression during sustained visuospatial attention. *J. Neurophysiol.* 95 (6), 3844–3851.

Lange, J., Oostenveld, R., Fries, P., 2011. Perception of the touch-induced visual double-flash illusion correlates with changes of rhythmic neuronal activity in human visual and somatosensory areas. *Neuroimage* 54 (2), 1395–1405.

Maris, E., Oostenveld, R., 2007. Nonparametric statistical testing of EEG- and MEG-data. *J. Neurosci. Methods* 164 (1), 177–190.

Mazaheri, A., Nieuwenhuis, I.L.C., van Dijk, H., Jensen, O., 2009. Prestimulus alpha and mu activity predicts failure to inhibit motor responses. *Hum. Brain Mapp.* 30 (6), 1791–1800.

Miron, D., Duncan, G.H., Bushnell, M.C., 1989. Effects of attention on the intensity and unpleasantness of thermal pain. *Pain* 39 (3), 345–352.

Müller, N., Weisz, N., 2011. Lateralized auditory cortical alpha band activity and inter-regional connectivity pattern reflect anticipation of target sounds. *Cereb. Cortex.* <http://dx.doi.org/10.1093/cercor/bhr232>.

Niedermeyer, E., Lopes da Silva, F.H., 2005. *Electroencephalography: Basic Principles, Clinical Applications, and Related Fields*, fifth ed. Lippincott Williams & Wilkins, Philadelphia.

Ohara, S., Crone, N.E., Weiss, N., Lenz, F.A., 2004. Attention to a painful cutaneous laser stimulus modulates electrocorticographic event-related desynchronization in humans. *Clin. Neurophysiol.* 115 (7), 1641–1652.

Oostenveld, R., Fries, P., Maris, E., Schoffelen, J.-M., 2011. FieldTrip: open source software for advanced analysis of MEG, EEG, and invasive electrophysiological data. *Comput. Intell. Neurosci.* 2011, 156869.

Petrovic, P., Petersson, K.M., Ghata, P.H., Stone-Elander, S., Ingvar, M., 2000. Pain-related cerebral activation is altered by a distracting cognitive task. *Pain* 85 (1–2), 19–30.

Pfurtscheller, G., Stancák Jr., A., Neuper, C., 1996. Event-related synchronization (ERS) in the alpha band—an electrophysiological correlate of cortical idling: a review. *Int. J. Psychophysiol.* 24 (1–2), 39–46.

Ploner, M., Gross, J., Timmermann, L., Pollak, B., Schnitzler, A., 2006a. Pain suppresses spontaneous brain rhythms. *Cereb. Cortex* 16 (4), 537–540.

Ploner, M., Gross, J., Timmermann, L., Pollak, B., Schnitzler, A., 2006b. Oscillatory activity reflects the excitability of the human somatosensory system. *Neuroimage* 32 (3), 1231–1236.

- Rohenkohl, G., Nobre, A.C., 2011. Alpha oscillations related to anticipatory attention follow temporal expectations. *J. Neurosci.* 31 (40), 14076–14084.
- Schlereth, T., Magerl, W., Treede, R., 2001. Spatial discrimination thresholds for pain and touch in human hairy skin. *Pain* 92 (1–2), 187–194.
- Schlereth, T., Baumgärtner, U., Magerl, W., Stoeter, P., Treede, R.-D., 2003. Left-hemisphere dominance in early nociceptive processing in the human parasyllian cortex. *Neuroimage* 20 (1), 441–454.
- Schulz, E., Tiemann, L., Schuster, T., Gross, J., Ploner, M., 2011. Neurophysiological coding of traits and states in the perception of pain. *Cereb. Cortex* 21 (10), 2408–2414.
- Schulz, E., Zherdin, A., Tiemann, L., Plant, C., Ploner, M., 2012. Decoding an individual's sensitivity to pain from the multivariate analysis of EEG data. *Cereb. Cortex* 22 (5), 1118–1123.
- Thorpe, S., D'Zmura, M., Srinivasan, R., 2012. Lateralization of frequency-specific networks for covert spatial attention to auditory stimuli. *Brain Topogr.* 25 (1), 39–54.
- Thut, G., Nietzel, A., Brandt, S.A., Pascual-Leone, A., 2006. Alpha-band electroencephalographic activity over occipital cortex indexes visuospatial attention bias and predicts visual target detection. *J. Neurosci.* 26 (37), 9494–9502.
- Treede, R.-D., 2003. Neurophysiological studies of pain pathways in peripheral and central nervous system disorders. *J. Neurol.* 250 (10), 1152–1161.
- van Dijk, H., Schoffelen, J.-M., Oostenveld, R., Jensen, O., 2008. Prestimulus oscillatory activity in the alpha band predicts visual discrimination ability. *J. Neurosci.* 28 (8), 1816–1823.
- van Ede, F., de Lange, F., Jensen, O., Maris, E., 2011. Orienting attention to an upcoming tactile event involves a spatially and temporally specific modulation of sensorimotor alpha- and beta-band oscillations. *J. Neurosci.* 31 (6), 2016–2024.
- Whitmarsh, S., Nieuwenhuis, I.L.C., Barendregt, H.P., Jensen, O., 2011. Sensorimotor alpha activity is modulated in response to the observation of pain in others. *Front. Hum. Neurosci.* 5, 91.
- Zanto, T.P., Pan, P., Liu, H., Bollinger, J., Nobre, A.C., Gazzaley, A., 2011. Age-related changes in orienting attention in time. *J. Neurosci.* 31 (35), 12461–12470.

Hepatic encephalopathy slows and delays stimulus-associated somatosensory alpha activity

Elisabeth S. May, MSc, Markus Butz, PhD, Nina Kahlbrock, PhD, Meike Brenner, MD, Nienke Hoogenboom, MSc, Gerald Kircheis, MD, Dieter Häussinger, MD, Alfons Schnitzler, MD

Affiliations:

Heinrich-Heine-University Düsseldorf, Medical Faculty, Institute of Clinical Neuroscience and Medical Psychology, Universitätsstrasse 1, D-40225 Düsseldorf, Germany (E.S.M., M.Bu., N.K., M.Br., N.H., A.S.)

Sobell Department of Motor Neuroscience and Movement Disorders, UCL Institute of Neurology, Queen Square, London, WC1N 3BG, United Kingdom (M.Bu.)

Heinrich-Heine-University Düsseldorf, Medical Faculty, Department of Gastroenterology, Hepatology and Infectious Disease, Universitätsstraße 1, D-40225 Düsseldorf, Germany (G.K., D.H.)

Corresponding Author:

Markus Butz, Sobell Department of Motor Neuroscience and Movement Disorders, UCL Institute of Neurology, Queen Square, London, WC1N 3BG, United Kingdom, email: m.butz@ucl.ac.uk, phone: +44 20 3448 8756, fax: +44 20 72789836

Search terms: All clinical neurophysiology [283], evoked potentials/somatosensory [288], all medical/systemic disease [146], neuropsychological assessment [205], attention [208]

Study funding: Supported by the German Research Foundation (SFB 575, SFB 974).

Author's email addresses:

Elisabeth S. May: elisabethsusanne.may@uni-duesseldorf.de

Markus Butz: m.butz@ucl.ac.uk

Nina Kahlbrock: nina.kahlbrock@uni-duesseldorf.de

Meike Brenner: meike.brenner@uni-duesseldorf.de

Nienke Hoogenboom: nienke.hoogenboom@med.uni-duesseldorf.de

Gerald Kircheis: kircheis@med.uni-duesseldorf.de

Dieter Häussinger: haeussin@uni-duesseldorf.de

Alfons Schnitzler: alfons.schnitzler@uni-duesseldorf.de

Manuscript specifications:

- Character count title: 88
- Word count abstract: 248
- Word count manuscript text: 3000
- Number of tables: 2
- Number of figures: 3
- Number of references: 37

Author contributions:

Ms. May: Study design, analysis and interpretation of data, drafting of manuscript.

Dr. Butz: Study design, analysis and interpretation of data, drafting of manuscript.

Dr. Kahlbrock: Interpretation of data, manuscript revision.

Ms. Brenner: Interpretation of data, manuscript revision.

Ms. Hoogenboom: Analysis and interpretation of data, manuscript revision.

Dr. Kircheis: Analysis and interpretation of data, manuscript revision.

Prof. Häussinger: Manuscript revision.

Prof. Schnitzler: Study design, interpretation of data, manuscript revision.

Disclosure:

Ms. May was supported by travel allowances by the Boehringer Ingelheim Fonds (B.I.F.) and the German Academic Exchange Service (DAAD). Dr. Butz was supported by a Marie Curie Fellowship of the EU (FP7-PEOPLE-2009-IEF-253965).

Dr. Kahlbrock received funding by the Studienstiftung des Deutschen Volkes and a travel allowance by the Boehringer Ingelheim Fonds (B.I.F.). Ms. Brenner and Ms. Hoogenboom report no disclosures. Dr. Kircheis and Prof. Häussinger belong to a group of patent holders for a bedside device for determination of critical flicker frequency. Prof. Schnitzler reports no disclosures.

Acknowledgements:

We are very thankful to Prof. Dr. Joachim Gross from the University of Glasgow and Dr. Tolga Özkurt from the Middle East Technical University Ankara for technical advice regarding data analysis. We furthermore thank Mr. Diethelm Plate from the Department of Gastroenterology, Hepatology and Infectious Diseases of the University of Düsseldorf for help in patient recruitment and psychometric testing,

Ms. Alla Solutuchin and Mr. Ulf Zierhut for help with the MEG data collection and Ms. Erika Rädisch for help with MRI acquisitions. Last but not least, we thank all participants who kindly took part in this study.

Abstract

Objectives: Motor and attentional symptoms of hepatic encephalopathy (HE) have recently been associated with slowed and pathologically synchronized oscillatory activity in related brain areas. Earlier studies already indicated an impaired processing of somatosensory stimuli in HE. However, oscillatory activity in this context has not been characterized so far. Here, we investigated the modulation of oscillatory alpha activity associated with median nerve stimulation within the primary somatosensory cortex (S1).

Methods: 21 patients with liver cirrhosis and varying degrees of low-grade HE and 7 healthy control subjects received electrical stimulation of the right median nerve while brain activity was recorded using magnetoencephalography (MEG). S1 oscillatory alpha activity contralateral to the stimulated hand and its stimulus-induced modulation were analyzed as a function of HE severity quantified by a clinical assessment including the critical flicker frequency (CFF).

Results: Median nerve stimuli evoked an early broadband power increase followed by suppression and later rebound of alpha activity. This rebound significantly differed between patients with manifest HE and healthy control subjects. Increasing HE severity as quantified by the CFF was associated with a slowing of the alpha peak frequency in S1 and a delayed alpha rebound.

Conclusions: The present results provide evidence for a slowing of S1 alpha activity, extending previous findings of slowed oscillatory activity as a hallmark in the pathophysiology of HE to the somatosensory system. The delayed alpha rebound can be interpreted as an impaired, i.e. slowed, capability of S1 to adjust activation levels back to the default state in HE.

1. Introduction

Hepatic encephalopathy (HE) is associated with slowed and pathologically synchronized neuronal oscillatory activity. Magneto- and electroencephalography studies (M/EEG) demonstrated a slowing of the peak frequency of spontaneous brain activity¹⁻³ and a stronger but slowed thalamo-cortico-muscular coupling associated with the motor symptoms of HE⁴⁻⁶. In addition, a slowing and impaired attentional modulation of stimulus-induced visual gamma band activity was shown⁷. Interestingly, studies using the critical flicker frequency (CFF) as a marker of HE severity⁸⁻¹¹ revealed a correlation of the slowing of oscillatory activity with the CFF^{5,7}. Hence, slowed oscillatory activity in various subsystems of the brain is thought to be a key pathophysiological mechanism underlying the different clinical symptoms in HE^{5,12}.

Somatosensory evoked potentials (SEP) allow insights into somatosensory processing in HE. A prolongation of peak and inter peak latencies in combination with a deformation or loss of SEP components indicated altered and delayed processing of simple somatosensory stimuli¹³⁻¹⁶. A predominant feature of the somatosensory system is oscillatory alpha activity (8 to 12 Hz) reflecting the degree of engagement/disengagement of a cortical region¹⁷⁻¹⁹. The processing of somatosensory stimuli in early somatosensory cortices is associated with an initial suppression of alpha activity followed by a rebound to or above baseline levels²⁰⁻²².

In the present study, we used MEG to characterize alpha activity in primary somatosensory areas in the context of median nerve stimulation in HE. Our findings provide evidence for a slowing of somatosensory alpha activity and a delayed stimulus-associated alpha rebound.

2. Methods

2.1 Standard protocol approvals, registrations, and patient consents

The study was approved by the local ethics committee (study no. 2895) of the University hospital Düsseldorf and conducted in conformity with the Declaration of Helsinki. All subjects participated in the study after giving written informed consent.

2.2 Subjects and clinical evaluation

21 patients with liver cirrhosis and 7 healthy controls underwent a clinical assessment and standard blood examination including venous ammonia levels. A battery of 5 computerized neuropsychological tests from the Vienna Test System (Dr. Schuhfried GmbH, Mödling, Austria)²³ with 22 evaluable neurophysiologic parameters directed to cognition, emotion and behavior was used as previously described^{6,8}. Test results were considered abnormal, when they were outside 1 standard deviation from the mean of a large age-matched control population²³. Patients without evidence for manifest HE according to the mental state were defined as having *HE0* when ≤ 1 of the computerpsychometric test results were abnormal and as *mHE* (minimal HE) when ≥ 2 were abnormal. Patients were classified as having *HE1* according to the mental state as defined by the West-Haven criteria²⁴. A fourth group comprised age-matched, healthy control subjects. Determinations of CFF thresholds were performed as previously described^{6,8,12,23,25}. Please see table 1 for single subject characteristics.

Exclusion criteria were neurological and psychiatric diseases other than HE, intake of psychoactive drugs, a history of severe HE (HE3 or HE4), acute gastrointestinal

haemorrhage or spontaneous bacterial peritonitis during the last 7 days and significant non-hepatic diseases. Patients with a history of alcohol abuse had to have remained abstinent for at least 4 weeks. Sensory neuropathy of the median and radial nerves was ruled out clinically and by bilateral sensory nerve conduction measures.

– Please insert Table 1 about here –

2.3 Paradigm and MEG recording

Non-painful 0.3 ms pulses of electric current were applied to the right median nerve at the wrist. Stimulation intensity was individually adjusted to be slightly above motor threshold and to elicit a small thumb twitch (mean amplitude \pm SD: 4.3 ± 1.3 mA). 300 stimuli were administered with a constant interstimulus interval of 2 s. Subjects passively perceived the stimuli with open eyes and no other task. Neuromagnetic brain activity was measured with a 306-channel MEG system (Elekta Oy, Helsinki, Finland). Individual structural magnetic resonance images (MRIs) were obtained with a 3 T Siemens Magnetom MRI scanner (Munich/Erlangen, Germany) for co-registration with MEG data. For three participants, a template MRI was used²⁶.

2.4 MEG data analysis

Data were analyzed using Matlab 7.1 (Mathworks, Natick, MA, USA), FieldTrip²⁷ and IBM SPSS Statistics 20 (IBM Corporation, Somers, USA).

2.4.1 Preprocessing

MEG data were divided into non-overlapping epochs of interest surrounding each median nerve stimulus using data of the 204 planar gradiometers only. Epochs and sensors with high variance due to artifacts were removed.

2.4.2 Virtual sensor analysis

Analysis of oscillatory brain activity was performed in source space using a linearly constrained minimum variance (LCMV)²⁸ beamformer. First, the strongest source of evoked responses to median nerve stimulation was localized for each individual. Then, this source was used as a virtual sensor location and single-trial time courses within the source were estimated. The obtained source waveforms were then used for further analysis.

To determine the source of evoked responses to median nerve stimulation, covariance matrices across all MEG sensors were calculated from the average across all trials after filtering the preprocessed data between 3 and 50 Hz. This was done separately for a pre-stimulus baseline (-0.5 to -0.3 s) and a post-stimulus interval (0 to 0.2 s) including strongest stimulus-evoked responses. From these covariance matrices, neural activity during both intervals was localized using individual, realistically shaped single-shell volume conduction models²⁹. Spatial filters were constructed to estimate source activity for points along a regular 5-mm grid. For each grid point, the ratio of post-stimulus to pre-stimulus activity was computed. The grid point showing the highest activity-ratio in response to median nerve stimulation was selected as virtual sensor location. The brain areas closest to the virtual sensor location were identified using the AFNI atlas (<http://afni.nimh.nih.gov/afni>).

For each individual, source waveforms at the virtual sensor location were then reconstructed. To this end, covariance matrices were computed for the averaged, non-overlapping trials from -1 to 1 s with respect to stimulus onset after filtering (3 and 50 Hz) and baseline-correction (-0.5 to -0.3 s). From these covariance matrices, a spatial filter was created. Single trial sensor data of ± 2.5 s length were projected through this filter to obtain the source waveforms.

2.4.3 Time frequency analysis

Time-frequency representations (TFRs) of power were estimated using the fast Fourier transform (FFT). For each trial, an adaptive time window of 4 cycles length was shifted in 10 ms time-steps across the complete source waveform of each trial. After applying a Hanning taper, power was estimated for frequencies between 1 and 25 Hz in steps of 1 Hz. Then, TFRs were averaged across trials for each subject. Subsequent analysis focused on the time interval from 0 to 2 s, comprising the time period from the onset of the stimulus to the onset of the subsequent stimulus, i.e. one complete stimulus cycle. To normalize for inter-individual differences, power values were divided by the mean power across the complete time-interval.

2.4.4 Alpha peak frequencies

To obtain estimates of the individual peak frequency of somatosensory alpha activity, segments of data from 0 to 2 s were extracted from the source waveforms and multiplied with a Hanning taper prior to applying a fast Fourier transform (FFT). Power spectra were computed between 1 and 25 Hz and the frequency between 6 and 14 Hz with the highest power was determined for each subject. To confirm that the determined alpha peak frequencies were not mainly driven by early stimulus-

evoked activity, alpha peak frequency determination was repeated on a time interval from 0.7 to 2 s.

2.4.5 Time of maximal alpha rebound

To quantify the time of the maximal rebound of alpha activity to or above baseline levels after its initial stimulus-induced suppression, the time course of alpha activity was estimated for each subject. Power obtained from TFRs was averaged across a 4 Hz frequency band comprising the individual alpha peak frequency \pm 2 Hz. Then, the time point of alpha rebound defined as the maximum alpha power during the period of 0.7 to 1.8 s after stimulus onset was extracted. The time window was chosen to start after the initial alpha suppression and end 0.2 s prior to the subsequent stimulus to avoid an intermixture of alpha activity estimates with stimulus-induced alpha increases from the next stimulus.

2.4.6 Statistics

Differences between TFRs from the four subject groups were examined by statistical group comparisons. Independent sample t-tests were calculated for each time-frequency-point between 5 and 25 Hz. Statistical inference was based on a non-parametric cluster-based randomization test^{30,31}.

Differences of stimulation intensities for median nerve stimulation, alpha peak frequencies and the time of alpha rebound between the different subject groups were analyzed using analysis of variance (ANOVA). Post-hoc tests were performed using one-sided independent samples *t*-tests, applying Bonferroni-Holm correction (13) to all *p*-values. To test for relations between stimulation intensities, blood levels of ammonia, the alpha peak frequency, the time of alpha rebound and the CFF,

partial one-sided Pearson's correlation coefficients were calculated, correcting for effects of age.

3. Results

Stimulation intensities used for median nerve stimulation (Table 2) were not significantly different between the four groups ($F_{(3,24)} = 2.97, p > .05$). In addition, no significant correlation with the CFF was found ($r = .33, p > .05$), indicating that individually adjusted stimulation intensities did not depend on HE disease severity.

– Please insert Table 2 about here –

3.1 Localization of evoked responses for virtual sensor analysis

For each subject, the strongest source of evoked responses during the first 0.2 s after median nerve stimulation was localized for placement of a virtual sensor. Localizations were consistent with the primary somatosensory cortex (S1) contralateral to the stimulated hand (Table 2 & Fig. 1).

– Please insert Figure 1 about here –

3.2 Time frequency analysis

In all four groups under study, median nerve stimuli elicited an early broadband power increase reflecting the evoked response, followed by a suppression of activity in alpha and beta frequency bands and a rebound to or above baseline levels (Fig. 2A). Cluster-based randomization statistics revealed a cluster of increased alpha activity from 5 to 13 Hz and 0.9 to 1.9 s for the comparison between HE1 patients

and healthy controls (Fig. 2B, $p < .01$), in line with a stronger and/or delayed rebound of alpha activity in patients with overt symptoms of HE. No other group differences were observed.

– Please insert Figure 2 about here –

3.3 Alpha peak frequencies

To examine a possible slowing of S1 alpha activity, individual alpha peak frequencies were determined (Table 2). An ANOVA revealed a significant effect of the subject group (Fig. 3A, left panel; $F_{(3,24)} = 3.83$, $p = .02$). Post-hoc tests showed lower alpha peak frequencies for mHE patients compared to controls ($p = .03$) and a trend towards lower alpha peak frequencies for HE1 patients compared to controls ($p = .06$). Correlations between the CFF and the alpha peak frequency revealed a positive relation between the two measures, across all subjects (Fig. 3A, middle panel; $r = .44$, $p = .01$) as well as for patients only (Fig. 3A, right panel; $r = .50$, $p = .02$). Further analysis showed a trend for a negative relation between the alpha peak frequency and the blood level of ammonia for all subjects ($r = -.26$, $p = .098$). Thus, the individual alpha peak frequency was slowed with increasing HE severity and there was a trend for an association of lower alpha peak frequencies with higher blood ammonia levels.

To confirm that the obtained alpha peak frequencies were not mainly driven by early stimulus-induced alpha activity increases, alpha peak frequency analysis was repeated based on the time interval from 0.7 to 2 s covering the alpha rebound. Again, the same pattern of results was found (ANOVA: $F_{(3,24)} = 3.33$, $p = .04$, post-hoc test controls vs. mHE: $p < .05$, post-hoc test controls vs. HE1: $p = .06$;

correlation CFF vs. alpha peak frequency: all subjects: $r = .38$, $p = .03$, patients only: $r = .49$, $p = .02$). For subsequent analyses, peak frequencies determined from the complete period were used.

– Please insert Figure 3 about here –

3.4 Time of maximal alpha rebound

To investigate a possible delay of the alpha rebound in HE, the time point of maximal alpha power during the rebound period was determined (Table 2). An ANOVA did not reveal significant differences between the four groups (Fig. 3B, left panel; $F_{(3,24)} = 1.21$, $p > .05$). However, the time of alpha rebound inversely correlated with the CFF across all subjects (Fig. 3B, middle panel; $r = -.36$, $p = .04$) and showed a trend for a correlation for patients only (Fig. 3B, right panel; $r = -.32$, $p = .09$). Further analyses revealed a positive relation between the time of alpha rebound and the blood ammonia level across all subjects ($r = .36$, $p = .03$) and a trend for patients only ($r = .34$, $p = .07$). Thus, a later time of alpha rebound was associated with higher blood ammonia levels and increasing disease severity as quantified by the CFF.

4. Discussion

The aim of the current study was to investigate potential pathological alterations of oscillatory alpha activity associated with the processing of somatosensory stimuli in HE. Our results provide first time evidence for a slowing of alpha activity in primary somatosensory cortex in combination with a delayed stimulus-induced modulation.

Even in the early stages of HE examined here, these neurophysiological alterations depended on disease severity as quantified by the CFF.

The current results were composed of several key findings. Initial time-frequency analyses of S1 source waveforms demonstrated that S1 alpha activity was first suppressed by median nerve stimulation and then rebounded to or above baseline levels, thereby tallying previous findings²⁰⁻²². Compared to healthy controls, group statistics revealed that this rebound was altered in HE1 patients, showing enhanced alpha activity in the frequency band of 5 to 13 Hz between 0.9 to 1.9 s after stimulation. Further analyses indicated that different features of S1 alpha activity are affected in HE and most likely contribute to this pattern. First, the peak frequency of S1 alpha activity was slowed in HE, as shown by both comparisons of the clinical groups and correlations with the CFF. Second, the time of alpha rebound in individually-adjusted frequency bands showed a negative correlation with the CFF, indicating a later rebound with increasing disease severity.

The observed slowed peak frequency of S1 alpha activity matches previous findings in HE patients showing slowed neuronal oscillatory activity of spontaneous brain activity¹⁻³ and in relation to motor symptoms⁴⁻⁶ and visual attention deficits⁷.

Therefore, the present findings extend these previous results to the somatosensory system and provide further evidence that HE affects oscillatory activity across different neuronal (sub-)systems and frequency bands. Thereby, the hypothesis of slowed oscillatory brain activity as a key hallmark of HE^{5,12} is further substantiated, expanding our understanding of the pathophysiological mechanisms of this disease.

The delayed rebound of alpha activity reported here is in line with previous SEP studies which showed delayed stimulus processing with increasing HE severity¹³⁻¹⁶.

These studies focused on immediate stimulus processing measured by evoked

responses in the first few hundred milliseconds after median nerve stimulation. Here, we studied modulations of oscillatory alpha activity at a larger time scale and up to 2 s after stimulation, reflecting changes in the overall activation state of the corresponding cortical area rather than immediate stimulus processing. The alpha rebound is part of a typical sequence of alpha modulation in response to simple somatosensory stimuli and follows an initial suppression of oscillatory alpha activity reflecting cortical activation²⁰⁻²². A delay of this rebound in HE can be interpreted as an impaired capability to return to the pre-stimulus or default state of cortical activation and a reduced flexibility of the somatosensory system to adjust activation levels back to baseline levels. These results are in accordance with a study on covert visual attention processes in a large cohort of cirrhotic patients without overt HE³², which demonstrated a reduced capability of cirrhotic patients to disengage visual attention previously focused on a cued location. Together with the current results, these data suggest a decreased capability to detach attentional resources from a stimulus, already present in low-grade HE. This compromised efficiency might be reflected by an impaired ability to modulate oscillatory activity to allocate attention, particularly in the alpha frequency band.

Stimulation intensities used for median nerve stimulation in the current study were individually adjusted to be slightly above motor threshold, but did not show a relation to disease severity. Up to now, no studies have been published, which systematically characterized somatosensory function in HE on a behavioral level. However, it is conceivable that the delayed stimulus processing shown here impairs associated behavioral responses and/or hinders subsequent stimulus processing. Future studies need to combine neurophysiological with psychophysical measures

of somatosensory processing in HE to investigate how altered oscillatory activity affects behavior.

Correlations between the CFF and neurophysiological parameters were found both when considering all subjects and when the analysis was restricted to patients only, demonstrating that correlations were not mainly due to differences in parameters between patients and healthy control subjects. Instead, even within the patient population comprising HE0 and low-grade HE, i.e. mHE and HE1, neurophysiological measures were closely related to HE severity as quantified by the CFF. Ongoing discussions question the usefulness of the common classification scheme of HE and suggest to approach the neurocognitive changes in HE as a continuum rather than defining a limited number of distinct stages of the disease^{33–35}. The current study tallies the notion that the CFF as a continuous measure is most sensitive in detecting relations between neurophysiological measures, behavior and disease severity^{7,8,36}. In line with the role suggested for ammonia in the pathophysiology of HE³⁴, the current results furthermore provide evidence that the neurophysiological alterations reported here are associated with a higher blood ammonia level.

In conclusion, the present study demonstrates alterations of somatosensory alpha activity and its stimulus-induced modulation in early stages of HE as a function of disease severity. The finding of slowed oscillatory alpha activity in primary somatosensory cortex extends results of slowed oscillatory activity from the motor and visual to the somatosensory system, extending our understanding of the pathophysiological processes in HE. The delayed processing of simple somatosensory stimuli in HE patients indicates an impaired capability of the

somatosensory system to return to the pre-stimulus or default state of activation, of which the behavioral consequences still need to be examined further.

References

1. Kullmann F, Hollerbach S, Lock G, Holstege A, Dierks T, Schölmerich J. Brain electrical activity mapping of EEG for the diagnosis of (sub)clinical hepatic encephalopathy in chronic liver disease. *Eur J Gastroenterol Hepatol* 2001;13:513–522.
2. Montagnese S, Jackson C, Morgan MY. Spatio-temporal decomposition of the electroencephalogram in patients with cirrhosis. *J Hepatol* 2007;46:447–458.
3. Amodio P, Orsato R, Marchetti P, et al. Electroencephalographic analysis for the assessment of hepatic encephalopathy: comparison of non-parametric and parametric spectral estimation techniques. *Neurophysiol Clin* 2009;39:107–115.
4. Timmermann L, Gross J, Kircheis G, Häussinger D, Schnitzler A. Cortical origin of mini-asterixis in hepatic encephalopathy. *Neurology* 2002;58:295–298.
5. Timmermann L, Butz M, Gross J, et al. Impaired cerebral oscillatory processing in hepatic encephalopathy. *Clin Neurophysiol* 2008;119:265–272.
6. Timmermann L, Gross J, Butz M, Kircheis G, Häussinger D, Schnitzler A. Mini-asterixis in hepatic encephalopathy induced by pathologic thalamo-motor-cortical coupling. *Neurology* 2003;61:689–692.
7. Kahlbrock N, Butz M, May ES, et al. Lowered frequency and impaired modulation of gamma band oscillations in a bimodal attention task are associated with reduced critical flicker frequency. *Neuroimage* 2012;61:216–227.
8. Kircheis G, Wettstein M, Timmermann L, Schnitzler A, Häussinger D. Critical flicker frequency for quantification of low-grade hepatic encephalopathy. *Hepatology* 2002;35:357–366.

9. Sharma P, Sharma BC, Puri V, Sarin SK. Critical flicker frequency: diagnostic tool for minimal hepatic encephalopathy. *J Hepatol* 2007;47:67–73.
10. Romero-Gómez M, Córdoba J, Jover R, et al. Value of the critical flicker frequency in patients with minimal hepatic encephalopathy. *Hepatology* 2007;45:879–885.
11. Prakash R, Mullen KD. Mechanisms, diagnosis and management of hepatic encephalopathy. *Nat Rev Gastroenterol Hepatol* 2010;7:515–525.
12. Timmermann L, Butz M, Gross J, Kircheis G, Häussinger D, Schnitzler A. Neural synchronization in hepatic encephalopathy. *Metab Brain Dis* 2005;20:337–346.
13. Blauenfeldt RA, Olesen SS, Hansen JB, Graversen C, Drewes AM. Abnormal brain processing in hepatic encephalopathy: evidence of cerebral reorganization? *Eur J Gastroenterol Hepatol* 2010;22:1323–1330.
14. Chu NS, Yang SS. Somatosensory and brainstem auditory evoked potentials in alcoholic liver disease with and without encephalopathy. *Alcohol* 1987;4:225–230.
15. Yang SS, Chu NS, Liaw YF. Somatosensory evoked potentials in hepatic encephalopathy. *Gastroenterology* 1985;89:625–630.
16. Davies MG, Rowan MJ, Feely J. EEG and event related potentials in hepatic encephalopathy. *Metab Brain Dis* 1991;6:175–186.
17. Pfurtscheller G, Stancák A Jr, Neuper C. Event-related synchronization (ERS) in the alpha band--an electrophysiological correlate of cortical idling: a review. *Int J Psychophysiol* 1996;24:39–46.

18. Jensen O, Mazaheri A. Shaping functional architecture by oscillatory alpha activity: gating by inhibition. *Front Hum Neurosci* 2010;4:186.
19. Foxe JJ, Snyder AC. The role of alpha-band brain oscillations as a sensory suppression mechanism during selective attention. *Front Psychol* 2011;2:154.
20. Nikouline VV, Linkenkaer-Hansen K, Wikström H, et al. Dynamics of mu-rhythm suppression caused by median nerve stimulation: a magnetoencephalographic study in human subjects. *Neurosci Lett* 2000;294:163–166.
21. Della Penna S, Torquati K, Pizzella V, et al. Temporal dynamics of alpha and beta rhythms in human SI and SII after galvanic median nerve stimulation. A MEG study. *Neuroimage* 2004;22:1438–1446.
22. Salenius S, Schnitzler A, Salmelin R, Jousmäki V, Hari R. Modulation of human cortical rolandic rhythms during natural sensorimotor tasks. *Neuroimage* 1997;5:221–228.
23. Vienna test system (WINWTS) Version 4.50. Dr. G. Schuhfried GmbH, Mödling, Austria; 1999.
24. Ferenci P, Lockwood A, Mullen K, Tarter R, Weissenborn K, Blei AT. Hepatic encephalopathy--definition, nomenclature, diagnosis, and quantification: final report of the working party at the 11th World Congresses of Gastroenterology, Vienna, 1998. *Hepatology* 2002;35:716–721.
25. Eberhardt G. Flimmerfrequenz-Analysator. Automatische Messmethode. Version 3.00. Dr. G. Schuhfried GmbH, Mödling, Austria; 1994.
26. Litvak V, Mattout J, Kiebel S, et al. EEG and MEG data analysis in SPM8. *Comput Intell Neurosci* 2011;2011:852961.

27. Oostenveld R, Fries P, Maris E, Schoffelen J-M. FieldTrip: Open source software for advanced analysis of MEG, EEG, and invasive electrophysiological data. *Comput Intell Neurosci* 2011;2011:156869.
28. Van Veen BD, van Drongelen W, Yuchtman M, Suzuki A. Localization of brain electrical activity via linearly constrained minimum variance spatial filtering. *IEEE Trans Biomed Eng* 1997;44:867–880.
29. Nolte G. The magnetic lead field theorem in the quasi-static approximation and its use for magnetoencephalography forward calculation in realistic volume conductors. *Phys Med Biol* 2003;48:3637–3652.
30. Maris E, Oostenveld R. Nonparametric statistical testing of EEG- and MEG-data. *J Neurosci Methods* 2007;164:177–190.
31. Nichols TE, Holmes AP. Nonparametric permutation tests for functional neuroimaging: a primer with examples. *Hum Brain Mapp* 2002;15:1–25.
32. Amodio P, Schiff S, Del Piccolo F, Mapelli D, Gatta A, Umiltà C. Attention dysfunction in cirrhotic patients: an inquiry on the role of executive control, attention orienting and focusing. *Metab Brain Dis* 2005;20:115–127.
33. Bajaj JS, Wade JB, Sanyal AJ. Spectrum of neurocognitive impairment in cirrhosis: Implications for the assessment of hepatic encephalopathy. *Hepatology* 2009;50:2014–2021.
34. Häussinger D, Kircheis G, Schliess F. *Hepatic Encephalopathy and Nitrogen Metabolism*. 1st ed. Dordrecht: Springer; 2006.
35. Kircheis G, Fleig WE, Görtelmeyer R, Grafe S, Häussinger D. Assessment of low-grade hepatic encephalopathy: a critical analysis. *J Hepatol* 2007;47:642–650.

36. Butz M, Timmermann L, Braun M, et al. Motor impairment in liver cirrhosis without and with minimal hepatic encephalopathy. *Acta Neurol Scand* 2010;122:27–35.
37. Pugh RN, Murray-Lyon IM, Dawson JL, Pietroni MC, Williams R. Transection of the oesophagus for bleeding oesophageal varices. *Br J Surg* 1973;60:646–649.

Table 1: Participant data.

Individual subject characteristics are given for the four groups as graded by the *West-Haven-Criteria*²⁴ and neuropsychometric test results⁸: Controls = healthy, age-matched control subjects, HE0 = cirrhotic patients showing no signs of HE, mHE = cirrhotic patients without clinical signs of HE but pathological results in ≥ 2 neuropsychometric tests, HE1 = cirrhotic patients showing clinically overt symptoms of HE. Age, gender, the critical flicker frequency and characteristics of the liver cirrhosis are given. Data from the different groups is summarized using mean values \pm standard deviation. Etiology of liver cirrhosis was assessed by each patient's medical history. Liver cirrhosis was confirmed by histology or fibroscan (> 13 kPa). Grading of liver cirrhosis was performed according to the European *Child-Pugh-classification*³⁷. F = female, M = male, CFF = critical flicker frequency, ALC = alcoholic, CRYP = cryptogenic, HCV= hepatitis C virus, PBC = primary biliary cirrhosis, PSC = primary sclerosing cholangitis. Please note that subject 19 had reduced eyesight of only 25% on one eye, disallowing a valid CFF measurement.

<i>Group</i>	<i>Subj. no.</i>	<i>Age (y)</i>	<i>Sex</i>	<i>CFF (Hz)</i>	<i>Cirrhosis etiology</i>	<i>Child Pugh score</i>
Controls	1	52	M	44.6	-	-
	2	58	F	41.4	-	-
	3	61	F	39.4	-	-
	4	74	M	38.1	-	-
	5	67	M	46.2	-	-
	6	48	M	39.3	-	-
	7	69	M	38.1	-	-
	n = 7	61.3 ± 9.4		41.0 ± 3.2		
HE0	8	50	M	43.2	ALC	A
	9	44	F	43.3	PSC	A
	10	70	F	42.2	HCV	A
	11	76	F	39.6	CRYP	B
	12	62	F	39.6	PBC	A
	13	54	M	42.7	HCV	A
		n = 6	59.3 ± 12.2		41.8 ± 1.7	
mHE	14	67	F	40.2	HCV	A
	15	63	M	39.3	ALC	A
	16	52	M	39.3	HCV	A
	17	62	M	40.4	CRYP	A
	18	56	M	42.0	HCV	A
	19	77	M	-	HCV	A
	20	53	F	41.3	ALC	B
	21	43	F	37.1	ALC	C
	n = 8	59.1 ± 10.4		39.9 ± 1.6		
	22	57	M	38.0	ALC	B

23	58	M	36.7	HCV	C
24	45	M	36.2	PSC	B
25	61	M	35.5	HCV	C
26	70	M	37.6	ALC	A
27	63	M	36.7	ALC	A
28	47	M	36.2	ALC	B
n = 7	57.3 ± 8.8		36.7 ± 0.9		

Table 2: MEG-related data.

Individual MEG-related data are given for the four groups as described in table 1.

Individual stimulation intensities used for median nerve stimulation, the alpha peak frequency in the primary somatosensory cortex, the time of maximal alpha power during the rebound period and details on the virtual sensor location are given. Data from the different groups is summarized using mean values \pm standard deviation.

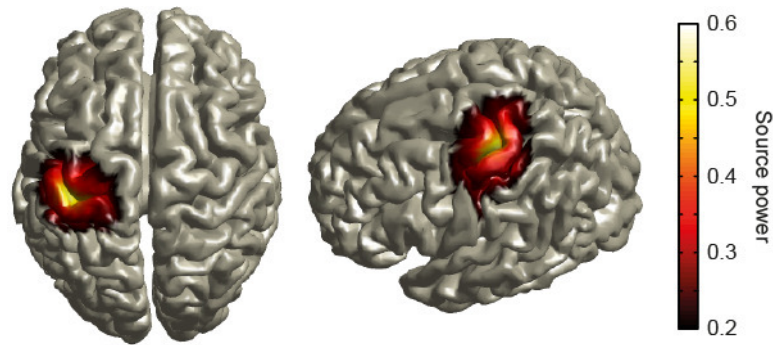
MNI = Montreal Neurological Institute. For subjects 11, 27 and 28, a template MRI was used for co-registration with MEG data.²⁶

Group	Subj. no.	Stimulation intensity (mA)	Alpha peak frequency (Hz)	Time of maximal alpha rebound (s)	Virtual sensor location			
					MNI coordinates			Closest label(s)
					x	y	z	
Controls	1	3.2	14	0.9	-3.7	1.9	8.5	Postcentral gyrus, BA 3
	2	4.5	13	1.8	-3.7	-0.3	8.5	Postcentral gyrus, BA 3
	3	5.0	13	1.0	-3.2	-0.0	8.6	Precentral gyrus
	4	7.0	11	1.8	-3.8	-0.6	9.3	Postcentral gyrus, BA 3
	5	7.5	9	0.9	-4.6	0.3	8.9	Postcentral gyrus
	6	4.0	9	1.0	-3.3	0.2	9.0	Precentral gyrus
	7	3.0	11	0.9	-4.5	-0.2	8.8	Postcentral gyrus
	n = 7	4.9 ± 1.8	11.4 ± 2.0	1.2 ± 0.4				
HE0	8	4.5	13	1.1	-3.9	0.9	8.9	Postcentral gyrus, BA 3
	9	3.2	10	0.8	-4.3	-0.5	8.1	Postcentral gyrus
	10	3.4	14	0.9	-4.5	0.3	9.4	Precentral gyrus
	11	2.7	9	1.8	-5.0	0.2	8.8	Precentral gyrus
	12	3.2	7	1.4	-3.7	-0.9	7.8	Postcentral gyrus
	13	3.5	12	1.1	-3.5	-0.6	9.7	No label found
	n = 6	3.4 ± 0.6	10.8 ± 2.6	1.2 ± 0.4				

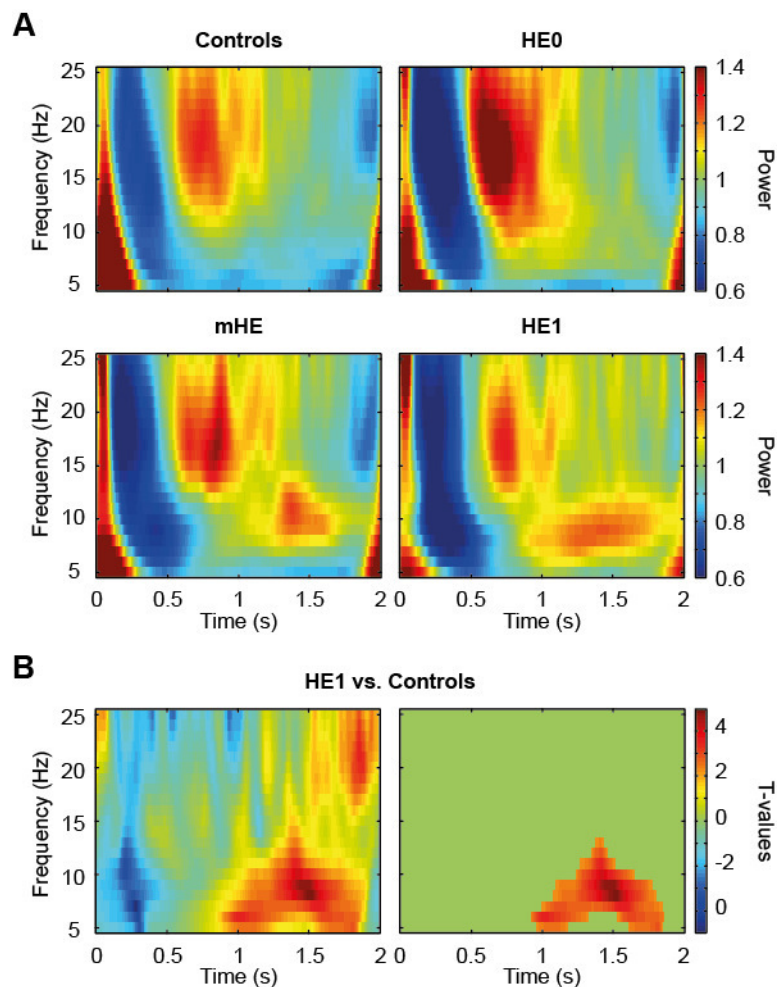
	14	5.0	9	1.8	-4.3	-0.4	8.1	Postcentral gyrus
	15	4.6	8	1.7	-4.3	-0.9	6.9	Inferior parietal lobule
	16	5.0	8	1.7	-3.9	0.1	7.6	Postcentral gyrus, BA 3
	17	4.5	9	1.5	-5.0	1.3	8.7	Postcentral gyrus
mHE	18	5.5	10	1.1	-3.6	-0.4	9.6	Postcentral gyrus, BA 3/1
	19	4.4	11	1.6	-4.2	0.5	9.0	Precentral gyrus
	20	6.5	7	1.3	-3.8	0.5	8.3	Postcentral gyrus, BA 3
	21	3.4	6	1.1	-3.8	0.3	8.9	Postcentral gyrus, BA 3
	n = 8	4.9 ± 0.9	8.5 ± 1.6	1.5 ± 0.3				
	22	4.0	8	1.8	-4.7	-0.0	8.3	Postcentral gyrus
	23	5.0	9	1.6	-3.9	-0.5	10.6	Precentral gyrus
	24	3.0	10	1.1	-4.8	0.0	9.3	Postcentral gyrus
HE1	25	4.0	8	1.4	-4.4	0.1	8.4	Postcentral gyrus
	26	4.6	8	1.4	-4.4	0.8	8.5	Precentral gyrus
	27	3.4	12	0.9	-4.0	-1.3	7.1	BA 13
	28	2.0	7	1.3	-4.4	-0.6	8.5	Precentral gyrus
	n = 7	3.7 ± 1.0	8.9 ± 1.7	1.4 ± 0.3				

Figure titles and legends

Figure 1: Localization of evoked responses for virtual sensor analysis



Locations for the virtual sensor analysis were obtained from analysis of evoked responses to median nerve stimuli and were consistent with the contralateral primary somatosensory cortex contralateral to the stimulated hand. For visualization, individual maps of stimulus-evoked power increases were normalized by setting their maximum value to 1 and averaged across all subjects. This resulted in an average power increase with dimension-less values (color-coded). Values below 0.2 are masked. Please note that for each subject the point of the individual maximum of the power increase was used as virtual sensor location.

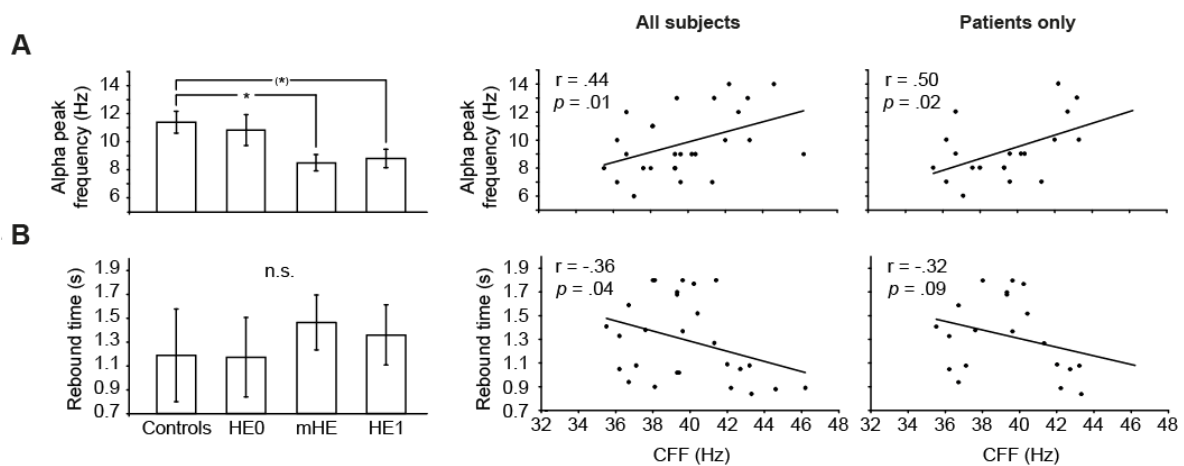
Figure 2: Time frequency representations and statistical results

A. Virtual sensor time frequency representations (TFRs) averaged across subjects in the four different subject groups (controls, HE0, mHE, HE1). Time-point 0 represents the onset of the median nerve stimulus (please note that the subsequent stimulus was administered at 2 s). Color-coded are power values normalized to the average power across the complete time interval (0 to 2 s). A value of 1 corresponds to the average power, while values higher than 1 indicate power above and values smaller than 1 power below average.

B. Statistical comparison of TFRs between the groups of HE1 patients and healthy control subjects. Color-coded are t -values quantifying the contrast between the two

groups. Positive values indicate higher, negative values lower power for HE1 patients. In the left panel, t -values are shown for all time-frequency points. In the right panel, non-significant time-frequency points are masked. Statistical analysis revealed a significant cluster ($p < .01$) of increased alpha power in HE1 patients compared to healthy controls. This cluster extends from 5 to 15 Hz and between 0.9 and 1.9 s, indicating an increased and/or delayed alpha rebound in HE1 patients.

Figure 3: Analysis of alpha peak frequencies and time of alpha rebound



A. Left panel: Mean values of alpha peak frequencies for all four groups (controls, HE0, mHE, HE1). Error bars indicate the standard error of measurement. Analysis of variance and subsequent post-hoc tests were performed to investigate group differences in alpha peak frequencies. Comparisons showing differences between groups are marked (*) $p < 0.1$, $*$ $p < 0.05$). Compared to healthy controls, statistics revealed lower alpha peak frequencies in mHE patients and a trend towards lower alpha peak frequencies in HE1 patients. Middle and right panel: Correlation of the critical flicker frequency (CFF) with the alpha peak frequency for all subjects (middle

panel) and patients only (right panel). Correlation coefficients and corresponding p -values are given in the figure. Please note that all correlation coefficients were corrected for effects of age. Correlations revealed that a lower CFF is associated with a lower alpha peak frequency.

B. Same as A. but for the time of maximal alpha rebound, i.e. the time point of maximum alpha power between 0.7 and 1.8 s (n.s. = not significant). While no significant group differences were observed, an inverse correlation between the CFF and the time of alpha rebound for all subjects and a trend towards an inverse correlation for patients only were found. Thus, a lower CFF was associated with a later alpha rebound.



Contents lists available at ScienceDirect

NeuroImage

journal homepage: www.elsevier.com/locate/ynimg

Sustained gamma band synchronization in early visual areas reflects the level of selective attention

Nina Kahlbrock^{a,*}, Markus Butz^{a,b,1}, Elisabeth S. May^a, Alfons Schnitzler^{a,c}

^a Heinrich-Heine-University Düsseldorf, Medical Faculty, Institute of Clinical Neuroscience and Medical Psychology, Universitätsstraße 1, D-40225 Düsseldorf, Germany

^b University College London, Institute of Neurology, 33 Queen Square, WC1N 3BG, London, United Kingdom

^c Heinrich-Heine-University Düsseldorf, Medical Faculty, Department of Neurology, Universitätsstraße 1, D-40225 Düsseldorf, Germany

ARTICLE INFO

Available online 23 July 2011

Keywords:

Synchronization
Gamma
Attention
Biased competition
MEG
Audiovisual

ABSTRACT

Cortical gamma band synchronization is associated with attention. Accordingly, directing attention to certain visual stimuli modulates gamma band activity in visual cortical areas. However, gradual effects of attention and behavior on gamma band activity in early visual areas have not yet been reported.

In the present study, the degree of selective visual attention was gradually varied in a cued bimodal reaction time paradigm using audio-visual stimuli. Brain activity was recorded with magnetoencephalography (MEG) and analyzed with respect to time, frequency, and location of strongest response.

Reaction times to visual and auditory stimuli reflected three presumed graded levels of visual attention (high, medium, and low). MEG data showed sustained gamma band synchronization in all three conditions in early visual areas (V1 and V2), while the intensity of gamma band synchronization increased with the level of visual attention (from low to high). Differences between conditions were seen for up to 1600 ms.

The current results show that in early visual areas the level of gamma band synchronization is related to the level of attention directed to a visual stimulus. These gradual and long-lasting effects highlight the key role of gamma band synchronization in early visual areas for selective attention.

© 2011 Elsevier Inc. All rights reserved.

Introduction

In our complex multisensory environment, it is essential to process relevant information while ignoring the rest. In case of competing input from two different modalities, stimuli in the attended modality receive amplified processing compared to stimuli in the non-attended modality (Gherri and Eimer, 2011; Spence and Driver, 1997). As stimulus processing is believed to be capacity-limited, allocating resources to one attended modality gradually subtracts resources from the available supply of all modalities (Bonnell and Hafter, 1998). Consequently, modulation of attentive processing in one modality can be studied by reallocating available resources between competing modality specific stimuli.

In the brain, attentional modulation of sensory processing has been associated with gamma band (30–100 Hz) synchronization (Fries et al., 2001; Hoogenboom et al., 2006, 2010; Kaiser et al., 2006; Lachaux et al., 2005; Steinmetz et al., 2000). Previous studies reported modulation of visually induced gamma band oscillations by attention in animals (Khayat et al., 2010) and humans (Gruber et al., 1999;

Siegel et al., 2008; Tallon-Baudry et al., 2005; Vidal et al., 2006; Wyart and Tallon-Baudry, 2008). In all these studies, states of ‘attention’ versus ‘no attention’ were compared. In an EEG study, Simos et al. (2002) provided first evidence that gamma band synchronization gradually increases with task complexity. However, changes remained unspecific and could not be attributed to modality specific regions.

Previous studies on selective visual attention suggest that the attended of two competing visual stimuli gets a competitive advantage over the other by enhancing its gamma band synchronization (Fries et al., 2001, 2008). This effect has been addressed in the hypothesis of biased competition through enhanced synchronization (Fries, 2005), which bases its assumptions on the biased competition hypothesis (Desimone and Duncan, 1995; Reynolds et al., 1999). Nevertheless, the conceptual framework of the biased competition hypothesis has yet to be tested for its application in cross-modal attention designs as for cross-modal designs it has only been addressed on a theoretical level for the visual-tactile domain (Magosso et al., 2010).

While several functional Magnetic Resonance Imaging studies showed that attention modulates processing of sensory information in early visual areas (Gandhi et al., 1999; Munneke et al., 2008), attention dependent modulation of gamma band synchronization has primarily been recorded in mid- and high level stages in the visual processing hierarchy (Fries et al., 2001; Gregoriou et al., 2009;

* Corresponding author at: Heinrich-Heine-University Düsseldorf, Medical Faculty, Institute of Clinical Neuroscience and Medical Psychology, Universitätsstraße 1, D-40225 Düsseldorf, Germany. Fax: +49 211 81 19033.

E-mail address: Nina.Kahlbrock@uni-duesseldorf.de (N. Kahlbrock).

¹ These two authors contributed equally to this work.

Womelsdorf et al., 2006). One study (Chalk et al., 2010) found decreased local field potential gamma band power and decreased gamma band spike field coherence with attention in monkey primary visual cortex. Previous works in humans using magnetoencephalography (MEG) have shown increased induced gamma band synchronization in visual areas V1–V3 during attention demanding tasks (Hoogenboom et al., 2006, 2010). Nevertheless, these neurophysiological results did not show graded attentional modulation of gamma band synchronization in early visual areas. In fact, up to now, studies on graded attentional modulation of induced gamma band synchronization in early visual areas in humans are lacking.

The present study is the first to systematically manipulate the level of visual attention, relate it to behavioral performance and to the intensity of gamma band synchronization in early visual areas. Subjects were simultaneously presented with visual (Hoogenboom et al., 2006) and auditory stimuli in a cued bimodal reaction time paradigm resulting in a gradual modulation of visual attention.

Materials and methods

Subjects

Sixteen healthy right-handed subjects with normal or corrected to normal vision participated in this study (8 female, mean age: 25.5 ± 4.3 years; SD). All subjects gave their written informed consent. The

study was approved by the local ethics committee (study no. 2895) and was performed in accordance with the Declaration of Helsinki.

Paradigm

Fig. 1 provides an overview of the paradigm. Each trial started with a cue presented for 1000 ms indicating the specific task of one of three experimental conditions: (i) *selective visual*, (ii) *selective auditory*, or (iii) *divided*, i.e. visual and auditory. Irrespective of the condition, the cue was followed by a 2000 ms fixation period. Then, a visual stimulus (an inwardly contracting grating) and an auditory stimulus (a constant tone) appeared simultaneously. After a randomly assigned period of 500, 1000, 2000, or 3000 ms, either the visual or the auditory stimulus changed its quality (change 1). 750 or 1000 ms later, the other stimulus also changed (change 2). In half of the trials, the visual stimulus changed first followed by a change in the auditory stimulus and vice versa. The order of these changes was randomized. A change of the visual stimulus was implemented as an increase in speed of the stimulus that either continued to move inwards or changed its direction and then moved outwards (inward/outward). A change in the auditory stimulus was implemented as a change in pitch to a higher or lower pitch (high/low). Please see section on [stimuli and stimulus delivery](#) for a detailed description of the properties and delivery of the stimuli.

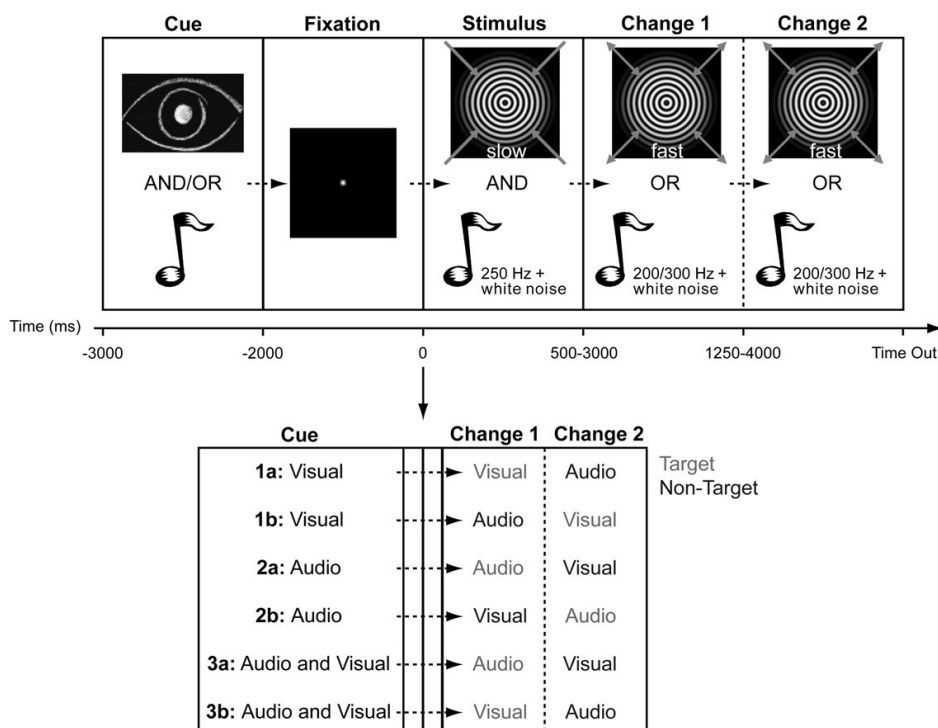


Fig. 1. Paradigm. Upper part: general overview of one trial. Each trial started with a cue indicating the condition (Cue). After presentation of a fixation dot (Fixation), visual and auditory stimuli were presented simultaneously (Stimulus; 0 = start of stimulus). After a randomly assigned period of 500 to 3000 ms, either the visual or the auditory stimulus changed its quality (Change 1). After 750 or 1000 ms also the other stimulus changed (Change 2). Depending on the condition, one of the two stimulus changes served as target. Subjects had to give a speeded response indicating quality of target as soon as it appeared in the cued modality (see section on [stimuli and stimulus delivery](#) for exact description of target qualities). A response or a reaction time > 2000 ms (Time out) terminated stimulus presentation. Feedback was given after each trial. Periods used for later analysis were Fixation (baseline) and Stimulus. Lower part: detailed description of variable parts of each trial. With a visual cue (1a/1b; condition *selective visual*, $n = 108$ trials) the change in visual stimulus became target and the change in auditory stimulus non-target. If the cue was auditory (2a/2b; condition *selective auditory*, $n = 108$ trials) the change in auditory stimulus became target and the change in visual stimulus non-target. Two target positions were possible in the *selective* conditions. When auditory and visual cues were presented together (3a/3b; condition *divided*; 3a: *divided auditory*, $n = 108$ trials, 3b: *divided visual*, $n = 108$ trials) the first changing stimulus became target, the second one non-target. Targets are depicted in light grey, non-targets in dark grey. Please note that fixation and stimulus periods consisted of the same stimulation in each trial, only duration of stimulus period varied. Thus, these trial periods are depicted as small empty boxes in the lower part.

Depending on the experimental condition, as indicated by the cue at the beginning of the trial, a change of one of the stimuli became the target. Subjects were required to give a speeded response to the change in the stimulus' quality, i.e. a change in speed of the visual or a change of pitch of the auditory stimulus. In condition *selective visual*, subjects had to exclusively react to the change in the visual stimulus (target), irrespective of its position in the trial (change 1 or 2) and ignore the change in the auditory stimulus (non-target). In condition *selective auditory*, accordingly, subjects had to react to the change in the auditory stimulus (target) only and ignore the change in the visual stimulus (non-target). In the *divided* condition, subjects had to respond to the stimulus that changed first (change 1 = target) and ignore the change in the other stimulus (change 2 = non-target).

The subject's task was thus to react to the target and indicate the quality of this stimulus change by pressing one of four buttons operated with the index and middle fingers of both hands. Thereby, each hand was assigned to one modality (visual and auditory) and each finger to one quality change, i.e. for the visual stimulus an index finger press indicated inward and a middle finger press outward movement, for the auditory stimulus an index finger press indicated a high tone, a middle finger press a low tone. Feedback was given after each trial. If subjects did not respond within 2000 ms after target appearance, the trial was counted as missed. The assignment of the left or right hand to the auditory or visual modality was balanced between subjects, finger assignment was kept fixed.

The paradigm consisted of 432 trials: 108 trials in conditions *selective visual* and *selective auditory* each and 216 in condition *divided* (subdivided into 108 trials where the visual stimulus changed first and thereby became target, *divided visual*; and 108 trials where the auditory stimulus changed first, *divided auditory*). Trials from the different conditions were presented in two blocks in a random order. Each block was subdivided into smaller blocks of twelve trials separated by self-paced breaks to avoid fatigue. Prior to data acquisition, subjects were trained on the paradigm until they thoroughly understood the task.

Three levels of visual attention were sought to be obtained by these conditions; high in condition *selective visual*, medium in condition *divided*, and low in condition *selective auditory*. In analogy to Coull et al. (2004), attentional allocation was obtained by varying the likelihood of whether the motor response was based on changes in the visual or the auditory stimulus (*selective visual*: 100% visual, 0% auditory, *selective auditory*: 0% visual, 100% auditory, *divided*: 50% visual, 50% auditory).

Stimuli and stimulus delivery

The fixation point was of a Gaussian (0.56° in diameter), which increased its contrast by 40% after 1000 ms, thereby informing the subject that the stimulation was about to start. The visual stimulus was adapted from Hoogenboom et al. (2006). It consisted of a foveal circular sine wave grating (diameter: 5.6°, spatial frequency: 2 cycles/°, contrast: 100%) continuously contracting towards the center of the screen (velocity: 1.6°/s). The change in visual stimulus (potential target) was characterized by an increase in velocity (3.38°/s). The sine wave grating was then either still contracting towards the center of the screen or changed its direction and expanded outwards.

The auditory stimulus was a binaurally presented 250 Hz sine tone embedded in white noise (white noise reduced by 9 dB compared to sine tone). The change in auditory stimulus (potential target) consisted of a change in pitch of the tone to either 200 Hz or 300 Hz. The auditory stimulus intensity was adjusted to subjectively match the visual stimulus intensity. Thus, auditory stimuli were well audible for all subjects, but at individual volumes.

Stimulus timing was controlled using Presentation® software (version 13.0, www.neurobs.com). Visual stimuli were projected onto

a screen with a dlp projector (PLUS Vision Corp. of America) with 60 Hz refresh rate. Participants were seated approximately 76 cm away from the screen. Auditory stimuli were produced using Audacity® (<http://audacity.sourceforge.net/>). They were sent into the shielded room via a mixing desk and earphone transducers (E-ARTONE, Aearo Technologies Inc., Indianapolis, USA), which converted the electrical to a sonic signal. The earphone transducers had two equal lengths plastic tubes and earplugs attached which were inserted into participants' ears.

Data acquisition

Neuromagnetic activity was measured in a magnetically shielded room with a whole-head Neuromag-122 MEG system (Elekta Neuromag Oy, Helsinki, Finland). Vertical and horizontal electrooculograms were recorded to later reject epochs contaminated with blink artifacts and eye movements. Individual high-resolution standard T1-weighted structural magnetic resonance images (MRIs) were obtained from a 3 T Siemens Magnetom MRI scanner (Munich/Erlangen, Germany).

Data analysis: behavioral data

Behavioral data were analyzed by means of error rates and reaction times. Trials were divided into conditions *selective visual*, *selective auditory*, and *divided*. For analyses of the behavioral data, the divided condition was further split up into two subcategories *divided visual* and *divided auditory*. Only correct trials with reaction times faster than 2000 ms were subjected to further analysis. Reaction times were analyzed using repeated measures analysis of variance (ANOVA) with factors modality (auditory versus visual) and condition (*selective* versus *divided*).

Data analysis: MEG data general

MEG data were analyzed using FieldTrip, an open source Matlab toolbox (Oostenveld et al., 2011), and Matlab 7.1 (MathWorks, Natick, MA). Continuously recorded MEG data were divided into epochs of interest, starting at the time of first fixation point and ending with appearance of change in either of the stimuli. Please note that for analyses of neurophysiological data, trials of the condition *divided* were not split up, as only periods prior to stimulus change were analyzed. Semi-automatic routines and visual artifact rejection were applied to discard epochs contaminated with eye, muscle, and sensor artifacts. Partial and complete artifact rejection procedures were applied, rejecting either only parts of the trial contaminated by artifacts or the whole trial in case of multiple artifacts. During partial artifact rejection, for each of the different artifact types (eye, muscle, and sensor artifacts), a z-score with specific sensitivity for the respective artifacts was computed. This was done by selecting either only EOG channels or all MEG sensors. Then, data were band-pass filtered in order to only include frequencies in which the artifacts are known to be most dominant. Subsequently, the envelope of the signal was computed using Hilbert transform and normalized by calculating the z-scores for each sensor. Next, one summed z-value was obtained for each moment in time. For this purpose, the z-scores of all selected sensors were added, and this sum was normalized by dividing it by the root of the number of summed sensors. A rejection threshold was then determined separately for each subject and applied automatically to its entire dataset. This adaptation of z-values between subjects was necessary because of differences in noise levels and in the signal-to-noise ratio. After partial artifact rejection, trials were inspected visually and excluded completely in case of remaining artifacts. Power line noise was removed by estimating and subtracting the 50-, 100- and 150-Hz components in the MEG data, using a discrete Fourier transform. The linear trend was removed from each epoch.

Data analysis: individual gamma band peaks

Rhythmic neuronal activity was estimated determining spectral power of the MEG signals. For the time period of 500 to 1000 ms (0 being the start of stimulus presentation) and frequencies of 30 to 100 Hz power spectra were calculated for each participant averaged over all trials of all conditions and over occipital sensors (± 1 Hz smoothing, hanning window). Each participant's absolute maximal gamma band frequency was obtained. Please note that to exclude purely stimulus-evoked components, the first 500 ms were excluded from those analyses steps not involving timely evolution of the signal. To include the strongest gamma band peak and the maximally possible amount of trials, periods from 500 to 1000 ms were used to calculate peak gamma band responses and their localization.

Data analysis: individual gamma sources

The source of the strongest gamma band peak (as obtained from the power spectra), averaged over all trials of all conditions, was localized for each individual using Dynamic Imaging of Coherent Sources (Gross et al., 2001), an adaptive spatial filtering technique in the frequency domain. Leadfield matrices were determined for realistically shaped single-shell volume conduction models (Nolte, 2003) derived from the individual structural MRIs. The grid of locations was constructed as a regular 5 mm grid. In order to account for each subject's strongest gamma band response crossspectral density matrices between all MEG sensor pairs at individual gamma band peaks ± 5 Hz were determined separately for time frequency windows from -1000 to -500 ms, i.e. before stimulus start (baseline), and from 500 to 1000 ms after stimulus start (stimulus period). Spatial filters were determined based on the crossspectral density matrices averaged over all trials of all conditions of a given subject. Relative changes between pre-stimulus and stimulus periods were calculated and locations of each subject's strongest relative gamma band peak were retrieved. Each subject's source parameters were displayed on their individual brains. Each structural MRI was spatially normalized to a smoothed template MRI based on multiple subjects (Statistical Parametric Mapping; SPM2; <http://www.fil.ion.ucl.ac.uk/spm/>). Differences between MNI and Talairach coordinates were adjusted (<http://imaging.mrc-cbu.cam.ac.uk/imaging/MniTalairach>) and individual virtual sensor locations were identified, Brodmann areas were estimated from Talairach and Tournoux (Talairach and Tournoux, 1988) using 'Talairach Client – Version 2.4.2' (Lancaster et al., 2000).

Data analysis: time course of signal at individual gamma sources

To quantify the time course of the signal at each subject's strongest relative gamma source, virtual sensors were generated by linear constrained minimum variance (LCMV) beamformer reconstructions. The time courses of the source wave forms were obtained using covariance matrices for pre-stimulus (-1000 to -500 ms) and stimulus periods (500 to 1000 ms) separately, band-pass filtered for each subject's strongest gamma band peak. Spatial filters were calculated averaged over all trials of a given subject. For each individual, equal numbers of trials for all three conditions and pre-stimulus and stimulus times, were randomly drawn from the available preprocessed trials. Single trial time courses were then projected through those filters, providing single trial estimates of source power. For further analyses, dipole moments' time courses were projected on the direction of maximal power in the individual gamma band frequency. On the resulting source wave forms, time frequency representations of power (TFRs) were calculated for frequencies between 30 and 100 Hz using windows of 400 ms moved in steps of 50 ms. Multitaper spectral estimation was used with ± 5 Hz smoothing (3 tapers) in steps of 0.5 Hz. Relative changes of power in the

stimulus period (0 to 2000 ms) to the pre-stimulus baseline (-1000 to -500 ms) were calculated. For each subject, average TFRs were calculated for each of the three conditions. Due to the special tuning of the virtual sensors for the subjects' individual gamma band frequencies, lower frequencies were not subjected to further analyses here.

Data analysis: statistical comparison of conditions

To examine differences between the three conditions, average TFRs were subjected to statistical group analysis. The stimulus period relative to the pre-stimulus baseline and the absolute baseline period were analyzed separately. Dependent samples two-sided t-tests for each time- and frequency-point across epochs were performed for all three comparisons (*selective visual/selective auditory*, *selective visual/divided*, and *divided/selective auditory*). Statistical inference was based on a non-parametric randomization test, correcting for multiple comparisons due to a multitude of time- and frequency-points (Maris and Oostenveld, 2007; Nichols and Holmes, 2002). Bonferroni-Holm correction (Holm, 1979) was applied to the alpha level to correct for multiple comparisons between the three conditions.

Data analysis: signal phase-locked to stimulus onset

In the analysis performed earlier (Data analysis: time course of signal at individual gamma sources and Data analysis: statistical comparison of conditions), trials were averaged after conducting time frequency analysis. This approach significantly favors identification of non-phase-locked (induced) activities. Applying time frequency analysis after averaging mainly provides information on phase-locked (evoked) oscillatory bursts (Tallon-Baudry et al., 1996). To determine whether the here observed statistical effects stem from induced or evoked activity, the analysis was repeated for responses phase-locked to stimulus onset and averaged before performing time frequency analysis. Data were aligned to stimulus onset, baseline corrected with a time window of 200 ms before stimulus onset, projected through the common spatial filters, averaged over trials, and subjected to a time frequency analysis. The same non-parametric randomization test as described earlier was applied.

Data analysis: evoked magnetic fields

The analysis was repeated for modulations in evoked magnetic fields. For a direct comparison with the spectral power analysis, the same source locations (virtual sensors) and trial selections were used. Data were filtered with a band-pass filter from 0.03 to 30 Hz. A baseline of 200 ms prior to stimulus onset was subtracted. The statistical group analysis was repeated (dependent samples two-sided t-tests for all three comparisons).

Results

Behavioral data

In all four behavioral conditions (*selective visual*, *selective auditory*, *divided visual*, and *divided auditory*), error rates were below 10%. Mean reaction times were 586.39 ms \pm 14.61 for condition *selective visual*, 669.96 ms \pm 22.79 for condition *divided visual*, 299.20 ms \pm 21.99 for condition *selective auditory*, and 430.74 ms \pm 23.50 for condition *divided auditory* (SEM reported here; Fig. 2). For reaction times a repeated measures analysis of variance (ANOVA) resulted in significant main effects for factors modality ($F_{(1,15)} = 426.57$, $p < 0.001$) and condition ($F_{(1,15)} = 90.61$, $p < 0.001$) and in a significant interaction ($F_{(1,15)} = 10.00$, $p = 0.006$) between both factors. Reaction times were faster in the selective compared to the respective divided attention conditions and in the auditory than in the visual conditions. The

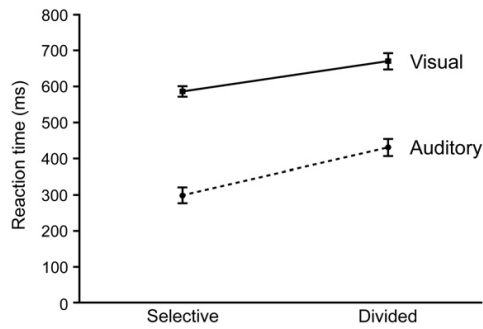


Fig. 2. Reaction times. Reaction times were faster in the selective, compared to the respective divided conditions, in both the visual and the auditory modality ($p < 0.001$). Thus, effects of attention between conditions were confirmed. Differences between conditions *selective auditory* and *divided auditory* were more pronounced than differences between conditions *selective visual* and *divided visual* ($p = 0.006$). Reaction times were faster in the auditory, than in the visual modality ($p < 0.001$; SEM displayed).

difference between selective and divided conditions was more pronounced in the auditory than in the visual modality.

Frequency and location of strongest gamma band source

For MEG data analyses an average of 326 ± 9.48 (SEM reported) trials remained for each subject after rejecting invalid trials and artifacts. Thus, 75% of the previously recorded trials remained. Using only these trials, each subject's strongest gamma band frequency peak was retrieved. Power spectra averaged over each subject's occipital sensors revealed individual peak gamma band frequencies ranging from 54 to 69 Hz (see Table 1 for individual peak frequencies). The maximum gamma band power was localized and a virtual sensor was constructed for each subject. Virtual sensors were mostly localized in early visual cortex. In fourteen of sixteen subjects, the virtual sensor accounting for strongest gamma band activity in response to the visual stimulus was located in Brodmann areas 17 or 18. In one subject, it was located in Brodmann area 19 and in one subject in lingual gyrus, close to the cerebellum (Table 1 and Fig. 3).

Table 1

Characterization of single subject gamma band frequencies and locations. For each subject, individual peak gamma band frequencies and locations of virtual sensors as Brodmann areas and Talairach coordinates are displayed. Please note that for subject 8, the virtual sensor was localized in lingual gyrus, close to the cerebellum, no Brodmann area is specified in this case.

Subject no.	Maximal γ	Brodmann area	Talairach coordinates (x, y, z)		
1	60 Hz	18	-6	-81	20
2	54 Hz	17	14	-82	1
3	66 Hz	18	4	-88	-5
4	65 Hz	18	5	-76	25
5	56 Hz	19	-7	-79	35
6	69 Hz	17	-17	-79	9
7	56 Hz	18	-4	-90	17
8	60 Hz	-	-1	-78	-7
9	58 Hz	18	-17	-95	20
10	54 Hz	18	-6	-98	7
11	58 Hz	17	6	-90	-1
12	66 Hz	17	-8	-84	12
13	64 Hz	18	-21	-99	2
14	54 Hz	17	-11	-84	9
15	60 Hz	17	-2	-84	9
16	56 Hz	18	-19	-95	6

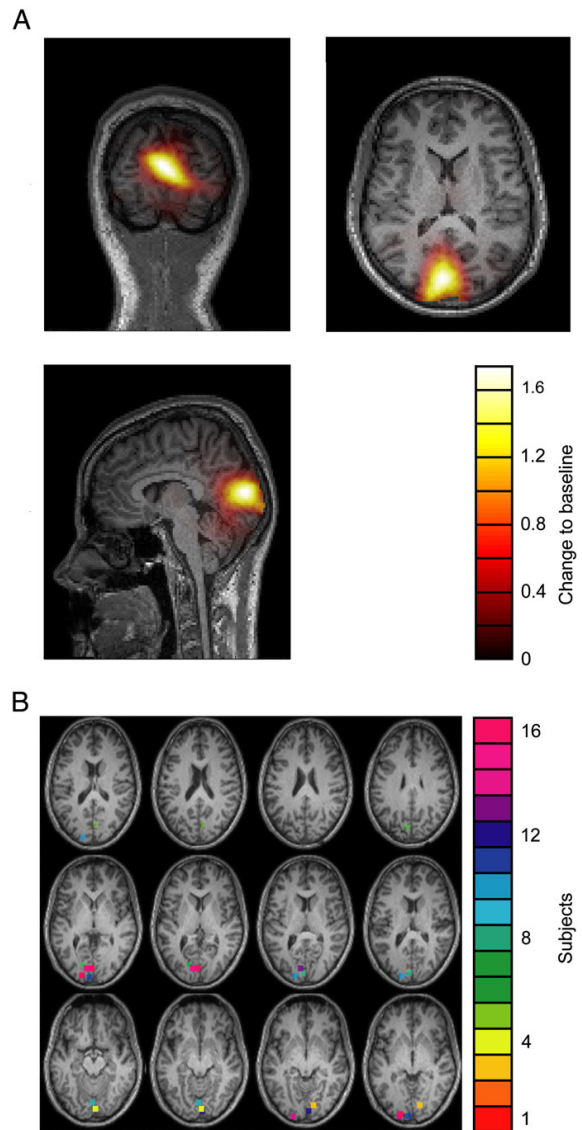


Fig. 3. Localization of gamma band power. A. Gamma band power relative to pre-stimulus baseline activity was localized in early visual areas. Displayed here is the grand average over all correct trials of all conditions for one representative subject (Subject 2). Colors indicate intensity of relative change to the pre-stimulus baseline. Values below 0.5 are masked. B. Virtual sensors were localized in areas V1 and V2 in 14 of 16 subjects. Shown here are virtual sensor locations for all subjects displayed on one individual brain normalized to a smoothed template MRI based on multiple subjects (Statistical Parametric Mapping; SPM2; <http://www.fil.ion.ucl.ac.uk/spm/>). Each colored point represents the virtual sensor of one subject. Please note that for visualization purposes, the kernels of the virtual sensors were extended to 9 mm. Slice thickness was 3 mm. For that reason, some virtual sensors are present in multiple slices.

Comparing conditions: similar baseline activity between attention conditions

When comparing conditions, the same numbers of trials were retrieved for each of the three conditions (*selective visual*, *selective auditory* and *divided*) and the pre-stimulus baseline and stimulus periods. On average, 79 ± 2.48 (SEM) trials remained per condition.

Between the three conditions no significant differences were found in pre-stimulus baseline activity ($p > 0.37$). Thus, further results are based on relative changes in power with respect to a pre-stimulus baseline.

Comparing conditions: differences in gamma band activity between attention conditions

On virtual sensor level, all subjects showed sustained visually induced gamma band synchronization compared to the pre-stimulus baseline in all three conditions (see Fig. 4A for grand averages over all subjects). Pairwise comparisons on group level between all three conditions resulted in significant power differences in the gamma band frequency range. Relative gamma band power was significantly higher in condition *selective visual* than in condition *selective auditory* between 53 and 80 Hz from 400 to 2000 ms ($p < 0.001$); it was significantly higher in condition *selective visual* than in condition *divided* between 54 and 74 Hz from 450 to 1550 ms ($p = 0.009$); and it was significantly higher in condition *divided* than in condition *selective auditory* between 54 and 75 Hz from 700 to 2000 ms ($p = 0.002$; all p -values corrected for multiple comparisons). Thus, relative visual gamma band synchronization was highest in condition *selective visual*, medium in condition *divided*, and lowest in condition *selective auditory* (Fig. 4B). Averaged over all subjects, over time (500 to 2000 ms) and individual gamma peak frequencies ± 5 Hz mean relative power values were 2.21 ± 0.44 (SEM) for *selective visual*, 2.13 ± 0.41 (SEM) for *divided*, and 1.92 ± 0.38 (SEM) for *selective auditory*. Please note that big standard errors are due to a big variance

in overall relative gamma power between subjects (range: 0.16 to 6.91).

Signal phase-locked to stimulus onset and evoked magnetic fields

To examine differences in evoked spectral power between conditions, time frequency representations of power phase-locked to stimulus onset were calculated. No statistically significant differences were observed between the three conditions in gamma band power phase-locked to stimulus onset.

Furthermore, it was investigated, whether attentional modulations were preceded by attentional modulations of evoked magnetic fields. Again, no statistically significant differences were observed between the three conditions.

Discussion

The aim of the present study was to gradually modulate visual attention, thereby examining its relation to gamma band synchronization in visual cortical areas. A bimodal paradigm designed to elicit three levels of visual attention (high, medium, and low) was used and three graded levels of visual attention were confirmed on the behavioral side. In response to the visual stimulus, prominent long lasting local gamma band synchronization in visual cortex was found. Gamma band power was gradually modulated in early visual areas according to the amount of attention directed to the visual stimulus. This gradual modulation suggests that by being precisely adjustable

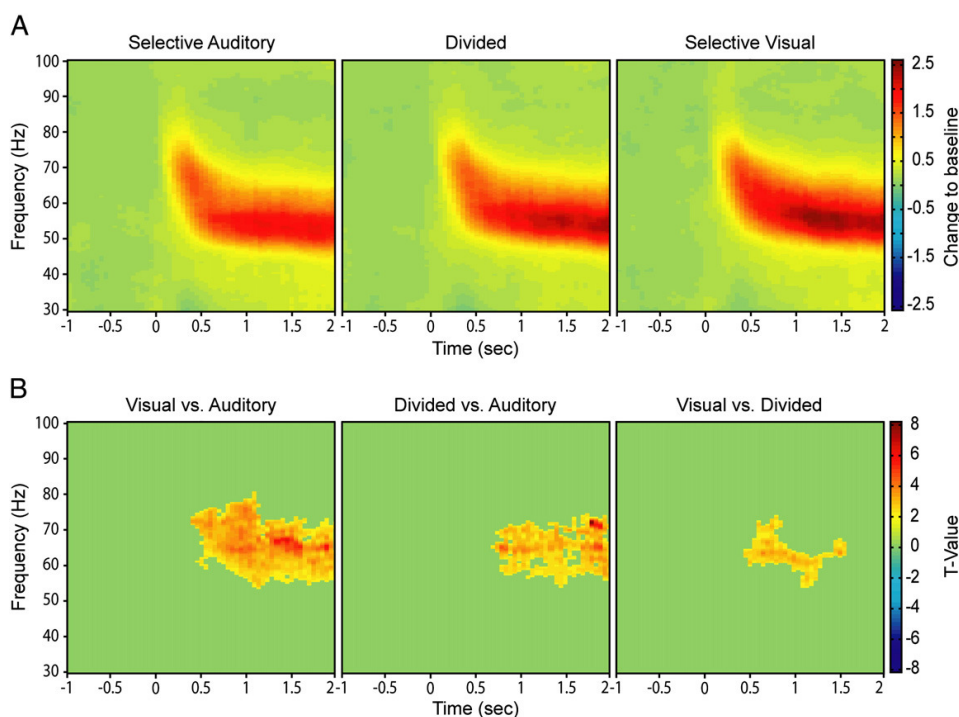


Fig. 4. Virtual sensor time frequency representations and statistics. A. Grand average time frequency representations relative to baseline from each subject's virtual sensor. In all three conditions (*selective auditory*; left, *divided*; middle, and *selective visual*; right) a prominent gamma band response relative to pre-stimulus baseline activity was observed during stimulation (onset of stimulation at $t = 0$). Color-coding: 0 corresponds to no change and 2.5 to a 250% increase in power relative to baseline. B. Statistical comparisons between all three conditions. Results are shown as t-values; all non-significant frequencies are masked green. Relative gamma band power was stronger in condition *selective visual* compared to condition *selective auditory* ($p < 0.001$; left), it was stronger in condition *divided* compared to condition *selective auditory* ($p = 0.002$; middle), and stronger in condition *selective visual* compared to condition *divided* ($p = 0.009$; right; p -values corrected for multiple comparisons).

to current attentional needs gamma band synchronization represents a mechanism enabling an efficient use of cognitive resources.

Behavioral data and induced gamma band synchronization support gradual modulation of attention

Behavioral data confirmed different reaction times for the three attention levels. Thus, one can assume that graded levels of visual attention were reached by the applied bimodal reaction time paradigm and that attention was shifted between the visual and auditory modalities. Extending earlier behavioral work (Posner et al., 1980; Schroeger et al., 2000; Spence and Driver, 1997), a third medium state of visual attention is introduced, thereby enabling measurement of gradually modulated attention.

In line with earlier research (Edden et al., 2009; Fries et al., 2001; Hoogenboom et al., 2006; Muthukumaraswamy et al., 2009), subjects showed prominent long lasting visual gamma band activity in all conditions when presented with the visual stimulus. Underlining the pivotal behavioral relevance of this neurophysiological effect, gamma band activity in early visual cortex was highest in condition *selective visual*, medium in condition *divided*, and lowest in condition *selective auditory*. Thus, three increasing levels of visual attention are associated with a corresponding modulation on the neurophysiological side. While previous works investigated the influence of 'attention' versus 'no attention' on gamma band synchronization (Fries et al., 2001; Gruber et al., 1999; Mueller et al., 2000; Siegel et al., 2008; Wyart and Tallon-Baudry, 2008), the present study extends these findings by establishing gradual attention modulation. Furthermore, attentional effects on gamma band synchronization have never been shown for such long periods of time (lasting up to 1600 ms). Previous studies have provided data either averaged over certain time periods, frequency bands or both (Fries et al., 2001; Gruber et al., 1999; Mueller et al., 2000; Tallon-Baudry et al., 2005; Vidal et al., 2006). Thus, our data provide new insights into long lasting attention modulation and its relation to gamma band synchronization.

Gamma band power phase-locked to stimulus onset and evoked magnetic field strengths were not significantly different between conditions. Tallying with non-existent predictive properties of evoked magnetic fields for reaction times (Hoogenboom et al., 2010) gamma band modulation in this paradigm is assumed to stem from differences in induced and not in evoked gamma band power. These findings oppose animal data, showing attentional modulation of early evoked gamma band responses in primary visual and auditory areas (Lakatos et al., 2009). However, the described work is based on multiunit recordings from macaque primary areas. This different approach and the restriction to primary areas might be an explanation for these dissimilar results. Furthermore, the present restriction to areas of strongest gamma band synchronization, allows no deeper conclusions about the order of processing in visual areas from these data.

The difference in gamma band synchronization between conditions *selective visual* and *divided* was less prominent and shorter lasting than differences between conditions *selective visual* and *selective auditory* and between conditions *divided* and *selective auditory*. In behavioral analogy, we observed a stronger orientation to the visual modality reflected by a greater difference in reaction times between conditions *selective auditory* and *divided auditory* than between conditions *selective visual* and *divided visual*. While emphasizing the relation between behavioral and neurophysiological data, these findings tally with the ventriloquist effect (Alais and Burr, 2004), stating that vision often dominates audition when attentive processes are involved. A very recent study substantiates this by showing that visual dominance is based on less vulnerability of the visual system to competition from auditory stimuli than vice versa (Schmid et al., 2011).

One might speculate that prolonged reaction times in the *divided* compared to the *selective* conditions reflect an effect of task difficulty. Indeed, earlier studies showed that gamma band oscillations can be modulated by overall task difficulty (Posada et al., 2003) and perceptual load (Howard et al., 2003). However, if task difficulty was higher in the *divided* condition, gamma band power would also have been expected to be highest in this condition and similar in the two *selective* conditions. As this is not the case in the current study, we claim to see modulation of gamma band synchronization that is due to modulation of attention by a limited capacity of attention resources (Bonnel and Hafer, 1998) and not due to task difficulty or perceptual load.

The discrepancy in frequencies, observed between highest relative gamma band power and the statistical difference between these two, might firstly be caused by smearing due to frequency smoothing used in time frequency analysis. Secondly, the strong gamma band power peak in the group average is dominated by power values of some subjects. The statistical effects are most likely due to subjects with higher frequency gamma band power peaks showing consistent modulations between conditions.

Gamma band synchronization in the auditory system

The data reported here were also scanned for effects of auditory stimulation (see Supplementary Figs. 1 and 2 for further information). Auditory evoked responses to auditory stimulation were found (see Supplementary Fig. 2). However, most likely due to stimulus characteristics, we were not able to find any systematic sustained stimulus related gamma band responses in auditory cortex. Certainly, intracranial studies have reported evoked short-lasting (Lakatos et al., 2009) and induced auditory gamma band synchronization (Crone et al., 2001). There have also been MEG studies, showing auditory evoked gamma band activity (Joliot et al., 1994; Pantev et al., 1991; Tiitinen et al., 1993). However, to the best of our knowledge, there are no studies using auditory stimuli inducing long-lasting gamma band synchronization in auditory cortex. One possible explanation might be that, MEG sensors are less sensitive to radial sources at the surface of gyri, e.g. superior temporal gyrus (Crone et al., 2001). Thus one might speculate that the signal to noise ratio of a potentially induced auditory gamma band response in our study might have been too low, especially compared to the visual response, to be seen in the MEG recording. Thus, due to the absence of an adequate auditory stimulus, we confined our analysis to the visual system.

The interpretation of the present findings is limited to some degree by the fact that gamma band activity could not be observed in the auditory system. While a shift of attention between the auditory and visual system can be assumed from behavioral data, explicit corresponding evidence from the neurophysiological data is missing. Hence, the proposed shift of attention between modalities remains speculative. Finding stimuli that permit showing mirror effects of modulated gamma band synchronization in auditory cortex, as shown with steady state stimuli at lower frequencies (Saupe et al., 2009) would be a desirable task for future works. This would permit firm conclusions about the relation between gamma band synchronization and resource allocation between modalities.

Modulation of induced gamma band synchronization in early visual areas

Subjects' strongest induced gamma band sources were located in early visual areas (V1 and V2) in fourteen of sixteen subjects. Modulation of gamma band synchronization was also found in these locations. Relative gamma band power in early visual cortical areas increased with the amount of attention directed to the visual stimulus. While some studies showed pronounced gamma band synchronization in visual areas V1–V3 in humans, when attentively

monitoring a visual stimulus (Hoogenboom et al., 2006, 2010), attention dependent modulations of gamma band synchronization have primarily been recorded in mid- and high level stages in the visual processing hierarchy (Fries et al., 2001; Gregoriou et al., 2009). One study (Chalk et al., 2010) however, found decreased local field potential gamma band power and decreased gamma band spike field coherence with attention in V1 of the macaque monkey. The authors suggest that by a reduction of center surround inhibition, gamma band synchronization decreases with attention, which only holds if an experimental design is used where attention is tightly focused at the center of the classical receptive field. The stimuli used in our study were relatively complex gratings, not restricted to the center of one receptive field, but exciting multiple neurons in visual cortex. The here applicable mechanism behind gamma band synchronization has been described in a recent review, which proposes that gamma band synchronization is driven by rhythmically synchronized inhibition through cortical interneurons (Fries, 2009).

Thus, our results substantiate that graded attentional modulation of gamma band synchronization takes place in early visual areas and support the theory that synchronized inhibition of cortical interneurons can serve as a mechanism for gamma band synchronization.

Biased competition model applied gradually

Previous studies on selective visual attention suggest that the attended of two competing visual stimuli gets a competitive advantage over the other by enhancing its gamma band synchronization (Fries et al., 2001, 2008). This effect has been addressed in the hypothesis of biased competition through enhanced synchronization (Fries, 2005), which bases its assumptions on the biased competition hypothesis (Desimone and Duncan, 1995; Reynolds et al., 1999). From the present results one might speculate that the conceptual framework of the biased competition model can also be applied to gradual attention modulation in the visual system. In this respect, enhanced gamma band synchronization could be seen as an adaptive mechanism enhancing the selective processing of a stimulus in a gradual manner, thereby reflecting the amount of selective attention a stimulus receives.

From the current results, one could furthermore speculate on the application of the biased competition model in an intermodal context, as shown in a modeling study for the visual and tactile domains (Magosso et al., 2010). With the attention related increase in gamma band synchronization in visual areas, one could assume a connection of the competitive advantage of the visual over the auditory stimulus to the amount of gamma band synchronization. However, one important aspect of the biased competition model is that responses to the non-preferred stimulus are suppressed, when the other stimulus 'wins' the competition for processing. The current study cannot directly proof suppressive effects of one of the two stimuli over the other. To substantiate the application of the biased competition model in an intermodal context, future studies are needed. These could employ bimodal stimuli, inducing long-lasting gamma band synchronization in visual and auditory areas at the same time and could thereby address suppressive and enhancing effects in modality specific cortical areas. Furthermore, interactions with and between other modalities such as the somatosensory system will be of great interest.

Conclusions

The current study is the first to show gradual and long lasting changes of gamma band synchronization in early visual areas related to the level of attention given to a visual stimulus. These attention effects, potentially achieved by resource allocation between the visual and auditory modality, may extend the biased competition model

of selective attention and highlight the key role of gamma band synchronization in visual attention.

Role of the funding source

This study was supported by Deutsche Forschungsgemeinschaft (SFB 575, project C4). N.K. was supported by Studienstiftung des deutschen Volkes and a travel allowance of Boehringer Ingelheim Foundation (B.I.F.).

Supplementary materials related to this article can be found online at doi:10.1016/j.neuroimage.2011.07.017.

Acknowledgments

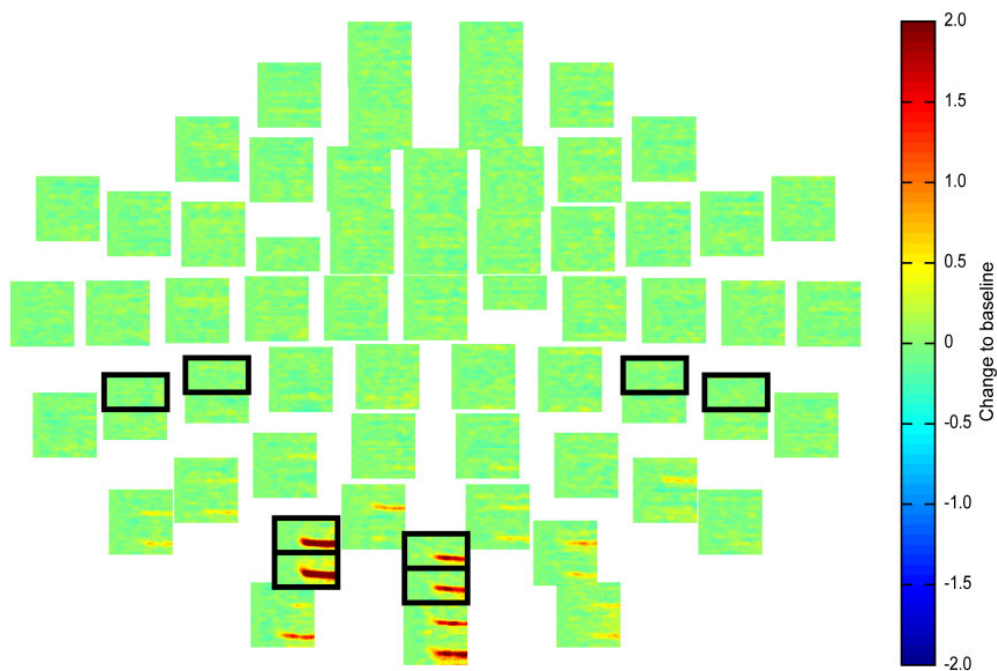
We thank Mrs. E. Rädisch and Mrs. A. Solutchin for technical support with MRI scans. We are thankful to Prof. Joachim Gross (CCNI, Glasgow), Dr. Hanneke van Dijk, and Dr. Nienke Hoogenboom (both University Düsseldorf) for helpful suggestions and discussion on data analysis. For critically revising the manuscript we thank Dr. Joachim Lange (University Düsseldorf).

References

- Alais, D., Burr, D., 2004. The ventriloquist effect results from near-optimal bimodal integration. *Curr. Biol.* 14 (3), 257–262.
- Bonnel, A.M., Hafter, E.R., 1998. Divided attention between simultaneous auditory and visual signals. *Percept. Psychophys.* 60 (2), 179–190.
- Chalk, M., Herrero, J.L., Gieselmann, M.A., Delicato, L.S., Gotthardt, S., Thiele, A., 2010. Attention reduces stimulus-driven gamma frequency oscillations and spike field coherence in V1. *Neuron* 66 (1), 114–125.
- Coull, J.T., Vidal, F., Nazarian, B., Macar, F., 2004. Functional anatomy of the attentional modulation of time estimation. *Science* 303 (5663), 1506–1508.
- Crone, N.E., Boatman, D., Gordon, B., Hao, L., 2001. Induced electrocorticographic gamma activity during auditory perception. *Clin. Neurophysiol.* 112 (4), 565–582.
- Desimone, R., Duncan, J., 1995. Neural mechanisms of selective visual attention. *Annu. Rev. Neurosci.* 18 (1), 193–222.
- Edden, R.A.E., Muthukumaraswamy, S.D., Freeman, T.C.A., Singh, K.D., 2009. Orientation discrimination performance is predicted by GABA concentration and gamma oscillation frequency in human primary visual cortex. *J. Neurosci.* 29 (50), 15721–15726.
- Fries, P., 2005. A mechanism for cognitive dynamics: neuronal communication through neuronal coherence. *Trends Cogn. Sci.* 9 (10), 474–480.
- Fries, P., 2009. Neuronal gamma-band synchronization as a fundamental process in cortical computation. *Annu. Rev. Neurosci.* 32, 209–224.
- Fries, P., Reynolds, J.H., Rorie, A.E., Desimone, R., 2001. Modulation of oscillatory neuronal synchronization by selective visual attention. *Science* 291 (5508), 1560–1563.
- Fries, P., Womelsdorf, T., Oostenveld, R., Desimone, R., 2008. The effects of visual stimulation and selective visual attention on rhythmic neuronal synchronization in macaque area V4. *J. Neurosci.* 28 (18), 4823–4835.
- Gandhi, S.P., Heeger, D.J., Boynton, G.M., 1999. Spatial attention affects brain activity in human primary visual cortex. *Proc. Natl. Acad. Sci. U.S.A.* 96 (6), 3314–3319.
- Gherri, E., Eimer, M., 2011. Active listening impairs visual perception and selectivity: an ERP study of auditory dual-task costs on visual attention. *J. Cogn. Neurosci.* 23 (4), 832–844.
- Gregoriou, G.G., Gotts, S.J., Zhou, H., Desimone, R., 2009. High-frequency, long-range coupling between prefrontal and visual cortex during attention. *Science* 324 (5931), 1207–1210.
- Gross, J., Kujala, J., Hämäläinen, M., Timmermann, L., Schnitzler, A., Salmelin, R., 2001. Dynamic imaging of coherent sources: studying neural interactions in the human brain. *Proc. Natl. Acad. Sci. U.S.A.* 98 (2), 694–699.
- Gruber, T., Mueller, M.M., Keil, A., Elbert, T., 1999. Selective visual-spatial attention alters induced gamma band responses in the human EEG. *Clin. Neurophysiol.* 110 (12), 2074–2085.
- Holm, S., 1979. A simple sequentially rejective multiple test procedure. *Scand. J. Stat.* 6 (2), 65–70.
- Hoogenboom, N., Schoffelen, J.M., Oostenveld, R., Parkes, L.M., Fries, P., 2006. Localizing human visual gamma-band activity in frequency, time and space. *Neuroimage* 29 (3), 764–773.
- Hoogenboom, N., Schoffelen, J.M., Oostenveld, R., Fries, P., 2010. Visually induced gamma-band activity predicts speed of change detection in humans. *Neuroimage* 51 (3), 1162–1167.
- Howard, M.W., Rizzuto, D.S., Caplan, J.B., Madsen, J.R., Lisman, J., Aschenbrenner-Scheibe, R., Schulze-Bonhage, A., Kahana, M.J., 2003. Gamma oscillations correlate with working memory load in humans. *Cereb. Cortex* 13 (12), 1369–1374.
- Joliot, M., Ribary, U., Llinás, R., 1994. Human oscillatory brain activity near 40 Hz coexists with cognitive temporal binding. *Proc. Natl. Acad. Sci. U.S.A.* 91 (24), 11748–11751.

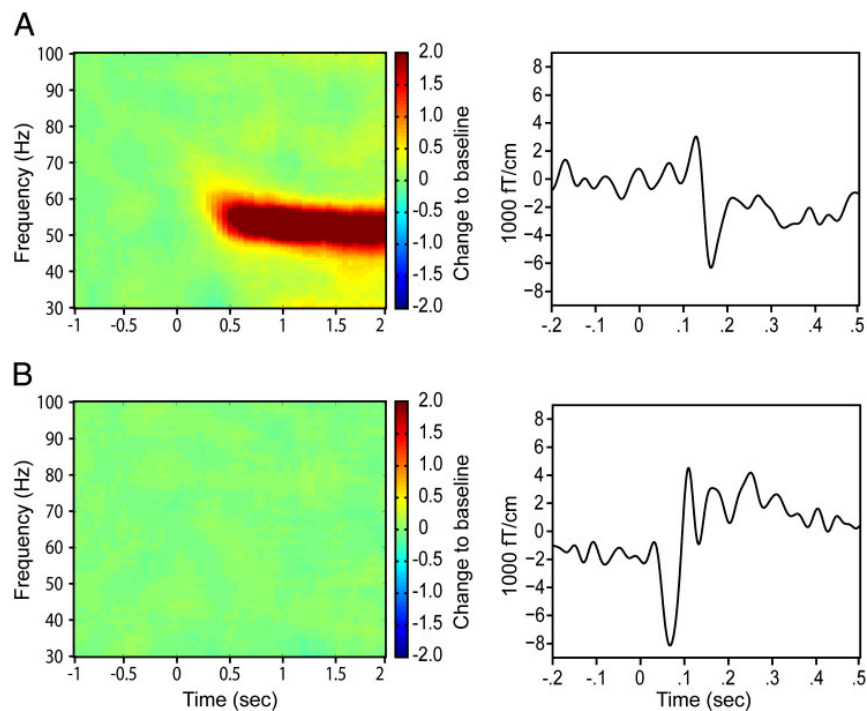
- Kaiser, J., Hertrich, I., Ackermann, H., Lutzenberger, W., 2006. Gamma-band activity over early sensory areas predicts detection of changes in audiovisual speech stimuli. *NeuroImage* 30 (4), 1376–1382.
- Khayat, P.S., Niebergall, R., Martinez-Trujillo, J.C., 2010. Frequency-dependent attentional modulation of local field potential signals in macaque area MT. *J. Neurosci.* 30 (20), 7037–7048.
- Lachaux, J.P., George, N., Tallon-Baudry, C., Martinerie, J., Hugueville, L., Minotti, L., Kahane, P., Renault, B., 2005. The many faces of the gamma band response to complex visual stimuli. *NeuroImage* 25 (2), 491–501.
- Lakatos, P., O'Connell, M.N., Barczak, A., Mills, A., Javitt, D.C., Schroeder, C.E., 2009. The leading sense: supramodal control of neurophysiological context by attention. *Neuron* 64 (3), 419–430.
- Lancaster, J.L., Woldorff, M.G., Parsons, L.M., Liotti, M., Freitas, C.S., Rainey, L., Kochunov, P.V., Nickerson, D., Mikiten, S.A., Fox, P.T., 2000. Automated Talairach atlas labels for functional brain mapping. *Hum. Brain Mapp.* 10 (3), 120–131.
- Magosso, E., Serino, A., di Pellegrino, G., Ursino, M., 2010. Crossmodal links between vision and touch in spatial attention: a computational modelling study. *Comput. Intell. Neurosci.* 304941. (Electronic publication ahead of print 2009 Oct 22).
- Maris, E., Oostenveld, R., 2007. Nonparametric statistical testing of EEG- and MEG-data. *J. Neurosci. Methods* 164 (1), 177–190.
- Mueller, M.M., Gruber, T., Keil, A., 2000. Modulation of induced gamma band activity in the human EEG by attention and visual information processing. *Int. J. Psychophysiol.* 38 (3), 283–299.
- Munneke, J., Heslenfeld, D.J., Theeuwes, J., 2008. Directing attention to a location in space results in retinotopic activation in primary visual cortex. *Brain Res.* 1222, 184–191.
- Muthukumaraswamy, S.D., Edden, R.A.E., Jones, D.K., Swettenham, J.B., Singh, K.D., 2009. Resting GABA concentration predicts peak gamma frequency and fMRI amplitude in response to visual stimulation in humans. *Proc. Natl. Acad. Sci. U.S.A.* 106 (20), 8356–8361.
- Nichols, T.E., Holmes, A.P., 2002. Nonparametric permutation tests for functional neuroimaging: a primer with examples. *Hum. Brain Mapp.* 15 (1), 1–25.
- Nolte, G., 2003. The magnetic lead field theorem in the quasi-static approximation and its use for magnetoencephalography forward calculation in realistic volume conductors. *Phys. Med. Biol.* 48 (22), 3637–3652.
- Oostenveld, R., Fries, P., Maris, E., Schoffelen, J., 2011. FieldTrip: open source software for advanced analysis of MEG, EEG, and invasive electrophysiological data. *Comput. Intell. Neurosci.* 2011, 156869.
- Pantev, C., Makeig, S., Hoke, M., Galambos, R., Hampson, S., Gallen, C., 1991. Human auditory evoked gamma-band magnetic fields. *Proc. Natl. Acad. Sci.* 88 (20), 8996–9000.
- Posada, A., Hugues, E., Franck, N., Vianin, P., Kilner, J., 2003. Augmentation of induced visual gamma activity by increased task complexity. *Eur. J. Neurosci.* 18 (8), 2351–2356.
- Posner, M.I., Snyder, C.R., Davidson, B.J., 1980. Attention and the detection of signals. *J. Exp. Psychol.* 109 (2), 160–174.
- Reynolds, J.H., Chelazzi, L., Desimone, R., 1999. Competitive mechanisms subserve attention in macaque areas V2 and V4. *J. Neurosci.* 19 (5), 1736–1753.
- Saupe, K., Schröger, E., Andersen, S.K., Müller, M.M., 2009. Neural mechanisms of intermodal sustained selective attention with concurrently presented auditory and visual stimuli. *Front. Hum. Neurosci.* 3, 58.
- Schmid, C., Büchel, C., Rose, M., 2011. The neural basis of visual dominance in the context of audio-visual object processing. *NeuroImage* 55 (1), 304–311.
- Schroeger, E., Giard, M.H., Wolff, C., 2000. Auditory distraction: event-related potential and behavioral indices. *Clin. Neurophysiol.* 111 (8), 1450–1460.
- Siegel, M., Donner, T.H., Oostenveld, R., Fries, P., Engel, A.K., 2008. Neuronal synchronization along the dorsal visual pathway reflects the focus of spatial attention. *Neuron* 60 (4), 709–719.
- Simos, P.G., Papanikolaou, E., Sakkalis, E., Micheloyannis, S., 2002. Modulation of gamma-band spectral power by cognitive task complexity. *Brain Topogr.* 14 (3), 191–196.
- Spence, C., Driver, J., 1997. On measuring selective attention to an expected sensory modality. *Percept. Psychophys.* 59 (3), 389–403.
- Steinmetz, P.N., Roy, A., Fitzgerald, P.J., Hsiao, S.S., Johnson, K.O., Niebur, E., 2000. Attention modulates synchronized neuronal firing in primate somatosensory cortex. *Nature* 404 (6774), 187–190.
- Talairach, J., Tournoux, P., 1988. Co-planar stereotaxic atlas of the human brain: 3-dimensional proportional system: an approach to cerebral imaging. Thieme, Stuttgart.
- Tallon-Baudry, C., Bertrand, O., Delpuech, C., Pernier, J., 1996. Stimulus specificity of phase-locked and non-phase-locked 40 Hz visual responses in human. *J. Neurosci.* 16 (13), 4240–4249.
- Tallon-Baudry, C., Bertrand, O., Henaff, M.A., Isnard, J., Fischer, C., 2005. Attention modulates gamma-band oscillations differently in the human lateral occipital cortex and fusiform gyrus. *Cereb. Cortex* 15 (5), 654–662.
- Tiitinen, H., Sinkkonen, J., Reinikainen, K., Alho, K., Lavikainen, J., Naatanen, R., 1993. Selective attention enhances the auditory 40-Hz transient response in humans. *Nature* 364 (6432), 59–60.
- Vidal, J.R., Chaumon, M., O'Regan, J.K., Tallon-Baudry, C., 2006. Visual grouping and the focusing of attention induce gamma-band oscillations at different frequencies in human magnetoencephalogram signals. *J. Cogn. Neurosci.* 18 (11), 1850–1862.
- Womelsdorf, T., Fries, P., Mitra, P.P., Desimone, R., 2006. Gamma-band synchronization in visual cortex predicts speed of change detection. *Nature* 439 (7077), 733–736.
- Wyart, V., Tallon-Baudry, C., 2008. Neural dissociation between visual awareness and spatial attention. *J. Neurosci.* 28 (10), 2667–2679.

Supplementary Figure 1



Supplementary Fig. 1. Sensor layout of time frequency representations of one subject.

Time frequency representations (30–100 Hz; –1000 to 2000 ms; 0 = start of stimulus; 400 ms time window in 50 ms steps; ± 5 Hz frequency resolution; 3 tapers) of all MEG sensors of one representative subject (subject 10) in condition *selective auditory*. Please note that the relative power values (compared to pre-stimulus baseline; –1000 to –500 ms) were limited in this plot, in order to be able to examine responses in auditory areas (going up to +2, whereas the maximum response over occipital sensors was $>+6$; color-coding: 0 corresponds to no change and 2.0 to a 200% increase in power relative to baseline). A strong gamma band response can be seen over occipital sensors. Over the auditory areas no such response could be observed.

Supplementary Figure 2**Supplementary Fig. 2. Occipital and temporal areas - high frequencies and evoked responses.**

A Left: Power relative to pre-stimulus baseline, averaged over the four occipital sensors (highlighted with a black box in Supplementary Fig. 1) of one representative subject (subject 10) in condition selective auditory. Right: Visual evoked field of the same subject, averaged over the same sensors as in A. To this end, sensor data were filtered with a band-pass filter from 0.03 to 30 Hz. A baseline of 200 ms prior to stimulus onset was subtracted.

B. The same data are displayed as in A, but averaged over the four bilateral temporal sensors as highlighted in Supplementary Fig. 1. These sensors were selected as they also showed the auditory evoked response in this subject. Please note that data of all participants were scanned on sensor level in order to identify long-lasting gamma band responses of the auditory cortex in reaction to auditory stimulation. No such response could be found in any subject recorded.

Gammaband-Oszillationen hängen mit dem Grad selektiv visueller Aufmerksamkeit zusammen

Gamma band oscillations are closely related to the level of selective visual attention

Autoren: Nina Kahlbrock^{a*}, Markus Butz^{a*}, Elisabeth S. May^a, Alfons Schnitzler^{a,b}

Institute: ^a Heinrich-Heine-Universität Düsseldorf, Medizinische Fakultät, Institut für Klinische Neurowissenschaften und Medizinische Psychologie, Universitätsstrasse 1, 40225 Düsseldorf

^b Heinrich-Heine-Universität Düsseldorf, Medizinische Fakultät, Neurologische Klinik, Universitätsstrasse 1, 40225 Düsseldorf

* gleichwertiger Beitrag dieser Autoren zur vorliegenden Arbeit

Korrespondenzadresse: Dr. Markus Butz, Heinrich-Heine-Universität Düsseldorf, Medizinische Fakultät, Institut für Klinische Neurowissenschaften und Medizinische Psychologie, Universitätsstrasse 1, 40225 Düsseldorf, mail: Markus.Butz@uni-duesseldorf.de

Schlüsselwörter: Synchronisation, Gamma, Aufmerksamkeit, MEG, audiovisuell

Keywords: synchronization, gamma, attention, MEG, audiovisual

Anmerkung: Die Ergebnisse der vorliegenden Arbeit wurden erstmals publiziert in: Kahlbrock N, Butz M, May ES, Schnitzler A (2012) Sustained gamma band synchronization in early visual areas reflects the level of selective attention. Neuroimage 59:673–681. Die vorliegende Zusammenfassung wurde genehmigt durch Elsevier.

Zusammenfassung

Kortikale Gammaband-Aktivität steht im engen Zusammenhang mit Aufmerksamkeit. Wird Aufmerksamkeit auf einen visuellen Reiz gerichtet, kommt es zu einer Modulation von Gammaband-Oszillationen im okzipitalen Kortex. Bis heute wurde jedoch noch keine graduelle Modulation von Gammaband-Oszillationen parallel zur Aufmerksamkeitsstärke in frühen visuellen Arealen untersucht. Graduelle Aufmerksamkeits-effekte können durch die Umverteilung von Ressourcen zwischen simultan präsentierten Reizen in zwei verschiedenen Modalitäten untersucht werden. In der vorliegenden Arbeit wurde die Stärke selektiv visueller Aufmerksamkeit graduell innerhalb eines audiovisuellen Reaktionszeitparadigmas variiert. Die Gehirnaktivität von 16 rechtshändigen Probanden (8 weiblich, mittleres Alter \pm Standardabweichung: 25.5 \pm 4,3 Jahre) wurde mittels Magnetenzephalographie (MEG) aufgezeichnet und bezüglich Zeit, Frequenz und Lokalisation der stärksten Gammaband-Antwort ausgewertet. Reaktionszeiten auf visuelle und auditorische Reize spiegelten die drei angenommenen Grade visueller Aufmerksamkeit wieder: hoch, mittel und gering ($p < 0,01$). Die MEG-Daten zeigten lang anhaltende Gammaband-Oszillationen in allen drei Bedingungen in primären und sekundären visuellen Arealen (V1 und V2), wobei die Stärke der Gammaband-Oszillationen mit dem Grad visueller Aufmerksamkeit anstieg (von gering zu hoch). Die Unterschiede zwischen den Bedingungen bestanden bis zu 1600 ms. Die vorliegenden Ergebnisse zeigen, dass die Stärke von Gammaband-Oszillationen in frühen visuellen Arealen mit dem Grad visueller Aufmerksamkeit variiert. Die dargestellten graduellen, lang anhaltenden Effekte erweitern das *biased competition* Modell selektiver Aufmerksamkeit und unterstreichen die Schlüsselrolle von Gammaband-Oszillationen in frühen visuellen Arealen für visuelle Aufmerksamkeit.

Abstract

Cortical gamma band synchronization is associated with attention. Accordingly, directing attention to a visual stimulus enhances gamma band activity in occipital brain areas. However, gradual effects of attention and behavior on gamma band activity in early visual areas have not been reported. Graded attention effects can be studied by reallocating available resources between simultaneously presented bimodal stimuli. In the present study, the degree of selective visual attention was gradually varied in a cued bimodal reaction time paradigm using audio-visual stimuli. From 16 healthy right handed subjects (8 female, mean age \pm standard deviation: 25.5 ± 4.3 years), brain activity was recorded using magnetoencephalography (MEG) and analyzed with respect to time, frequency, and location of strongest gamma band response.

Reaction times to visual and auditory stimuli reflected the three presumed graded levels of visual attention: high, medium, and low ($p < 0.01$). MEG data showed sustained gamma band synchronization in all three conditions in primary and secondary visual areas (V1 and V2). The intensity of gamma band synchronization increased with the level of visual attention (from low to high). Differences between conditions were seen for up to 1600 ms.

The current results show that the level of gamma band synchronization in early visual areas is related to the level of attention directed to a visual stimulus. These gradual and long-lasting effects expand the *biased competition* model of attention and highlight the key role of gamma band synchronization in early visual areas for selective attention.

Einleitung

In unserer Umwelt strömen meist viele unterschiedliche Reize gleichzeitig auf uns ein. Daher ist es unerlässlich, relevante von irrelevanter Information zu trennen, um relevante Informationen besser verarbeiten zu können. Werden beispielsweise gleichzeitig zwei Reize in unterschiedlichen Modalitäten verarbeitet, wird der Reiz in der beachteten Modalität in der Regel effizienter verarbeitet als der in der nicht beachteten Modalität (1, 2). Da angenommen wird, dass die Verarbeitung von Reizen eine begrenzte Kapazität hat, hat die Verarbeitung von Reizen in einer Modalität auch Einfluss auf die Verarbeitung von Reizen in anderen Modalitäten. Dementsprechend kann z.B. der Grad visueller Aufmerksamkeit durch gleichzeitige Darbietung eines auditorischen Reizes beeinflusst werden (3).

Aufmerksamkeitsrelevante Prozesse im menschlichen Gehirn sind mit einer Synchronisation der Hirnaktivität im Gammaband (30-100 Hz; den sogenannten Gammaband-Oszillationen) assoziiert (4–9). In früheren Studien wurde gezeigt, dass sich die Stärke visuell induzierter Gammaband-Oszillationen mit dem Aufmerksamkeitsgrad ändert, d.h. mit Aufmerksamkeit moduliert wird (10–14). Allerdings wurden in diesen Studien nur Zustände hoher und niedriger Aufmerksamkeit kontrastiert. Eine graduelle Modulation von Aufmerksamkeit und den korrespondierenden Gammaband-Oszillationen wurde bis jetzt noch nicht untersucht.

Studien mittels funktioneller Magnetresonanztomographie konnten zeigen, dass Aufmerksamkeit die Verarbeitung in frühen visuellen Arealen moduliert (15, 16). Obwohl frühere neurophysiologische Studien bereits ausgeprägte Gammaband-Oszillationen in visuellen Arealen (V1-V3) fanden (5, 6), zeigte sich die Modulation von Gammaband-Oszillationen durch Aufmerksamkeit meist in mittleren bis späten Stufen visueller Verarbeitung (4, 17, 18). Durch die Ergebnisse der vorangegangenen Studien kann angenommen werden, dass auch Gammaband-Oszillationen in frühen visuellen Arealen mit dem Aufmerksamkeitsgrad variieren.

Ziel dieser Arbeit war es, durch ein bimodales, audiovisuelles Reaktionszeitparadigma die Stärke der Aufmerksamkeit auf einen visuellen Reiz systematisch, graduell zu manipulieren und drei unterschiedliche Grade visueller Aufmerksamkeit zu induzieren. Neuromagnetische Gehirnaktivität wurde mithilfe von Magnetenzephalographie (MEG) aufgezeichnet, um die Modulation von Gammaband-Oszillationen in frühen visuellen Arealen zu untersuchen.

Material und Methoden

Probanden

An der Studie nahmen 16 gesunde, rechtshändige Probanden mit normaler Hör- und normaler oder korrigierter Sehkraft teil (8 weiblich, mittleres Alter \pm Standardabweichung: $25,5 \pm 4,3$ Jahre).

Paradigma

Die Probanden bearbeiteten ein Reaktionszeitparadigma (Abbildung 1). Jeder Durchgang begann mit einem Hinweisreiz (1000 ms), der anzeigte, welcher von drei experimentellen Bedingungen (*visuell selektiv*, *auditorisch selektiv* oder *geteilt*) der aktuelle Durchgang angehörte. Aus dem Hinweisreiz ergab sich dadurch die Aufgabenstellung des Durchgangs. Anschließend erschien ein Fixationspunkt (2000 ms). Darauf folgend startete die simultane visuelle (ein sich nach innen bewegendes Kreismuster) und auditorische (ein konstanter Sinuston, eingebettet in weißes Rauschen) Stimulation. Nach 500, 1000, 2000, oder 3000 ms veränderten entweder zuerst der visuelle oder der auditorische Reiz seine Qualität (Änderung 1). 750 oder 1000 ms später veränderte auch der andere Reiz seine Qualität (Änderung 2). In der Hälfte der Durchgänge veränderten erst der visuelle und dann der auditorische Reiz ihre jeweilige Qualität. In der anderen Hälfte der Durchgänge erfolgte die Änderung umgekehrt.

Die Änderung des visuellen Reizes bestand aus einer Geschwindigkeitserhöhung, während der sich der Reiz entweder nach außen oder weiterhin nach innen beschleunigte (außen/innen). Die Änderung des auditorischen Reizes war eine Tonhöhenänderung zu einer höheren oder tieferen Tonhöhe (hoch/tief).

Je nach experimenteller Bedingung ergaben sich verschiedene Aufgabenstellungen und die Änderungen eines der Reize wurde zum Zielreiz: der visuelle Reiz in der *visuell selektiven* Bedingung, der auditorische Reiz in der *auditorisch selektiven* Bedingung und der Reiz, der sich zuerst veränderte, in der *geteilten* Bedingung (in 50% der Fälle der visuelle und in 50% der Fälle der auditorische Reiz). Die Aufgabe des Probanden war es, so schnell wie möglich auf Veränderungen des Zielreizes zu reagieren und dabei anzugeben, welche Änderung stattgefunden hatte (innen/außen bzw. hoch/tief). Nach jedem Durchgang wurde ein Feedback über die Korrektheit der Antwort angezeigt. Jeder Proband bearbeitete 432 Durchgänge (je 108 der *visuell selektiven* und *auditorisch selektiven* Bedingungen und 216 der *geteilten* Bedingung). Das Ziel des Paradigmas war es, drei Grade visueller Aufmerksamkeit zu induzieren: ein hoher Grad in der *visuell selektiven* Bedingung, ein mittlerer in der *geteilten* Bedingung und ein geringer in der *auditorisch selektiven* Bedingung.

Eine genauere Beschreibung der Reize und ihrer Darbietungsform findet sich in Kahlbrock et al. (2012a; (19)).

Datenaufnahme

Die neuromagnetische Gehirnaktivität wurde mit einem Ganzkopf 122-Kanal MEG-System (Elekta Oy, Helsinki, Finnland) aufgezeichnet. Mittels Elektrookulogramm

wurden zudem vertikale und horizontale Augenbewegungen gemessen. Für jeden Probanden wurden weiterhin hochaufgelöste individuelle anatomische Magnetresonanztomographie (MRT) Aufnahmen des Kopfes erstellt (3 T Siemens Magnetom; München/Erlangen).

Datenanalyse

Verhaltensdaten

Zur Untersuchung der Effekte auf Verhaltensebene wurden die Reaktionszeiten mittels einer Varianzanalyse (ANOVA) mit Messwiederholung mit den Faktoren Modalität (visuell/auditorisch) und Bedingung (selektiv/geteilt) analysiert. Hierfür wurden die Durchgänge anhand der verschiedenen Bedingungen (*visuell selektiv*, *auditorisch selektiv* oder *geteilt*) aufgeteilt. Die *geteilte* Bedingung wurde weiterhin unterteilt in die Durchgänge, in denen auf den visuellen Reiz reagiert werden musste (*visuell geteilt*), und die Durchgänge, in denen auf den auditorischen Reiz reagiert werden musste (*auditorisch geteilt*). In diese und alle folgenden Analysen wurden ausschließlich korrekte Durchgänge mit Reaktionszeiten kleiner 2000 ms eingeschlossen.

MEG-Datenanalyse

Die MEG Daten wurden mittels der Toolbox FieldTrip (20) und Matlab 7.1 (MathWorks, Natick, MA) analysiert.

Zunächst wurden aus den kontinuierlichen Daten die relevanten Epochen identifiziert und artefaktbereinigt. Jede Epoche begann mit der Präsentation des Fixationspunktes und endete mit der Veränderung des ersten Reizes (Änderung 1). Zur Artefaktbereinigung wurden semiautomatische Routinen verwendet. Hierbei wurden, abhängig von der Anzahl der Artefakte pro Durchgang, entweder nur die Epochen, die ein Artefakt enthielten (partielle Korrektur) oder die gesamten Durchgänge, in denen Artefakte vorhanden waren (komplette Korrektur) verworfen. Zur partiellen Artefaktkorrektur wurden für die unterschiedlichen Artefakttypen (Blinzel-, Muskel-, und Sensorartefakte) und für jeden Probanden individuelle z-Werte berechnet und die Schwellenwerte zur Definition eines Artefaktes für jeden Probanden individuell festgelegt. Die komplette Artefaktkorrektur erfolgte mittels visueller Inspektion (eine genauere Beschreibung der Prozedur findet sich in Kahlbrock et al. (2012a; (19))). Für jeden Probanden wurden Leistungsspektren (Powerspektren) für die Zeit von 500 bis 1000 ms nach Beginn der Stimulation im Bereich von 30 bis 100 Hz berechnet, um die Frequenz mit der stärksten Gammaband-Antwort zu bestimmen.

Gemittelt über alle Durchgänge wurde die Quelle der stärksten Gammaband-Antwort relativ zur Baseline (-1000 bis -500 ms) lokalisiert, d.h. die Hirnregion mit der stärksten Aktivität in diesem Frequenzbereich. Hierfür wurde ein Verfahren verwendet, in dem adaptive räumliche Filter in der Frequenzdomäne zur Anwendung kommen (*Dynamic Imaging of Coherent Sources*; (21)). Die gefundenen Quelleninformationen wurden auf die individuelle MRT-Aufnahme des jeweiligen Einzelprobanden projiziert und das der individuellen Lokalisation der stärksten Gammaband-Antwort entsprechende Brodmann Areal nach Talairach und Tournoux (22) bestimmt.

Um den Zeitverlauf des Signals an der individuellen Stelle der stärksten Gammaband-Antwort zu quantifizieren, wurde eine weitere, zeitaufgelöste, Quellenanalyse durchgeführt. Zu diesem Zweck wurde für jeden Probanden für die Hirnregion mit der stärksten Gammaband-Antwort ein virtueller Sensor generiert. Mittels eines *linear constrained minimum variance (LCMV) Beamformers* wurden anschließend die Zeitverläufe der Quellen berechnet. Über diese Zeitverläufe konnte dann eine Zeit-Frequenz-Analyse mittels Multitapern berechnet werden. Diese Zeit-Frequenz-Analysen wurden für jeden Probanden separat für jede der drei Bedingungen berechnet (*visuell selektiv, auditorisch selektiv* und *geteilt*). Alle Durchgänge der *geteilten* Bedingung wurden verwendet, unabhängig davon, ob auf den visuellen oder den auditorischen Reiz reagiert wurde, da die Stimulation bis zur Änderung 1 in allen Durchgängen gleich war. Schließlich wurden die Unterschiede in der Stärke der Gammaband-Oszillationen zwischen den drei Bedingungen auf statistische Signifikanz geprüft. Hierfür wurden für jede Versuchsperson und jede der drei Bedingungen zufällig gleich viele Durchgänge ausgewählt und dann für jeden der drei Vergleiche (*visuell selektiv/auditorisch selektiv, geteilt/auditorisch selektiv* und *visuell selektiv/geteilt*) eine T-Statistik für abhängige Daten berechnet. Um eine Kumulierung des Alphafehlers aufgrund von multiplen Vergleichen einer großen Anzahl von Zeit- und Frequenzpunkten zu verhindern, wurde die statistische Signifikanz zwischen den Bedingungen mittels eines nonparametrischen Clusterbasierten Randomisationsverfahrens geprüft (23, 24). Mittels Bonferroni-Holm Korrektur (25) wurde außerdem für multiple Vergleiche zwischen den drei Bedingungen korrigiert.

Ergebnisse

Verhalten

Die mittleren Reaktionszeiten waren $586,39 \text{ ms} \pm 14,61$ für die *visuell selektive*, $669,96 \text{ ms} \pm 22,79$ für die *visuell geteilte*, $299,20 \text{ ms} \pm 21,99$ für die *auditorisch selektive* und $430,74 \text{ ms} \pm 23,50$ für die *auditorisch geteilte* Bedingung (Standardfehler des Mittelwertes angegeben). Eine ANOVA mit Messwiederholung zeigte Haupteffekte für die Faktoren Modalität ($F(1,15) = 426,57, p < 0,001$) und Bedingung ($F(1,15) = 90,61, p < 0,001$) sowie eine Interaktion ($F(1,15) = 10,00, p = 0,006$) zwischen den beiden Faktoren. Die Probanden reagierten schneller in den *selektiven* als in den *geteilten* Bedingungen. Zudem war der Unterschied zwischen der *selektiven* und *geteilten* Bedingung stärker in der *auditorischen* als in der *visuellen* Modalität.

MEG-Daten

Die Frequenz der individuell stärksten visuellen Gammaband-Antwort in Reaktion auf die audiovisuelle Stimulation lag für die einzelnen Probanden zwischen 54 und 69 Hz. Die Quelle dieser stärksten Gammaband-Antworten befand sich bei 14 von 16 Probanden in den Brodmann Arealen 17 oder 18 (V1 und V2, Abbildung 2 A, B), also Arealen früher visueller Verarbeitung. Alle Probanden zeigten in allen drei Bedingungen lang anhaltende visuelle Gammaband-Aktivität (eine Erhöhung der Leistung/Power im Vergleich zur Baseline; Abbildung 2 C).

Die Bedingungen wurden separat für die Baseline- und die Stimulationsphase auf Unterschiede untereinander getestet. Für die Baselinephase zeigte sich kein Unterschied zwischen den Bedingungen ($p > 0,1$), so dass die weiteren Analysen auf der relativen Veränderung der Leistung im Vergleich zur Baseline basieren. Paarweise Vergleiche zeigten Unterschiede in der Stärke der Gammaband-Oszillationen zwischen den drei Bedingungen (Abbildung 2 D). Die relative Gammaband-Antwort war stärker in der *visuell selektiven* als in der *auditorisch selektiven* Bedingung ($p < 0,001$). Zudem war sie stärker in der *geteilten* als in der *visuell selektiven* Bedingung ($p < 0,009$) und in der *geteilten* als in der *auditorisch selektiven* Bedingung ($p < 0,002$). So war die relative Gammaband-Antwort am stärksten in der *visuell selektiven*, mittel in der *geteilten* und am geringsten in der *auditorisch selektiven* Bedingung.

Diskussion

Mittels eines audiovisuellen Reaktionszeitparadigmas konnten wir in der vorliegenden Studie zeigen, dass visuelle Aufmerksamkeit und die damit assoziierten Gammaband-Oszillationen in frühen visuellen Arealen graduell moduliert werden können. Diese graduelle Modulation zeigt eine präzise Anpassung der Gammaband-Oszillationen an aktuelle Erfordernisse der Umwelt, was eine effiziente Nutzung kognitiver Ressourcen ermöglicht.

Im Verhalten zeigten sich unterschiedliche Reaktionszeiten für die drei Aufmerksamkeitsgrade, höchstwahrscheinlich begründet in einer Verschiebung der Aufmerksamkeit zwischen der visuellen und auditorischen Modalität. Somit wurden vorhergehende Verhaltensstudien (2, 26, 27) um eine dritte, mittlere Aufmerksamkeitsstufe erweitert, so dass graduelle Aufmerksamkeitsveränderungen untersucht werden konnten.

Wie bereits in früheren Studien (4, 5, 28, 29), zeigten die Probanden lang anhaltende Gammaband-Aktivität in allen Bedingungen. Die Gammaband-Antwort war am stärksten in der *visuell selektiven*, mittel in der *geteilten* und am geringsten in der *auditorisch selektiven* Bedingung. Dieses Ergebnis untermauert den Verhaltenseffekt und stützt die Annahme, dass drei Grade visueller Aufmerksamkeit gleichzeitig auch durch eine korrespondierende Modulation der neurophysiologischen Parameter repräsentiert sind. Dieses Ergebnis erweitert frühere Arbeiten zu Gammaband-Oszillationen, die lediglich Zustände mit und ohne Aufmerksamkeit kontrastiert hatten (4, 10, 11, 14, 30), um eine dritte, mittlere Stufe visueller Aufmerksamkeit.

Darüber hinaus konnten erstmals derart lang anhaltende Aufmerksamkeitseffekte (bis zu 1600 ms) auf Gammaband-Oszillationen gezeigt werden. In früheren Arbeiten wurden die Ergebnisse entweder über bestimmte Zeitperioden und/oder Frequenzen gemittelt (4, 10, 12, 13, 30). Daher geben die vorliegenden Daten neue Einblicke in lang anhaltende Aufmerksamkeitseffekte und deren Beziehung zu Gammaband-Oszillationen.

Die Quellen der stärksten Gammaband-Antwort wurden bei 14 von 16 Probanden in frühen visuellen Arealen (V1 und V2) lokalisiert. Ebenso zeigte sich die Modulation der

Gammaband-Oszillationen in diesen Arealen. Wenngleich frühere Studien bereits ausgeprägte Gammaband-Oszillationen in visuellen Arealen (V1-V3) fanden (5, 6), wurde eine aufmerksamkeitsrelevante Modulation von Gammaband-Oszillationen meist in mittleren bis späten Stufen visueller Verarbeitung gefunden (4, 17, 18). Somit ist die vorliegende Arbeit die erste, die in frühen visuellen Arealen zeigen konnte, dass die Stärke der Gammaband-Oszillationen mit dem Grad der visuellen Aufmerksamkeit korrespondiert.

Ein Modell, das im Zusammenhang mit selektiv visueller Aufmerksamkeit und Gammaband-Oszillationen diskutiert wird, ist das Modell der *biased competition through enhanced synchronization* (31), dessen Annahmen auf der *biased competition* Hypothese (32, 33) basieren. Dieses Modell besagt, dass durch die Erhöhung von Gammaband-Oszillationen der beachtete von zwei konkurrierenden Reizen effizienter verarbeitet wird. Vorherige Studien zu selektiv visueller Aufmerksamkeit konnten diese Annahme untermauern (4, 34). Die vorliegenden Daten deuten an, dass das *biased competition* Modell auch bei gradueller Modulation der Aufmerksamkeit im visuellen System zutrifft. Somit würde nicht nur entweder der eine oder der andere Reiz effizienter verarbeitet, sondern es wäre auch eine graduelle Verteilung der Aufmerksamkeit zwischen den beiden Reizen möglich. Gammaband-Oszillationen wären somit ein adaptiver Mechanismus, der die selektive Verarbeitung eines Reizes graduell erhöht und dabei den Grad der selektiven Aufmerksamkeit repräsentiert, die ein Reiz erhält. Aufgrund der vorliegenden Daten kann spekuliert werden, dass das *biased competition* Modell auch in einem intermodalen Kontext (hier zwischen der visuellen und auditorischen Modalität) Anwendung finden kann.

Zusammenfassend zeigt die vorliegende Arbeit erstmals eine graduelle Modulation lang anhaltender Gammaband-Oszillationen in frühen visuellen Arealen, die mit der Stärke der visuellen Aufmerksamkeit zusammenhängt. Diese Effekte erweitern das *biased competition* Modell um eine graduelle Dimension und unterstreichen die Schlüsselrolle von Gammaband-Oszillationen bei visueller Aufmerksamkeit.

Zukünftige Studien sollten dieses Wissen nutzen, um die funktionelle Rolle von Gammaband-Oszillationen im gesunden Gehirn und deren Beeinträchtigung im erkrankten Gehirn weiter zu untersuchen und aufzuklären. Erste Ergebnisse in diesem Bereich weisen bereits darauf hin, dass visuelle Gammaband-Oszillationen bei Patienten mit Aufmerksamkeitsstörungen verändert sind (35).

Referenzen

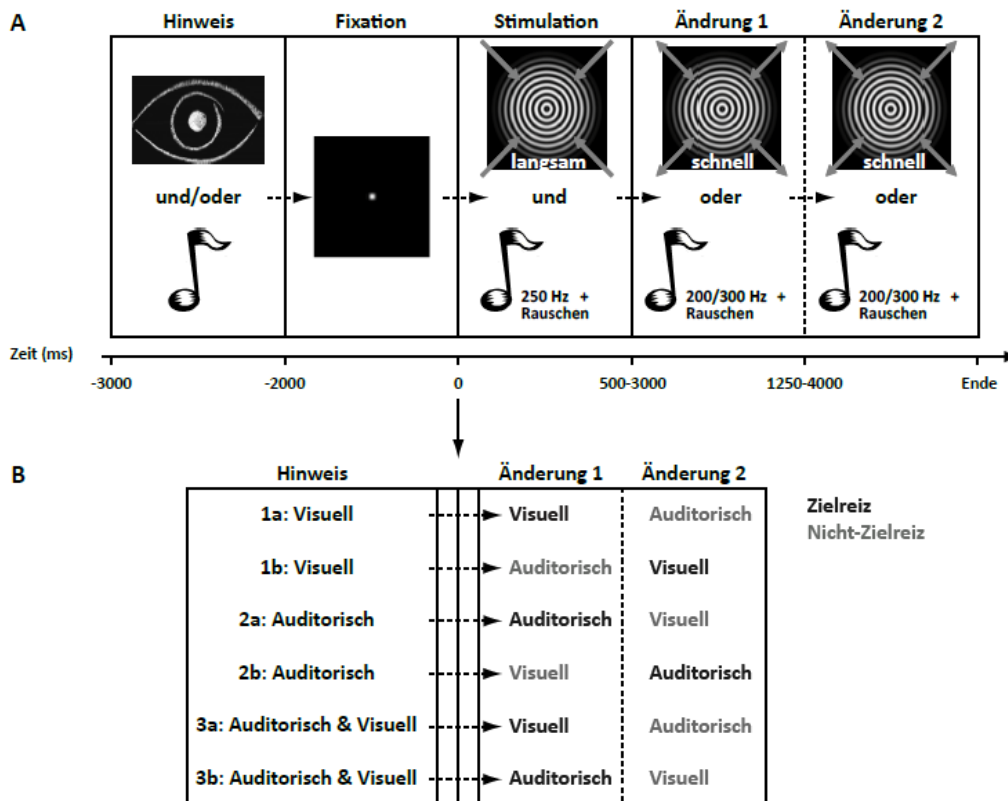
1. Ghetti E, Eimer M (2011) Active Listening Impairs Visual Perception and Selectivity: An ERP Study of Auditory Dual-task Costs on Visual Attention. *J Cogn Neurosci* 23:832–844.
2. Spence C, Driver J (1997) On measuring selective attention to an expected sensory modality. *Percept Psychophys* 59:389–403.
3. Bonnel AM, Hafter ER (1998) Divided attention between simultaneous auditory and visual signals. *Percept Psychophys* 60:179–90.
4. Fries P, Reynolds JH, Rorie AE, Desimone R (2001) Modulation of oscillatory neuronal synchronization by selective visual attention. *Science* 291:1560–3.
5. Hoogenboom N, Schoffelen JM, Oostenveld R, Parkes LM, Fries P (2006) Localizing human visual gamma-band activity in frequency, time and space. *Neuroimage* 29:764–73.
6. Hoogenboom N, Schoffelen JM, Oostenveld R, Fries P (2010) Visually induced gamma-band activity predicts speed of change detection in humans. *Neuroimage* 51:1162–1167.
7. Kaiser J, Hertrich I, Ackermann H, Lutzenberger W (2006) Gamma-band activity over early sensory areas predicts detection of changes in audiovisual speech stimuli. *Neuroimage* 30:1376–82.
8. Lachaux JP, George N, Tallon-Baudry C et al. (2005) The many faces of the gamma band response to complex visual stimuli. *Neuroimage* 25:491–501.
9. Steinmetz PN, Roy A, Fitzgerald PJ et al. (2000) Attention modulates synchronized neuronal firing in primate somatosensory cortex. *Nature* 404:187–190.
10. Gruber T, Müller MM, Keil A, Elbert T (1999) Selective visual-spatial attention alters induced gamma band responses in the human EEG. *Clin Neurophysiol* 110:2074–85.
11. Siegel M, Donner TH, Oostenveld R, Fries P, Engel AK (2008) Neuronal synchronization along the dorsal visual pathway reflects the focus of spatial attention. *Neuron* 60:709–19.
12. Tallon-Baudry C, Bertrand O, Henaff MA, Isnard J, Fischer C (2005) Attention modulates gamma-band oscillations differently in the human lateral occipital cortex and fusiform gyrus. *Cereb Cortex* 15:654–62.

13. Vidal JR, Chaumon M, O'Regan JK, Tallon-Baudry C (2006) Visual grouping and the focusing of attention induce gamma-band oscillations at different frequencies in human magnetoencephalogram signals. *J Cogn Neurosci* 18:1850–62.
14. Wyart V, Tallon-Baudry C (2008) Neural dissociation between visual awareness and spatial attention. *J Neurosci* 28:2667–2679.
15. Gandhi SP, Heeger DJ, Boynton GM (1999) Spatial attention affects brain activity in human primary visual cortex. *Proc Natl Acad Sci U S A* 96:3314–9.
16. Munneke J, Heslenfeld DJ, Theeuwes J (2008) Directing attention to a location in space results in retinotopic activation in primary visual cortex. *Brain Res* 1222:184–91.
17. Gregoriou GG, Gotts SJ, Zhou H, Desimone R (2009) High-frequency, long-range coupling between prefrontal and visual cortex during attention. *Science* 324:1207–10.
18. Womelsdorf T, Fries P, Mitra PP, Desimone R (2006) Gamma-band synchronization in visual cortex predicts speed of change detection. *Nature* 439:733–736.
19. Kahlbrock N, Butz M, May ES, Schnitzler A (2012) Sustained gamma band synchronization in early visual areas reflects the level of selective attention. *Neuroimage* 59:673–681.
20. Oostenveld R, Fries P, Maris E, Schoffelen J-M (2011) FieldTrip: Open source software for advanced analysis of MEG, EEG, and invasive electrophysiological data. *Comput Intell Neurosci* 2011:156869.
21. Gross J, Kujala J, Hamalainen M et al. (2001) Dynamic imaging of coherent sources: Studying neural interactions in the human brain. *Proc Natl Acad Sci U S A* 98:694–9.
22. Talairach J, Tournoux P (1988) *Co-planar stereotaxic atlas of the human brain: 3-dimensional proportional system: an approach to cerebral imaging* (Thieme, Stuttgart).
23. Maris E, Oostenveld R (2007) Nonparametric statistical testing of EEG- and MEG-data. *J Neurosci Methods* 164:177–90.
24. Nichols TE, Holmes AP (2002) Nonparametric permutation tests for functional neuroimaging: a primer with examples. *Hum Brain Mapp* 15:1–25.
25. Holm S (1979) A Simple Sequentially Rejective Multiple Test Procedure. *Scand J Statist* 6:65–70.

26. Posner MI, Snyder CR, Davidson BJ (1980) Attention and the detection of signals. *J Exp Psychol* 109:160–74.
27. Schroeger E, Giard MH, Wolff C (2000) Auditory distraction: event-related potential and behavioral indices. *Clin Neurophysiol* 111:1450–1460.
28. Edden RAE, Muthukumaraswamy SD, Freeman TCA, Singh KD (2009) Orientation discrimination performance is predicted by GABA concentration and gamma oscillation frequency in human primary visual cortex. *J Neurosci* 29:15721–6.
29. Muthukumaraswamy SD, Edden RAE, Jones DK, Swettenham JB, Singh KD (2009) Resting GABA concentration predicts peak gamma frequency and fMRI amplitude in response to visual stimulation in humans. *Proc Natl Acad Sci U S A* 106:8356–61.
30. Müller MM, Gruber T, Keil A (2000) Modulation of induced gamma band activity in the human EEG by attention and visual information processing. *Int J Psychophysiol* 38:283–99.
31. Fries P (2005) A mechanism for cognitive dynamics: neuronal communication through neuronal coherence. *Trends Cogn Sci* 9:474–480.
32. Desimone R, Duncan J (1995) Neural Mechanisms of Selective Visual Attention. *Annu Rev Neurosci* 18:193–222.
33. Reynolds JH, Chelazzi L, Desimone R (1999) Competitive Mechanisms Subserve Attention in Macaque Areas V2 and V4. *J Neurosci* 19:1736–1753.
34. Fries P, Womelsdorf T, Oostenveld R, Desimone R (2008) The effects of visual stimulation and selective visual attention on rhythmic neuronal synchronization in macaque area V4. *J Neurosci* 28:4823–4835.
35. Kahlbrock N, Butz M, May ES et al. (2012) Lowered frequency and impaired modulation of gamma band oscillations in a bimodal attention task are associated with reduced critical flicker frequency. *NeuroImage* 61:216–227.

Abbildungen

Abbildung 1

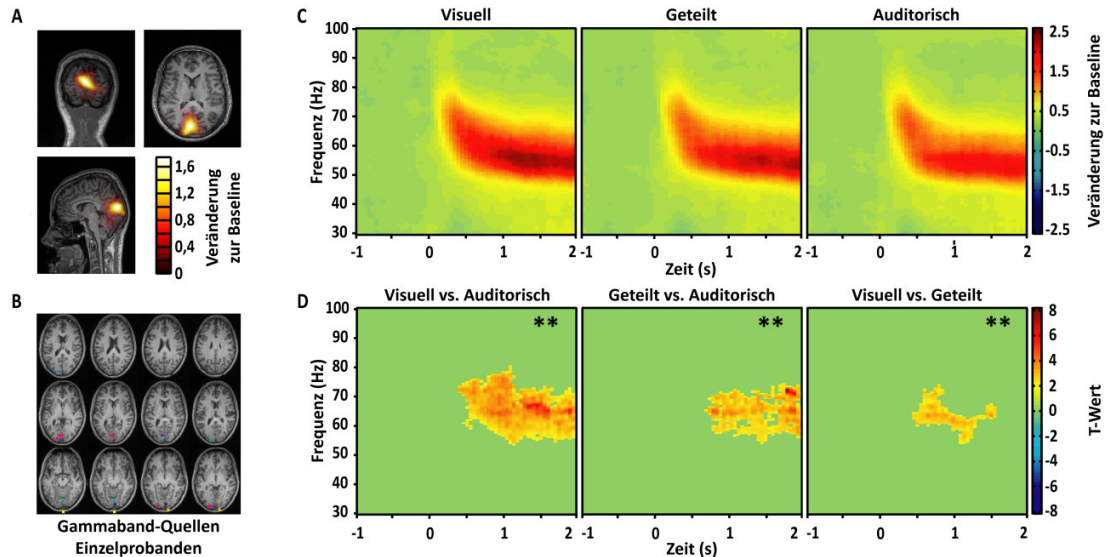


A) Exemplarische Darstellung eines Durchgangs des Reaktionszeitparadigmas. Zuerst wurde ein Hinweisreiz präsentiert, der anzeigte, welche der drei experimentellen Bedingungen (*visuell selektiv*, *auditorisch selektiv* oder *geteilt*) bearbeitet werden musste (Hinweis). Der Hinweisreiz wurde gefolgt von einem Fixationspunkt (Fixation). Daraufhin startete die gleichzeitige visuelle und auditorische Stimulation (Stimulation). Nach 500, 1000, 2000, oder 3000 ms veränderten entweder der visuelle oder der auditorische Reiz seine Qualität (Änderung 1, innen/außen oder hoch/tief). 750 oder 1000 ms später veränderte auch der andere Reiz seine Qualität (Änderung 2, innen/außen oder hoch/tief).

B) Experimentelle Bedingungen. Je nach experimenteller Bedingung wurde die Änderung eines der Reize zum Zielreiz (in schwarz dargestellt): der visuelle Reiz in der *visuell selektiven* Bedingung (1a und 1b), der auditorische Reiz in der *auditorisch selektiven* Bedingung (2a und 2b) und der Reiz, der sich zuerst veränderte, in der *geteilten* Bedingung (3a und 3b). Die Aufgabe des Probanden war es, so schnell wie möglich auf eine Veränderung des Zielreizes zu reagieren, und dabei anzugeben, welche Änderung stattgefunden hatte.

Eine genauere Beschreibung der Reize und der Darbietungsform findet sich in Kahlbrock et al. (19). Abbildung adaptiert von (19), mit Genehmigung von Elsevier.

Abbildung 2

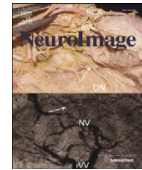


A) Gammaband-Quelle eines Einzelprobanden. Die Quelle der stärksten Gammaband-Antwort relativ zur Baseline exemplarisch für einen repräsentativen Einzelprobanden. Dargestellt ist die durchschnittliche Stärke der Quelle gemittelt über alle korrekten Durchgänge aller Bedingungen. Die Farbkodierung zeigt die relative Veränderung zur Baseline an.

B) Virtuelle Sensorpositionen der Einzelprobanden. Die virtuellen Sensoren befanden sich in den Arealen V1 und V2 bei 14 von 16 Probanden. Dargestellt sind Sensorpositionen für alle Probanden abgebildet auf einem individuellen, normalisierten Gehirn (Statistical Parametric Mapping; SPM2; <http://www.fil.ion.ucl.ac.uk/spm/>). Jeder farbige Punkt stellt die Position des virtuellen Sensors eines Probanden dar. Zur besseren Visualisierung wurden die Punkte der virtuellen Sensoren auf 9 mm erweitert. Da die einzelnen MRT-Schichten 3 mm dick sind, tauchen einzelne virtuelle Sensoren in mehreren Schichten auf.

C) Zeit-Frequenz-Repräsentationen. Durchschnittliche Zeit-Frequenz-Repräsentationen der Stärke der Oszillationen relativ zur Baseline (-1000 bis -500 ms), berechnet anhand des Signals an der virtuellen Sensorposition der Einzelprobanden, gemittelt über alle Probanden. In allen drei Bedingungen (*visuell selektiv*, links, *geteilt*, Mitte, *auditorisch selektiv*, rechts) zeigten sich lang anhaltende Gammaband-Oszillationen relativ zur Baseline (Reizbeginn zum Zeitpunkt 0). Farbkodierung: 0 bedeutet keine Veränderung, 2,5 eine 250% Erhöhung der Leistung (Power) relativ zur Baseline.

D) Statistische Vergleiche zwischen den drei Bedingungen. Die Ergebnisse sind als t-Werte der T-Statistik für abhängige Daten, die für die Vergleiche zwischen den jeweiligen Bedingungen berechnet wurden, dargestellt. Grün maskiert sind alle, nach Durchführung des Clusterbasierten Randomisationsverfahrens, nicht signifikanten Werte. Die relative Gammaband-Antwort war stärker in der *visuell selektiven* als in der *auditorisch selektiven Bedingung* (links), sie war stärker in der *geteilten* als in der *auditorisch selektiven Bedingung* (Mitte) und stärker in der *visuell selektiven* als in der *geteilten Bedingung* (rechts; ** = $p < 0,01$; alle p -Werte korrigiert).
Abbildung adaptiert von (19), mit Genehmigung von Elsevier.



Lowered frequency and impaired modulation of gamma band oscillations in a bimodal attention task are associated with reduced critical flicker frequency

Nina Kahlbrock^a, Markus Butz^{a,b,*}, Elisabeth S. May^a, Meike Brenner^a, Gerald Kircheis^c, Dieter Häussinger^c, Alfons Schnitzler^{a,d}

^a Heinrich-Heine-University Düsseldorf, Medical Faculty, Institute of Clinical Neuroscience and Medical Psychology, Universitätsstraße 1, D-40225 Düsseldorf, Germany

^b University College London, Institute of Neurology, 33 Queen Square, London, WC1N 3BG, UK

^c Heinrich-Heine-University Düsseldorf, Medical Faculty, Department of Gastroenterology, Hepatology and Infectious Disease, Universitätsstraße 1, D-40225 Düsseldorf, Germany

^d Heinrich-Heine-University Düsseldorf, Medical Faculty, Department of Neurology, Universitätsstraße 1, D-40225 Düsseldorf, Germany

ARTICLE INFO

Article history:

Accepted 21 February 2012

Available online 1 March 2012

Keywords:

MEG

Oscillations

Gamma

CFF

Hepatic encephalopathy

GABA

ABSTRACT

Visual attention is associated with occipital gamma band activity. While gamma band power can be modulated by attention, the frequency of gamma band activity is known to decrease with age. The present study tested the hypothesis that reduced visual attention is associated with a change in induced gamma band activity. To this end, 26 patients with liver cirrhosis and 8 healthy controls were tested. A subset of patients showed symptoms of hepatic encephalopathy (HE), a frequent neuropsychiatric complication in liver disease, which comprises a gradual increase of cognitive dysfunction including attention deficits. All participants completed a behavioral task requiring shifts of attention between simultaneously presented visual and auditory stimuli. Brain activity was recorded using magnetoencephalography (MEG). The individual critical flicker frequency (CFF) was assessed as it is known to reliably reflect the severity of HE.

Results showed correlations of behavioral data and HE severity, as indexed by CFF. Individual visual gamma band peak frequencies correlated positively with the CFF ($r = 0.41$). Only participants with normal, but not with pathological CFF values showed a modulation of gamma band power with attention.

The present results suggest that CFF and attentional performance are related. Moreover, a tight relation between the CFF and occipital gamma band activity both in frequency and power is shown. Thus, the present study provides evidence that a reduced CFF in HE, a disease associated with attention deficits, is closely linked to a slowing of gamma band activity and impaired modulation of gamma band power in a bimodal attention task.

© 2012 Elsevier Inc. All rights reserved.

Introduction

Cortical gamma band activity (30–100 Hz) is known as a key correlate of cognition (Fries et al., 2008) and has been associated with various cognitive functions (Gray et al., 1989; Roelfsema et al., 1997; Tallon-Baudry et al., 1998), including attention (Fries et al., 2001; Hoogenboom et al., 2006, 2010; Kaiser et al., 2006; Lachaux et al., 2005; Steinmetz et al., 2000). The power of visually induced gamma band activity can be modulated by attention (Gruber et al., 1999; Kahlbrock et al., 2012; Siegel et al., 2008; Tallon-Baudry et al., 2005; Vidal et al., 2006; Wyart and Tallon-Baudry, 2008). The frequency of visually induced gamma band activity seems to be specific to certain cognitive operations. Vidal et al. (2006) showed in their study that distinct frequencies of gamma band oscillations are related to attention and grouping related activity, respectively. However,

when stimuli, cognitive operation, and cognitive demand remain constant, gamma band power and frequency have been demonstrated to be very consistent across measurements within-subjects. Nevertheless, high inter-subject variability in power and frequency of gamma band responses can be observed (Hoogenboom et al., 2006; Muthukumaraswamy et al., 2010). The underlying causes of this variability have not been finally explained so far.

Two recent studies, including participants from first to fifth decade of life, have shown that the frequency of gamma band activity decreases with age (Gaetz et al., 2011b; Muthukumaraswamy et al., 2010). Moreover, in subjects suffering from schizophrenia, it has been shown that the frequency of phase-locked gamma band activity related to gestalt perception is decreased and correlates with specific symptoms of the disease, i.e. visual hallucinations, thought disorder, and disorganization (Spencer et al., 2004). Interestingly, these patients experience multiple cognitive deficits, which can be seen as core pathology of the disorder (Green, 1996).

Distinct oscillation features have been demonstrated in various neurological and psychiatric diseases (Schnitzler and Gross, 2005;

* Corresponding author.

E-mail address: m.butz@ucl.ac.uk (M. Butz).

Uhlhaas and Singer, 2006). Especially, a slowing of brain activity in lower frequencies, i.e. delta, alpha, and beta band activity has been demonstrated. For example, patients with brain infarct or brain tumor show increased activity in the delta band in perilesional areas (Butz et al., 2004; de Jongh et al., 2003). Patients with Alzheimer's disease show a reduction in resting state gamma band synchronization (Koenig et al., 2005).

Also in hepatic encephalopathy (HE), the neurological entity studied in the present work, spontaneous oscillatory activity and the mean resting activity electroencephalography (EEG) peak frequency have been shown to be progressively slowed (e.g., Amodio et al., 1999, 2009; Bajaj, 2010; Davies et al., 1991; Kullmann et al., 2001; Montagnese et al., 2007, 2011; Olesen et al., 2011; Parson-Smith et al., 1957; Van der Rijt et al., 1984). Alterations in the EEG are associated with the severity of HE (Marchetti et al., 2011). Hence, the EEG can be used to complement the neurological examination for HE, i.e., diagnosis, grading, and prediction (Amodio and Gatta, 2005; Guerit et al., 2009). HE is a frequent, potentially reversible, neuropsychiatric complication of chronic liver disease, involving multiple cognitive and motor symptoms, altered sleep patterns, and changes in vigilance state (for a review see Butterworth, 2000; Häussinger and Schliess, 2008). Of special relevance for the present study is one key symptom of HE – a gradual increase of attention deficits with increasing disease severity (Amodio et al., 2005; Kircheis et al., 2009; Pantiga et al., 2003; Weissenborn et al., 2001, 2005). Previous studies addressing the motor symptoms in HE revealed a pathologically slowed thalamo-cortico-muscular coupling with increasing severity of HE (Timmermann et al., 2002, 2003). Disease severity of HE can be quantified by determining the critical flicker frequency (CFF), which decreases with increasing disease severity (Kircheis et al., 2002; Prakash and Mullen, 2010; Romero-Gómez et al., 2007; Sharma et al., 2007). Accordingly, Timmermann et al. (2008) showed a strong correlation between the slowing of cortico-muscular coupling and the CFF. Based on the findings of slowed coupling in the motor systems of HE patients, Timmermann et al. (2005) hypothesized that a global slowing of oscillatory activity in various human cerebral subsystems could represent a key mechanism in the pathophysiology of HE. Along these lines, the question arises whether certain diseases that involve cognitive deficits are associated with a slowing of gamma band brain activity.

The present study aimed to test the relation of disease severity and the frequency of attention-related visually induced gamma band activity in a population of HE patients. In addition, the subject's capacity to modulate attention and concurrently modulate the power of attention-related occipital gamma band activity was scrutinized. Subjects completed a behavioral task requiring shifts of attention between simultaneously presented visual and auditory stimuli, while brain activity was recorded using magnetoencephalography (MEG). A reduction in attention-related gamma band peak frequencies with increasing disease severity was hypothesized, adhering to the hypothesis of slowed oscillatory brain activity as a key phenomenon in the pathophysiology of HE. Due to the known attentional deficits in this disease, a reduced capacity to modulate gamma band power with attention was expected.

Methods

Participants

Patients and controls

26 patients with liver cirrhosis, confirmed by sonography or fibroscan (> 13 kPa) and 8 healthy, age-matched controls underwent a comprehensive clinical assessment including blood tests, neuropsychometric computer tests (Vienna test system, WINWTS, Version 4.50, 1999), assorted subtests of the test battery of Tests of Attentional Performance (TAP; PSYTEST, Herzogenrath, Germany), and CFF

measurements (Eberhardt, 1994). As described in Kircheis et al. (2002) and according to West-Haven Criteria (Conn and Lieberthal, 1979) and psychometric test results, patients were classified into three groups: (i) HE0, i.e. patients showing no signs of HE, (ii) minimal HE (mHE), i.e., patients showing no clinical signs of HE, but pathological results in at least two psychometric tests, and (iii) HE1, i.e. manifest HE of grade 1, patients showing clinical signs of HE. The fourth group constituted of healthy control participants, i.e., (iv) controls (please see Table 1 for further details about subjects' characteristics). 24 patients performed the tests for grading of HE stage within two days, two patients within a week before or after the MEG measurement. All subjects had normal or corrected to normal vision and normal hearing. All of them gave their written informed consent. The study was approved by the local ethics committee (study no. 2895) and was performed in accordance with the Declaration of Helsinki.

General exclusion criteria were neurological/psychiatric illness, intake of psychoactive drugs, the existence of an HIV infection, Wilson's disease, Korsakoff's syndrome, and chronic pain syndrome. Patients with liver cirrhosis stemming from alcohol abuse had to be abstinent from alcohol for at least 6 months. To further control for this, blood

Table 1
Participant data.

Group	Subj. no.	Age	Sex	CFF	Cirrhosis etiology	Child Pugh Score
Control	1	51	m	44.3	–	–
	2	46	f	41.1	–	–
	3	67	m	39.8	–	–
	4	71	m	–	–	–
	5	69	f	40.8	–	–
	6	58	f	41.4	–	–
	7	61	f	38.4	–	–
	8	73	m	38.1	–	–
	n = 8	62.0 ± 3.5		40.6 ± 0.8		
HE0	9	55	f	39.4	Ethanol	A
	10	53	m	43.0	Ethanol	B
	11	48	m	41.8	Hepatitis C	C
	12	44	f	41.3	PBC	A
	13	69	f	38.4	Hepatitis C	A
	14	60	m	42.3	Ethanol	A
	15	70	m	39.0	Hepatitis C	A
	16	59	m	39.1	Hepatitis B	A
	n = 8	52.3 ± 3.3		40.5 ± 0.6		
mHE	17	60	m	38.6	Cryptogenic	B
	18	59	f	39.1	Hepatitis C	A
	19	57	m	38.3	Ethanol	A
	20	65	f	39.0	Ethanol	A
	21	56	m	35.7	Ethanol	B
	22	57	m	37.2	Ethanol	A
	23	62	m	39.9	Cryptogenic	A
	24	52	m	39.4	Hepatitis C	A
	n = 8	58.5 ± 1.3		38.4 ± 0.5		
HE1	25	69	m	38.6	Ethanol	B
	26	67	m	36.2	Autoimmune	C
	27	70	m	38.3	Hepatitis A/B	B
	28	72	m	35.5	Hepatitis C	B
	29	75	f	38.3	Cryptogenic	B
	30	65	f	37.7	Ethanol	C
	31	45	m	34.8	PSC	C
	32	45	f	32.6	Autoimmune	C
	33	63	m	36.4	Ethanol	A
	34	59	m	32.4	Ethanol	C
	n = 10	63.0 ± 3.3		36.1 ± 0.7		

Individual participant specific data are shown. For age and CFF, group mean values ± standard errors of the mean are given. Gender is coded as f = female and m = male. Etiology of liver cirrhosis was assessed by each patient's medical history, PSC = Primary sclerosing cholangitis, PBC = Primary biliary cirrhosis. Grading of liver cirrhosis was done according to the European Child-Pugh-classification (Pugh et al., 1973).

ethanol levels and carbohydrate deficient transferrin (CDT) were measured.

Groups of participants sorted by CFF

Due to an ongoing discussion of the validity of the common classification scheme of HE into groups of HE0, mHE, and HE1-HE4 (Häussinger et al., 2006; Kircheis et al., 2007), all analyses were performed on an alternative group classification scheme. According to Kircheis et al. (2002), a critical flicker frequency (CFF, see *Determination of the critical flicker frequency (CFF)* for more information) value of 39 Hz is described as being the critical cut-off frequency separating patients with manifest HE from controls and HE0 patients. Therefore, all participants showing significant gamma band activity in response to the visual stimulus (*visual condition, Bimodal reaction time paradigm and Individual gamma band peaks and power*) were sorted by CFF into one group of participants with low, i.e. pathological, CFF (< 39 Hz, $n = 12$) and one group of subjects with high, i.e. normal, CFF (≥ 39 Hz, $n = 14$). In a second step, all analyses were repeated, including patients only (low CFF: $n = 10$ and high CFF: $n = 10$). Henceforth, the groups defined by their CFF values will be referred to as low and high CFF groups respectively.

Data acquisition

Determination of the critical flicker frequency (CFF)

The critical flicker frequency (CFF) is the frequency threshold at which a flickering light is perceived as flickering and no longer as continuous (normally ≥ 39 Hz for healthy people). The CFF has been shown to reliably quantify and monitor the severity of HE, i.e. the lower the CFF the higher the severity of HE (Kircheis et al., 2002; Prakash and Mullen, 2010; Romero-Gómez et al., 2007; Sharma et al., 2007). CFF thresholds were assessed using the Schuhfried Test System (Dr. Schuhfried Inc., Mödling, Austria). In gradual steps of 0.5 to 0.1 Hz/s rectangular light pulses decreased their frequency from 60 Hz downwards until the subjects indicated by a button press that they perceived them as flickering. Details of the recording procedure can be found in Kircheis et al. (2002). Only mean CFF values with a standard deviation below 0.5 Hz were considered for further analyses. All subjects except for one control subject met this criterion. CFF data of this control subject were not used in further analyses.

Bimodal reaction time paradigm

A paradigm adapted and simplified from Kahlbrock et al. (2012) was used, as illustrated in Fig. 1. Subjects worked on three experimental conditions presented in separate blocks. A block design was chosen to make the task accomplishable for all HE patients. Each block was subdivided into smaller blocks of twelve trials separated by self-paced breaks to avoid fatigue.

Before each block, subjects were instructed and trained in the specific task of one of three experimental conditions: (i) *visual*, (ii) *auditory*, or (iii) *divided*. Irrespective of the condition, each trial always started with a 2000 ms fixation period. Then, a visual stimulus (an inwardly contracting grating) and an auditory stimulus (a constant tone) appeared simultaneously. After a randomly assigned period of 500, 1000, 1500, or 2000 ms, either the visual or the auditory stimulus changed its quality (Change 1). 750 or 1000 ms later, the other stimulus also changed (Change 2). In half of the trials, the visual stimulus changed first followed by a change in the auditory stimulus and vice versa. The order of trials was randomized. A change of the visual stimulus was implemented as an increase in speed of the stimulus that either continued to move inwards or changed its direction and then moved outwards (inward/outward). A change in the auditory stimulus was implemented as a change in pitch to a higher or lower pitch (high/low). Please see *Stimuli and stimulus delivery* for a detailed description of the properties and delivery of the stimuli.

Depending on the experimental condition, the change of one of the stimuli became the target. Subjects were required to give a speeded response to the change in the stimulus' quality, i.e. a change in speed of the visual or a change of pitch of the auditory stimulus. In the *visual* condition, subjects had to exclusively react to the change in the visual stimulus (Target), irrespective of its position in the trial (Change 1 or 2) and ignore the change in the auditory stimulus (Non-Target). In the *auditory* condition, accordingly, subjects had to react to the change in the auditory stimulus (Target) only and ignore the change in the visual stimulus (Non-Target). In the *divided* condition, subjects had to respond to the stimulus that changed first (Change 1 = Target) and ignore the change in the other stimulus (Change 2 = Non-Target).

In detail, the subject's task was to react to the target and indicate the quality of this stimulus change by pressing one of two buttons operated with the index fingers of both hands. Thereby, each hand was assigned to one quality change, i.e. in the *visual* condition, the index finger press of one hand indicated inward and the index finger press of the other hand outward movement of the visual stimulus. In the *auditory* condition, the index finger press of one hand indicated a high and the index finger press of the other hand a low tone. In the *divided* condition, the index finger press of one hand indicated a change in the visual and the index finger press of the other hand a change in the auditory stimulus. Feedback was given after each trial. If subjects did not respond within 2000 ms after target appearance, the trial was counted as missed. The assignment of the left or right hand to the target qualities was balanced between subjects.

The paradigm consisted of 540 trials (180 trials of each condition) including 72 catch trials. Catch trials consisted of trials without target appearance and required no response.

As shown in Kahlbrock et al. (2012), three levels of visual attention were sought to be obtained by these conditions; high in the *visual*, medium in the *divided*, and low in the *auditory* condition.

Stimuli and stimulus delivery

The fixation point consisted of a Gaussian (0.56° in diameter), which increased its contrast by 40% after 1000 ms, thereby informing the subject that the stimulation was about to start. The visual stimulus was adapted from Hoogenboom et al. (2006). It consisted of a foveal circular sine wave grating (diameter: 7.13° , spatial frequency: 2 cycles/deg, contrast: 100%) continuously contracting towards the center of the screen (velocity: $2.16^\circ/s$). The change in visual stimulus was characterized by an increase in velocity ($4.32^\circ/s$). The sine wave grating was then either still contracting towards the center of the screen (quality change inward) or changed its direction and expanded outwards (quality change outward).

The auditory stimulus was a binaurally presented 250 Hz sine tone. The change in auditory stimulus consisted of a change in pitch of the tone to either 200 Hz (quality change low) or 300 Hz (quality change high). The auditory stimulus intensity was adjusted to subjectively match the visual stimulus intensity. Thus, auditory stimuli were well audible for all subjects, but at individual volumes.

Stimulus timing was controlled using Presentation® software (version 13.0, www.neurobs.com). Visual stimuli were projected onto a screen with a DLP projector (Panasonic, Osaka, Japan) with 60 Hz refresh rate. Participants were seated approximately 96 cm away from the screen. Auditory stimuli were produced using Audacity® (<http://audacity.sourceforge.net/>). The analog tonal signal was generated in STIM Audio System (Neuroscan, Abbotstford, Victoria, Australia) and sent into the shielded room. Calibrated earphone transducers (TIP-300 Tubal Insert Phone, Nicolet Biomedical, Inc., Fitchburg, Wisconsin, USA) then converted the electrical to a sonic signal. The earphone transducers had two equal length plastic tubes and earplugs attached, which were inserted into participants' ears.

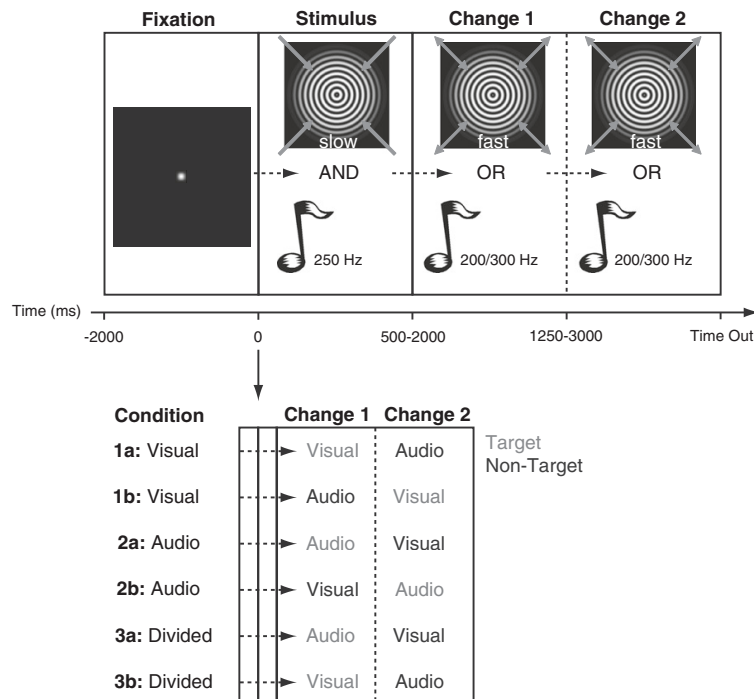


Fig. 1. Paradigm. Upper part: General overview of one trial. Each trial started with the presentation of a fixation dot (Fixation). Thereafter, visual and auditory stimuli were presented simultaneously (Stimulus; $t = 0$). After a randomly assigned period of 500 to 2000 ms, either the visual or the auditory stimulus changed its quality (Change 1). After another 750 or 1000 ms also the other stimulus changed (Change 2). Depending on the condition, one of the two stimulus changes served as target. Subjects had to give a speeded response indicating the quality of the target as soon as it appeared in the cued modality (see *Bimodal reaction time paradigm* for exact description of target qualities). A response or a reaction time > 2000 ms (Time Out) terminated stimulus presentation. Feedback was given after each trial. Periods used for later analysis were Fixation (baseline) and Stimulus. Lower part: Detailed description of variable parts of each trial. Depending on the condition, the change of either the visual or the auditory stimulus was target. In the *visual* condition (1a/1b), the change in visual stimulus was target and the change in auditory stimulus non-target. In the *auditory* condition (2a/2b), the change in auditory stimulus was target and the change in visual stimulus non-target. Two target positions were possible in these two conditions. In the *divided* condition (3a/3b), exclusively the first changing stimulus was target, irrespective if it occurred in the visual or auditory modality. Targets are depicted in light gray, non-targets in dark gray. Please note that fixation and stimulus periods consisted of the same stimulation in each trial, only duration of stimulus period varied. Thus, these trial periods are depicted as empty boxes in the lower part.

Neurophysiological and anatomical data

Brain activity was recorded using magnetoencephalography (MEG; 306-channel, ELEKTA Oy, Helsinki). Vertical and horizontal electrooculograms were recorded to later identify epochs with blink artifacts and eye movements. Individual high-resolution standard T1-weighted structural magnetic resonance images (MRIs) were obtained from a 3 T Siemens Magnetom MRI scanner (Munich/Erlangen, Germany). For three participants no MRIs could be obtained. Their data was projected to the single subject T1-weighted template MRI of the Statistical Parametric Mapping 2 software (SPM2; <http://www.fil.ion.ucl.ac.uk/spm/>).

Data analysis

Behavioral data

Age differences were scrutinized using two-sided Mann–Whitney U test. Behavioral data were analyzed by means of error rates and reaction times. To confirm behavioral effects described previously (Kahlbrock et al., 2012) trials were divided according to the different conditions (*visual*, *auditory*, and *divided*). The *divided* condition was further subdivided into those trials where the visual or the auditory stimulus changed first and therefore became the target (*divided visual* and *divided auditory* respectively). Mean reaction times were calculated for each participant and condition. Only trials with a correct response and reaction times ranging between ± 2 standard deviations

from the individual mean reaction time of each condition were counted as correct and subjected to further analysis.

Reaction times, percent correct responses, and CFF values were analyzed in two ways. Firstly, a non-parametric Friedman test was employed to determine differences in distributions of reaction times and correctness of responses between selective and divided conditions. Post-hoc one-sided Wilcoxon signed-rank tests were used to test for differences between the single conditions. Secondly, a one-sided Mann–Whitney U test was employed to test for differences in distributions of reaction times, correctness of responses and CFF values between groups (low vs. high CFF).

To confirm expected behavioral effects (Kahlbrock et al., 2012), reaction times and correctness of responses of all three behavioral conditions were analyzed in these first steps. As the highest contrast of visual attention was expected between the *visual* and the *auditory* condition, only these two conditions were considered in further analyses.

Partial one-sided correlations, correcting for effects of age, were calculated for reaction times, percent correctness of responses, and CFF. Bonferroni–Holm correction (Holm, 1979) was applied to all alpha levels to correct for multiple comparisons. All statistical analyses of behavioral data were performed using the statistics software package IBM SPSS Statistics 19 for Windows (IBM Corporation, Somers, USA).

MEG data general

MEG data were analyzed using FieldTrip, an open source Matlab toolbox (Oostenveld et al., 2011), and Matlab 7.1 (MathWorks,

Natick, MA). For artifact rejection, continuously recorded MEG data were divided into epochs of interest, starting at time of first fixation point and ending with time of response or time out in case of a catch trial. Semi-automatic routines and visual artifact rejection were applied to remove epochs contaminated with eye blink, muscle, and sensor artifacts. Partial and complete artifact rejection procedures were applied, rejecting either only parts of the trial contaminated by artifacts or the whole trial in case of multiple artifacts. Where necessary, independent component analysis was used to correct for eye blink artifacts. Power line noise was removed by estimating and subtracting the 50- and 100-Hz components in the MEG data, using a discrete Fourier transform. The linear trend was removed from each epoch. Further analyses were performed on the time window from time of first fixation point until the first stimulus change.

Again, analyses were confined to the *visual* and *auditory* conditions, as these two were expected to be most distinctive for effects of visual attention.

Stimulus induced gamma band activity

Oscillatory neuronal activity was estimated by determining time frequency representations of power (TFRs) for frequencies between 30 and 100 Hz using windows of 400 ms moved in steps of 50 ms. Multitaper spectral estimation was used with ± 5 Hz smoothing (3 tapers) in steps of 0.5 Hz. For each subject, TFRs were calculated for the *visual* and the *auditory* condition. As previous works showed gamma band activity in response to visual stimuli over occipital areas (Hoogenboom et al., 2006; Kahlbrock et al., 2012), data were averaged over all occipital and the six most caudal parietal sensor pairs (32 sensor pairs in total; Fig. 4A). Group averages were calculated for the two groups under study, i.e., low and high CFF.

Statistical comparison of power between conditions

To determine differences in visual gamma band power between attention conditions, data were first averaged over the above described sensors (Fig. 4A) for each subject. The same number of trials (depending on the condition with the smallest number of trials) was randomly drawn from the available trials for the two conditions. On a single trial basis and using independent samples *t*-tests, *t*-values were calculated for the difference in absolute power between these two conditions from -1500 to 1500 ms (0 being the start of stimulus presentation) and 30 to 100 Hz and resulted in time frequency *t*-maps. Subsequent group level statistics determined time frequency clusters with significant effects at random effects level. To obtain these time frequency clusters, time frequency *t*-maps were thresholded at the *t*-value corresponding to a one-sided *t*-test with an alpha level of 0.05, determined by the values of the permutation distribution. The summed *t*-values per cluster were used as test statistic. Statistical inference was based on a non-parametric randomization test, correcting for multiple comparisons due to a multitude of time- and frequency-points (Maris and Oostenveld, 2007; Nichols and Holmes, 2002). This second step was done for each subject and time frequency points from 500 to 1500 ms (thereby excluding purely stimulus evoked components in the first 500 ms) and 30 to 100 Hz. This analysis was once performed including all participants and repeated separately for each group under study (low and high CFF).

Individual gamma band peaks and power

For frequencies of 30 to 100 Hz, power spectra were calculated for each participant, condition, and all sensors described in *Stimulus induced gamma band activity* (Fig. 4A; ± 1 Hz smoothing, Hanning window). To exclude purely stimulus evoked components and to include the strongest gamma band power increase and the maximally possible amount of trials, periods from 500 to 1000 ms were used. Relative changes compared to the pre-stimulus baseline (-1000 to -500 ms) were calculated. For each sensor, the maximal relative gamma band peak frequency and its power were determined. In

order to increase the signal-to-noise ratio, the ten sensors showing highest gamma band power and lying in close proximity to each other were identified and averaged for each subject. The average gamma band peak frequency was determined. The power increase relative to baseline was tested for significance using one-sided dependent samples *t*-tests for each frequency point comparing stimulus with pre-stimulus baseline times. Statistical inference was based on a non-parametric randomization test, correcting for multiple comparisons (Maris and Oostenveld, 2007; Nichols and Holmes, 2002). The gamma band peak frequency and its corresponding relative power were only used for further analyses if the power of this peak was significantly different from baseline. This procedure was performed separately for the two conditions.

Statistics gamma band peaks

Non-parametrical one-sided Wilcoxon tests were employed to determine differences in distributions of gamma band peak frequencies between the *visual* and the *auditory* condition. This analysis was done including all participants and repeated for each individual group of participants (low and high CFF). In addition, Mann–Whitney U tests were employed to test for differences in distributions of gamma band peak frequencies between groups for both conditions separately.

To test for effects of age on gamma band peak frequencies, the median age of all participants was calculated. Frequency data were then split at the median age (one half of the subjects being equal/older and the other half being equal/younger than the median age) and compared using a Mann–Whitney U test. The same procedure was used to test for effects of age on the modulation of gamma band power between the *visual* and the *auditory* condition averaged in time and space (for details please see *Individual gamma band peaks and power*).

Partial one-sided correlation, correcting for age effects, was calculated for gamma band peak frequencies and CFF using IBM SPSS Statistics 19 for Windows (IBM Corporation, Somers, USA). Bonferroni–Holm correction (Holm, 1979) was applied to the alpha level to correct for multiple comparisons.

Sources of gamma band peaks

Sources of significant gamma band peaks were localized using *Dynamic Imaging of Coherent Sources* (DICS; Gross et al., 2001), an adaptive spatial filtering technique in the frequency domain. To this end, each individual structural MRI was spatially normalized to a smoothed template MRI based on multiple subjects (Statistical Parametric Mapping; SPM2; <http://www.fil.ion.ucl.ac.uk/spm/>). For the three subjects with missing individual MRI scans the single subject T1-weighted template MRI as given in SPM2 was used. Leadfield matrices were determined for realistically shaped single-shell volume conduction models (Nolte, 2003) derived from the individual normalized structural MRIs. The grid of locations was constructed as a regular 5 mm grid, which was then adjusted to the individuals' head shapes. To obtain the best possible estimate of the location of each subject's strongest gamma band response, cross spectral density matrices between all MEG sensor pairs at individual gamma band peaks ± 5 Hz were determined for time frequency windows from -1000 to -500 ms (baseline), and 500 to 1000 ms (stimulus period) averaged over all trials of the *visual* and the *auditory* conditions. These common spatial filters were then used to calculate cross spectral density matrices for the two conditions separately. Finally, relative changes between baseline and stimulus periods were calculated.

Results

Participants

No significant age differences were observed between low and high CFF groups. Details and individual subject dependent data are summarized in Table 1.

Behavioral attention effects

To confirm previously reported effects (Kahlbrock et al., 2012), reaction times and correctness of responses were examined for effects of condition (selective vs. divided) averaged over all subjects (please see Table 2 for individual reaction times).

Median reaction times and standard errors of the median were 714 ± 52 ms for the *visual*, 598 ± 52 ms for the *auditory*, 691 ± 50 ms for the *divided visual*, and 602 ± 52 ms for the *divided auditory* condition. Differences were observed in the distributions of the four conditions ($\chi^2_{(3)} = 26.10$, $p < 0.01$, $n = 32$). However, post-hoc tests showed no differences between the selective and the divided conditions.

Median percent correct and standard errors of the median were $91.0 \pm 0.7\%$ for the *visual*, $94.2 \pm 0.9\%$ for the *auditory*, $88.5 \pm 1.9\%$ for the *divided visual*, and $90.7 \pm 1.4\%$ for the *divided auditory* conditions. Differences in the distributions of the four conditions were observed ($\chi^2_{(3)} = 31.36$, $p < 0.01$, $n = 32$). Post-hoc analyses showed that the median differences between the *visual* and the *divided visual* condition ($Z = -3.45$, $p < 0.01$, $n = 32$) and the median difference between the *auditory* and the *divided auditory* condition

($Z = -3.35$, $p < 0.01$, $n = 32$) were different from zero. Thus, participants reacted more correctly in the selective compared to the divided conditions.

Low and high CFF groups show differential behavioral performance

The comparison of low and high CFF groups showed an overall better performance of the high CFF group (reaction times: *visual*: $U = 35$, $p = 0.02$; *auditory*: $U = 32$, $p = 0.01$; *divided visual*: $U = 41$, $p = 0.05$; *divided auditory*: $p > 0.1$; correctness of responses: *visual*: $U = 44$, $p = 0.04$; *auditory*: $p > 0.1$; *divided visual*: $U = 33$, $p = 0.03$; *divided auditory*: $U = 35$, $p = 0.03$; see Supplementary Table 1 for median values and standard deviations). A similar pattern, however not always reaching significance when corrected for multiple comparisons, was observed when comparing only patients with high and low CFF values (reaction times: *visual*: $U = 18$, $p = 0.03$; *auditory*: $U = 22$, $p = 0.054$; *divided visual*: $U = 24$, $p = 0.09$; *divided auditory*: $p > 0.1$; correctness of responses: *visual*: $p > 0.1$; *auditory*: $p > 0.1$; *divided visual*: $p > 0.1$; *divided auditory*: $U = 19$, $p = 0.06$; see Supplementary Table 1 for median values and standard deviations).

Table 2
Individual behavioral and gamma band data.

Group	Subj. no.	Reaction times		Correctness		Occipital γ frequency		Occipital γ amplitude		
		Visual	Auditory	Visual	Auditory	Visual	Auditory	Visual	Auditory	Visual–Auditory
Control	1	539	451	95	94	–	–	–	–	–
	2	714	672	91	95	56	52	0.64	0.62	0.02
	3	631	602	94	94	46	46	0.30	0.22	0.08
	4	740	489	93	95	–	–	–	–	–
	5	899	774	95	87	52	50	0.92	0.55	0.37
	6	555	489	95	95	52	52	0.43	0.59	–0.16
	7	1049	661	91	92	38	40	0.72	0.83	–0.11
	8	1127	949	90	94	46	–	0.45	–	–
	n = 8	727 ± 98	631 ± 74	93 ± 1	94 ± 1	49 ± 3	50 ± 3	0.55 ± 0.12	0.59 ± 0.12	0.02 ± 0.12
HE0	9	475	459	96	94	52	52	4.52	1.25	3.27
	10	732	556	95	97	52	56	0.82	0.32	0.50
	11	512	371	96	95	48	48	1.15	0.73	0.42
	12	732	522	94	96	62	–	0.20	–	–
	13	945	666	90	95	46	46	0.64	0.84	–0.20
	14	868	594	88	92	42	38	0.76	0.47	0.29
	15	576	524	91	93	–	–	–	–	–
	16	536	538	90	93	48	50	0.78	0.76	0.02
	n = 8	654 ± 77	531 ± 39	92 ± 1	95 ± 1	48 ± 3	49 ± 3	0.78 ± 0.69	0.74 ± 0.16	0.36 ± 0.65
mHE	17	1128	666	82	92	–	–	–	–	–
	18	701	570	92	95	50	50	1.17	0.93	0.24
	19	545	601	93	95	–	54	–	0.16	–
	20	1165	952	90	94	52	50	0.90	0.56	0.34
	21	504	412	92	94	36	40	0.21	0.26	–0.05
	22	706	963	94	76	54	52	1.39	1.45	–0.06
	23	678	522	91	94	52	52	0.70	0.54	0.16
	24	656	568	91	95	52	52	6.44	4.31	2.13
	n = 8	690 ± 111	586 ± 88	91 ± 2	94 ± 3	52 ± 3	52 ± 2	1.03 ± 1.18	0.56 ± 0.69	0.20 ± 0.43
HE1	25	574	530	89	96	–	–	–	–	–
	26	611	552	93	95	–	–	–	–	–
	27	1429	1036	91	87	54	48	0.29	0.31	–0.02
	28	1022	838	91	95	46	–	0.74	–	–
	29	912	864	87	94	44	44	0.30	2.10	–1.80
	30	1098	559	91	95	44	44	0.70	0.64	0.06
	31	786	996	87	86	48	48	1.92	2.05	–0.13
	32	1005	668	87	96	48	50	0.92	0.55	0.37
	33	776	625	94	96	38	–	0.38	–	–
	34	–	1594	–	87	–	–	–	–	–
n = 10	912 ± 111	753 ± 130	91 ± 1	95 ± 2	46 ± 2	48 ± 2	0.70 ± 0.27	0.64 ± 0.54	–0.02 ± 0.48	

Individual behavioral and gamma band data are shown. Reaction times and correctness of responses, gamma band peak frequencies and relative power over occipital sensors are depicted separately for the *visual* and the *auditory* condition. In the last column, individual power differences between the *visual* and the *auditory* condition are displayed. For all parameters, group median values \pm standard errors of the median are displayed.

CFF correlates with behavioral performance

Behavioral parameters correlated with the CFF, as a measure of HE disease severity. For the *auditory* condition, a negative correlation of CFF and reaction times was detected ($r = -0.53$, $p < 0.01$; Fig. 2A). No correlation of correctness of responses and CFF was found in the *auditory* condition.

In the *visual* condition, the CFF correlated positively with the number of correct responses ($r = 0.40$, $p = 0.02$; Fig. 2B). No correlation of reaction times and CFF was found in the *visual* condition.

Comparing gamma band power between groups and conditions

In all groups, sustained gamma band activity in response to the visual stimulus was observed at sensors overlaying visual cortex (Fig. 3A). Tallying a previous report (Kahlbrock et al., 2012), it was not possible to find any systematic sustained stimulus related gamma band responses in auditory cortex. This is most likely due to stimulus characteristics as discussed elsewhere (Kahlbrock et al., 2012). The analyses were thus confined to the visual system.

The strongest gamma band peaks were localized in visual areas in all groups under study (Fig. 3B). Averaged over individual gamma band peak frequencies and the time of strongest gamma band responses (500 to 1500 ms), no differences in relative gamma band power were observed between any of the compared groups ($p > 0.1$). Please see Table 2 for individual changes in gamma band power.

Comparing sensor level gamma band power between the *visual* and the *auditory* condition for each group separately, revealed a significant cluster from 575 to 1500 ms and 44 to 60 Hz ($p = 0.03$; Fig. 4B) for the high CFF group including all participants. A similar cluster was found for the high CFF group of patients only between the two conditions from 500 to 1500 ms and 43 to 58 Hz ($p = 0.02$). For the low CFF groups (either including all participants or patients only), no significant differences were observed

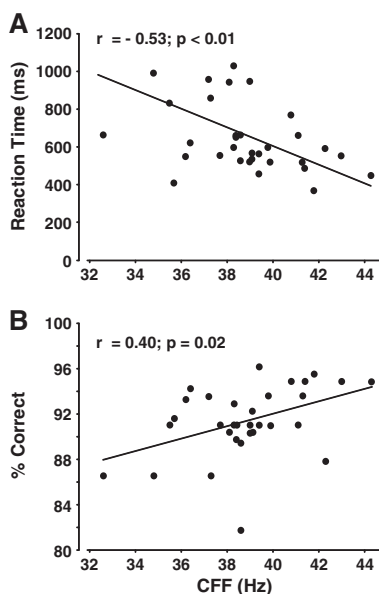


Fig. 2. Disease severity and behavioral performance correlate. A). In the *auditory* condition, the CFF correlated with reaction times ($r = -0.53$, $p < 0.01$, corrected). Thus, the lower the CFF, the slower the response given. B). In the *visual* condition, the CFF correlated with the percent of correct responses ($r = 0.40$, $p = 0.02$, corrected). Thus, the lower the CFF, the more incorrect responses were given.

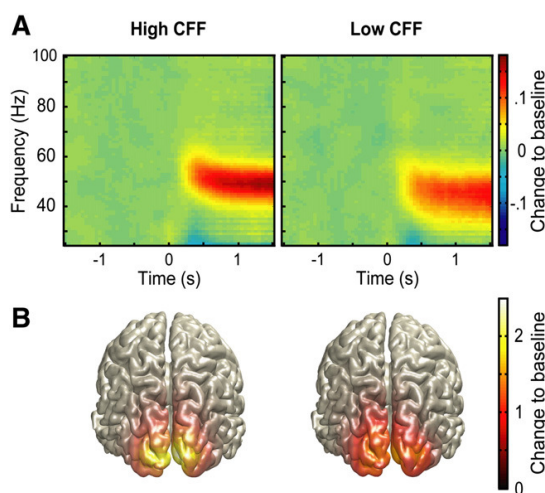


Fig. 3. Patients with HE show visually induced gamma band synchronization. A). For the two groups of participants (left: high CFF, $n = 14$; right: low CFF, $n = 12$) the average relative gamma band response in the *visual* condition is depicted. Only participants with significant gamma band peaks in the *visual* condition were included. Time-point zero constitutes the time of stimulus onset. Color-coding: 0 corresponds to no change, 0.15 to a 15% increase, and -0.15 to a 15% decrease in power relative to baseline (-1000 to -500 ms). B). Localization of strongest relative individual gamma band peaks ± 5 Hz from 500 to 1000 ms after start of stimulus for the two groups of participants in the *visual* condition. Color indexes intensity of relative change to the pre-stimulus baseline as described in A.

($p > 0.1$). This indicates that gamma band power was stronger in the *visual* than in the *auditory* condition for the high CFF groups only.

Effects of age on gamma band modulation between conditions were scrutinized by calculating a median split for age with the modulation of gamma band power between *visual* and *auditory* condition averaged over time and space. Median difference in gamma band power between *visual* and *auditory* condition for the lower age group (≤ 59 years, $n = 11$) was 0.02 ± 0.42 . For the higher age group (≥ 59 years, $n = 11$), the median difference in gamma power between the *visual* and *auditory* condition was 0.08 ± 0.23 (for all standard error of the median displayed). The Mann-Whitney U test resulted in no significant difference between the two age groups ($U = 48.5$, $p > 0.1$; Fig. 5C).

Gamma band peak frequency differs between groups

Significant differences of gamma band peak frequencies were found between low and high CFF groups (including all participants) for the *visual* ($U = 37.5$, $p = 0.01$; Fig. 5A) and the *auditory* condition ($U = 27$, $p = 0.01$). When looking at patients only, a similar difference for the *visual* and a trend for the *auditory* condition between low and high CFF groups were observed (*visual*: $U = 26.0$, $p = 0.03$; *auditory*: $U = 18.0$, $p = 0.07$). However, individual gamma band peak frequencies were not different between the *auditory* and the *visual* condition (please see Table 2 for individual gamma band peak frequencies).

Gamma band peak frequency is influenced by age

Effects of age on gamma band peak frequencies were examined by calculating a median split for age with the gamma band peak frequency data and comparing the two age groups (*visual* condition: lower age group: ≤ 59 years, $n = 14$; higher age group: > 59 years, $n = 14$). Median *visual* gamma band peak frequency for the lower age group was $52 \text{ Hz} \pm 2 \text{ Hz}$. For the higher age group, the median *visual*

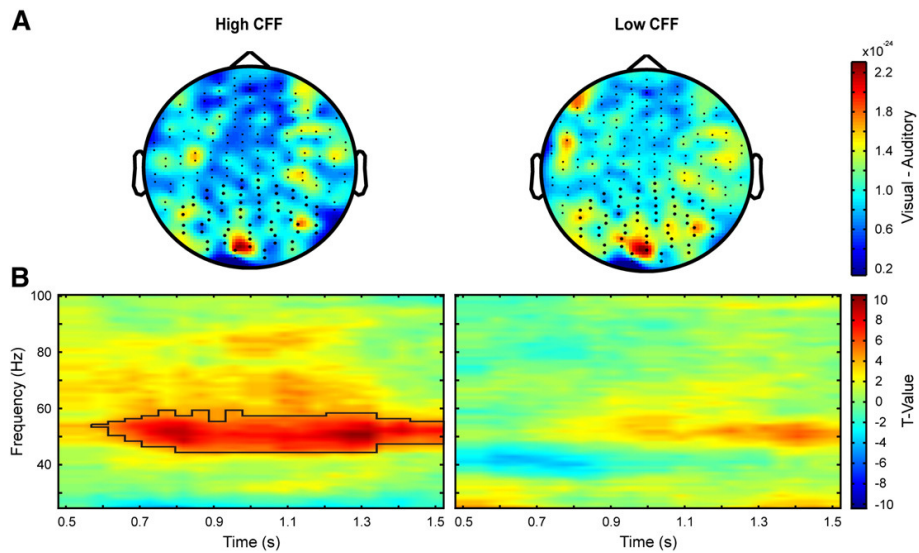


Fig. 4. Modulation of gamma band power with attention in participants with high CFF. A). Grand average difference plot of gamma band power between the *visual* and the *auditory* condition averaged over the period of 500 to 1000 ms at each subject's individual gamma band peak frequency ± 5 Hz. Low (left) and high (right) CFF groups are depicted separately. All sensors used for statistics and used to determine the ten sensors with strongest gamma band peaks are marked by asterisks. B). Statistical comparison of gamma band power in the *visual* and the *auditory* condition for the low (left) and high (right) CFF groups including all participants ($n = 12$ and $n = 14$ respectively). Results are shown as t -values. Subsequent non-parametric randomization statistics reveal a significant cluster as marked by the black frame. Gamma band power was stronger in the *visual* than in the *auditory* condition ($p = 0.03$, corrected). Please note that similar results were obtained when looking at the high CFF group including patients only ($p = 0.02$, corrected; $n = 10$).

gamma band peak frequency was $46 \text{ Hz} \pm 2 \text{ Hz}$. The Mann–Whitney U test revealed a higher median gamma band peak frequency in the *visual* condition for the lower than the higher age group ($U = 43.5$, $p = 0.02$; Fig. 5B). For the *auditory* condition the median gamma band peak frequency for the lower age group (≤ 59 years, $n = 12$) was $52 \text{ Hz} \pm 1 \text{ Hz}$. For the higher age group (≥ 59 years, $n = 11$), the median gamma band peak frequency was $46 \text{ Hz} \pm 2 \text{ Hz}$ (for all standard error of the median displayed). The Mann–Whitney U test showed that the median gamma band peak frequency in the *auditory*

condition was higher for the lower than the higher age group ($U = 26.0$, $p = 0.01$). For additional correlations of age with CFF and gamma band parameters see Supplementary Fig. 1.

Gamma band peak frequency correlates with CFF

Individual gamma band peak frequencies correlated with the CFF in the *visual* condition ($r = 0.41$, $p = 0.04$; Fig. 6, corrected for effects of

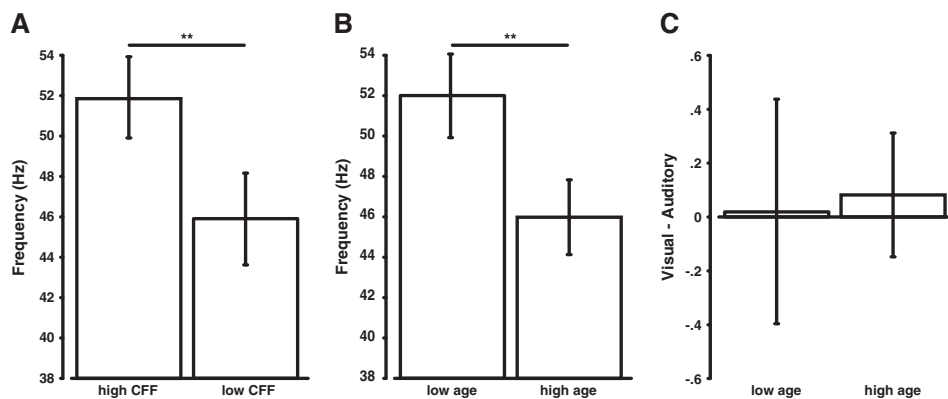


Fig. 5. Differences between high and low CFF and age groups for gamma band peak frequency and gamma band modulation over occipital areas. A). Median values of gamma band peak frequencies in the *visual* condition for high and low CFF groups including all participants (high CFF: $n = 14$; low CFF: $n = 12$). Gamma band peak frequencies were different between the two groups ($U = 37.5$, $p = 0.01$, corrected). Please note that when comparing high and low CFF groups including patients only (high CFF: $n = 10$; low CFF: $n = 10$), a similar difference was observed between groups ($U = 26.0$, $p = 0.03$, corrected). High CFF group: Median = 51.0 ± 1.5 , low CFF group: Median = 45.9 ± 2.1 (standard errors of the median reported). B). Median values of gamma band peak frequencies in the *visual* condition for low and high age groups including all participants (low age: ≤ 59 years, $n = 14$; high age: > 59 years, $n = 14$). Median visual gamma band frequency for the low age group was $52 \text{ Hz} \pm 2 \text{ Hz}$. Median visual gamma band frequency for the high age group was $46 \text{ Hz} \pm 2 \text{ Hz}$ (standard error of the median). Gamma band peak frequencies were different between groups ($U = 43.5$, $p = 0.02$, corrected). C). Median values of gamma band power modulation (changes in relative gamma band power between the *visual* and *auditory* condition) for low and high age groups including all participants (low age: ≤ 59 years, $n = 11$; high age: > 59 years, $n = 11$). The median difference for the lower age group was 0.02 ± 0.42 . For the higher age group, the median difference was 0.08 ± 0.23 (standard error of the median). Gamma band modulation was not different between groups ($U = 48.5$, $p > 0.1$, corrected).

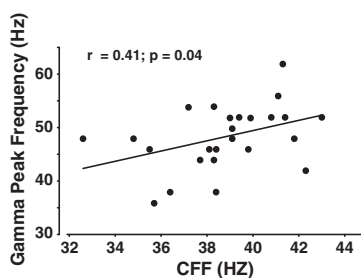


Fig. 6. Gamma band peak frequency over occipital areas correlates with disease severity. Individual peak frequencies of gamma band activity of the *visual* condition and corresponding CFF values are displayed. Gamma band peak frequencies correlated with the CFF ($r = 0.41$, $p = 0.04$, corrected). Thus, the lower the CFF, the lower the gamma band peak frequency.

age). In the *auditory* condition, no correlation of gamma band peak frequency with CFF was observed ($p > 0.1$, corrected for effects of age).

Discussion

Using a bimodal reaction time paradigm requiring modulation of visual attention, this study presents first time evidence of visually induced gamma band activity in HE patients. Moreover, both the frequency of this visual gamma band activity and behavioral performance correlate with the CFF, an indicator of HE disease severity. Thus, the current findings imply that HE disease severity is associated with a decrease of the gamma band peak frequency and a worsening of attentional performance. Furthermore, the current work shows that gamma band power is modulated by the level of visual attention in cirrhotic patients with normal CFF values only, while patients with pathological CFF values are lacking this ability. With these results, conclusions about underlying pathological mechanisms can be drawn, at the same time enhancing our understanding of normal brain functioning.

Behavioral data

Behavioral data, in particular the high percentages of correct responses, show that participants were able to perform all tasks and thereby shift their attention between the visual and the auditory domains. Reaction time differences as expected from a previous study using a similar paradigm (Kahlbrock et al., 2012) could not be reproduced. This is most likely due to the slightly different paradigm, which was simplified to a block design for the present study to make it accomplishable for patients with noticeable attention deficits. Furthermore, the higher age of the current group under study might explain these differences. It has been shown that young adults aim to balance speed and accuracy when working on speeded response tasks. Older adults, on the contrary, aim to minimize errors, irrespective of the time their responses take (Starns and Ratcliff, 2010). Thus, due to a different strategy in the present study, reaction times might not have been as informative as correctness of responses.

A worsening of behavioral performance was associated with a worsening of HE as revealed by correlation analyses with the CFF. Additionally, dividing the data into a high and a low CFF group also revealed that more impaired patients show inferior behavioral performance. This gives further evidence for the notion of a decline of attentional function with increased HE severity and tallies previous findings showing cognitive impairment in patients with HE (Amodio et al., 1998, 2005; Pantiga et al., 2003; Weissenborn et al., 2001, 2003, 2005). It is also in line with a previous study showing performance differences between healthy subjects, patients with mHE and HE1 in tests of attention and short-term memory (Mattarozzi et al., 2005) and studies, already

demonstrating the importance of testing for attention in this population (e.g., Amodio et al., 2010).

Gamma band activity in disease

This study is the first to show attention-related visual gamma band brain activity in a cohort of HE patients. This finding is by itself of special relevance as one might predict that due to decreased cognitive abilities in HE (Pantiga et al., 2003; Weissenborn et al., 2001, 2003) and the observed slowing of brain responses in the motor system (Timmermann et al., 2002, 2003, 2008), HE patients, in particular the more impaired ones, would not show substantial cognition related gamma band brain activity at all.

Impaired modulation of attention-related gamma band activity with reduced CFF

Present findings revealed that gamma band power was modulated by the level of visual attention in participants with normal CFF values. This corresponds with previous works in healthy subjects, reporting attentional modulation of induced visual gamma band responses (Gruber et al., 1999; Kahlbrock et al., 2012; Siegel et al., 2008; Tallon-Baudry et al., 2005; Vidal et al., 2006; Wyart and Tallon-Baudry, 2008). Interestingly, patients with low CFF values were lacking this ability. This finding is of high relevance as it shows that with a low CFF and thus higher HE disease severity, gamma band modulation with attention is impaired. This reduced ability to modulate gamma band power with attention could represent an inefficiency in shifting attention between the visual and the auditory modalities. It might be explained by the fact that more impaired HE patients are more easily distracted by irrelevant inputs (Amodio et al., 2005), i.e. the non-target inputs in this study. It could also be partially explained by a deficit in cerebral processing of oscillatory stimuli with reduced CFF, which is discussed in *Slowed oscillatory activity as a key mechanism of HE pathology*.

Slowed oscillatory activity as a key mechanism of HE pathology

The present work shows that the frequency of visually induced gamma band activity correlates with the severity of HE. This was revealed by a correlation of CFF values and individual gamma band frequencies in the *visual* condition and by differences in gamma band frequencies between low and high CFF groups in the *visual* and *auditory* condition.

The reduced frequency of attention-related gamma band activity in more severely impaired patients are in line with earlier findings showing a reduced mean dominant frequency and a general slowing of spontaneous oscillatory brain activity in HE patients (Amodio and Gatta, 2005; Amodio et al., 1999, 2009; Bajaj, 2010; Davies et al., 1991; Kullmann et al., 2001; Montagnese et al., 2007, 2011; Olesen et al., 2011; Parson-Smith et al., 1957; Van der Rijt et al., 1984). A recent study, for example, found a significant association of the alterations in the EEG with the severity of liver disease and HE, i.e. decreased EEG frequency and increased interhemispheric theta coherence (Marchetti et al., 2011). Moreover, these data tally previous reports of slowed oscillatory processes in the motor and visual system (Timmermann et al., 2002, 2003, 2008). Thus, the present results add further evidence to the hypothesis that slowed oscillatory activity is a key mechanism in the pathophysiology of HE (Timmermann et al., 2005). In line with research in patients with schizophrenia showing decreased frequency of phase-locked gamma band activity related to gestalt perception (Spencer et al., 2004), the slowing of gamma band oscillations might represent the pathophysiological mechanism responsible for the diverse cognitive deficits in patients with HE. Thereby the hypothesis of slowed oscillations in HE is extended to the cognitive domain.

The correlation of the gamma band peak frequency with the CFF in the *visual* but not in the *auditory* condition is most likely due to the smaller number of participants showing a significant occipital gamma band peak in the *auditory* condition. This is also supported by the finding that gamma band peak frequencies were not different between the two conditions.

Individual gamma band frequencies varied between 36 and 62 Hz. However, many subjects showed a similar gamma band frequency. This is in line with a previous study where younger subjects were measured with similar visual stimulation (Kahlbrock et al., 2012). From these works it appears that the employed visual stimulation drives, i.e. induces, gamma band oscillations in a specific frequency range. However, within this range, the individual frequency seems to be influenced, i.e. modulated, by other additional and 'stronger' factors, like the HE status here.

The current study focused on the relation between HE disease severity and gamma band oscillations. This focus is firstly due to the finding of a gradual increase of attention deficits with increasing disease severity (Amodio et al., 2005; Kircheis et al., 2009; Pantiga et al., 2003; Weissenborn et al., 2001, 2005). Secondly, cortical gamma band activity has been characterized as a key correlate of attention (Fries et al., 2001; Hoogenboom et al., 2006, 2010; Kaiser et al., 2006; Lachaux et al., 2005; Steinmetz et al., 2000). Attention also changes oscillatory activity in other frequency bands, e.g. the alpha (e.g., Rihs et al., 2009; Thut et al., 2006) and beta bands (Engel and Fries, 2010). In studies of resting state activity in HE patients, all frequency bands under study (usually delta, theta, alpha, and beta) were reported to be affected (e.g., Amodio et al., 2009; Olesen et al., 2011). Thus, during a cognitive task, slowed oscillatory activity in other frequency bands can also be expected. Future studies are needed to address the questions of how other frequency bands are affected by HE disease severity during attentional processing and how different frequencies interact.

Slowed gamma band frequency in disease

As a cognitive task was used, specific inferences can be drawn about the role of gamma band activity in cognitive tasks and its alteration in disease, i.e. with reduced attentional function. Based on the present data, it can be speculated that healthy and reduced attentional performance are encoded by differential mechanisms. Healthy performance seems to be encoded by power only, i.e. the strength of gamma band activity increases with the level of attention given to a stimulus (Gruber et al., 1999; Kahlbrock et al., 2012; Siegel et al., 2008; Tallon-Baudry et al., 2005; Vidal et al., 2006; Wyart and Tallon-Baudry, 2008). The within-subject frequency of gamma band oscillations has been shown to be considerably stable when keeping stimuli, cognitive operation, and cognitive demand constant between recordings (Hoogenboom et al., 2006; Muthukumaraswamy et al., 2010). However, reduced attentional performance seems to be encoded by either power or frequency of gamma band activity. A study in patients with schizophrenia showed for example decreases of gamma band power during visual stimulus processing (e.g., Green et al., 2003). In patients with Alzheimer's disease, decreased resting state gamma band synchronization was found (Koenig et al., 2005). In the current study, no such difference was observed between groups, however, only participants who were least affected by HE showed modulation of gamma band activity by attention. Reduced attentional performance can also be encoded by differences in the frequency of gamma band activity as shown in the current study by the relation of gamma band frequency and HE disease severity. A task for future research is to examine other patient populations with attention deficits and confirm that reduced attentional performance is encoded by gamma band power and frequency. Furthermore, follow-up measurements including patients with changes in HE severity, i.e. patients recovering from severely impaired stages

back to mild impairment or vice versa, are likely to substantiate the findings presented here.

An alternative explanation for the decreased gamma band frequency with higher HE severity could be that of a simple deficit in processing of oscillatory stimuli, the further the HE progresses. With higher HE disease severity lower CFF values are measured (Kircheis et al., 2002; Prakash and Mullen, 2010; Romero-Gómez et al., 2007; Sharma et al., 2007). The exact physiological mechanisms of this clinical measure are still unclear. Interestingly, human cortical visual areas are able to process flickering stimuli at frequencies higher than the maximum consciously perceived flicker frequency (Herrmann, 2001). Thus, it is possible that the observed impairment in perception of an oscillatory visual (flicker-) stimulus, i.e. reduced CFF in patients with HE, is due to a dysfunction in the cerebral processing of oscillatory visual stimuli as hypothesized by Timmermann et al. (2008). Hence, the reduced gamma band frequency would be explained by a cerebral processing deficit of oscillatory stimuli. However, in the present study cognitive performance correlates with disease severity. Thus, cognitive dysfunctions cannot be excluded as being involved in the gamma frequency reduction. Furthermore, behavioral performance deficits were shown in the attention task in both the *visual* and the *auditory* condition. Thus, it seems unlikely that pure processing deficits in the visual modality are by themselves responsible for the gamma band frequency reduction. A more global reduction of attentional functioning seems more likely.

The reduced gamma band peak frequency could also have been affected by the age of the participants. Indeed, the current data show an effect of age on gamma band peak frequency, in line with two recent studies showing decreased frequency of gamma band activity with age in a cohort of participants from first to fifth decade of life (Gaetz et al., 2011b; Muthukumaraswamy et al., 2010). Importantly, the reported correlations in the current study were corrected for effects of age by using partial correlation. The correlation between gamma band peak frequency and CFF remained, supporting the conclusion of a relationship between HE disease severity and gamma band peak frequency. However, the two effects cannot be completely disentangled finally.

Interestingly, the frequency of gamma band activity has been shown to positively correlate with resting gamma-Aminobutyric acid (GABA) concentrations measured with magnetic resonance spectroscopy in visual (Muthukumaraswamy et al., 2009) and motor cortices (Gaetz et al., 2011a). Altered inhibitory GABA mediated neurotransmission has been described to contribute to HE (Ahboucha, 2011; Ahboucha et al., 2004; Bassett et al., 1990; Jones et al., 1984). Thus, future research needs to examine the effects of GABA mediated neurotransmission on gamma band frequency in HE patients.

Conclusion

The present work reveals a relation between the attention-related gamma band peak frequency in visual areas and the severity of a disease prominently involving cognitive deficits – HE. Earlier results of slowed oscillatory processes in the motor system of patients with HE are thereby extended to the cognitive domain. The notion that pathologically slowed oscillatory activity is a key mechanism in the pathophysiology of HE is strongly supported. Slowed gamma band oscillations might represent the pathophysiological mechanism responsible for the diverse cognitive deficits in this patient population. Moreover, the present data reveal that only patients with high (normal) CFF values are able to show attention-related gamma band modulation. More impaired patients with low (pathological) CFF values, however, do not show this modulation, in line with previous findings of pronounced attentional deficits in HE. It can be speculated that generally, healthy and reduced cognitive performance are encoded by differential gamma

band modulations: gamma band power encodes healthy performance while reduced performance is encoded by both frequency and power of gamma band activity.

Role of funding source

This study was supported by Deutsche Forschungsgemeinschaft (SFB 575). N.K. was supported by Studienstiftung des deutschen Volkes. NK and EM were supported by a travel allowance of Boehringer Ingelheim Foundation (B.I.F.). M.Bu. was supported by a Marie Curie Fellowship of the EU (FP7-PEOPLE-2009-IEF-253965).

Disclosures

GK and DH belong to a group of patent holders for a portable bedside device for CFF analysis.

Acknowledgments

We thank all participants who kindly participated in this study. We thank Mr. Diethelm Plate for his unfailing support in all patient related issues. We thank Mrs. E. Rädisch and Mrs. A. Solutuchin for technical support with MRI scans, and Mrs. A. Solutuchin and Mr. Ulf Zierhut for assistance in data acquisition.

References

Ahboucha, S., 2011. Neurosteroids and hepatic encephalopathy: an update on possible pathophysiological mechanisms. *Curr. Mol. Pharmacol.* 4 (1), 1–13.

Ahboucha, S., Pomier-Layrargues, G., Butterworth, R.F., 2004. Increased brain concentrations of endogenous (non-benzodiazepine) GABA-A receptor ligands in human hepatic encephalopathy. *Metab. Brain Dis.* 19 (3–4), 241–251.

Amodio, P., Gatta, A., 2005. Neurophysiological investigation of hepatic encephalopathy. *Metab. Brain Dis.* 20 (4), 369–379.

Amodio, P., Marchetti, P., Del Piccolo, F., Campo, G., Rizzo, C., Iemmolo, R.M., Gerunda, G., Caregari, L., Merkel, C., Gatta, A., 1998. Visual attention in cirrhotic patients: a study on covert visual attention orienting. *Hepatology* 27 (6), 1517–1523.

Amodio, P., Marchetti, P., Del Piccolo, F., de Tourchaninoff, M., Varghese, P., Zuliani, C., Campo, G., Gatta, A., Guérit, J.M., 1999. Spectral versus visual EEG analysis in mild hepatic encephalopathy. *Clin. Neurophysiol.* 110 (8), 1334–1344.

Amodio, P., Schiff, S., Del Piccolo, F., Mapelli, D., Gatta, A., Umiltà, C., 2005. Attention dysfunction in cirrhotic patients: an inquiry on the role of executive control, attention orienting and focusing. *Metab. Brain Dis.* 20 (2), 115–127.

Amodio, P., Orsato, R., Marchetti, P., Schiff, S., Poci, C., Angeli, P., Gatta, A., Sparacino, G., Toffolo, G.M., 2009. Electroencephalographic analysis for the assessment of hepatic encephalopathy: comparison of non-parametric and parametric spectral estimation techniques. *Neurophysiol. Clin./Clin. Neurophysiol.* 39 (2), 107–115.

Amodio, P., Ridola, L., Schiff, S., Montagnese, S., Pasquale, C., Nardelli, S., Pentassuglio, I., Trezza, M., Marzano, C., Flaiban, C., Angeli, P., Cona, G., Bisiacchi, P., Gatta, A., Riggio, O., 2010. Improving the inhibitory control task to detect minimal hepatic encephalopathy. *Gastroenterology* 139 (2), 510–518. [518.e1-2](#).

Bajaj, J.S., 2010. Current and future diagnosis of hepatic encephalopathy. *Metab. Brain Dis.* 25 (1), 107–110.

Bassett, M.L., Mullen, K.D., Scholz, B., Fenstermacher, J.D., Jones, E.A., 1990. Increased brain uptake of gamma-aminobutyric acid in a rabbit model of hepatic encephalopathy. *Gastroenterology* 98 (3), 747–757.

Butterworth, R.F., 2000. Complications of cirrhosis III. Hepatic encephalopathy. *J. Hepatol.* 32 (1 Suppl), 171–180.

Butz, M., Gross, J., Timmermann, L., Moll, M., Freund, H.-J., Witte, O.W., Schnitzler, A., 2004. Perilesional pathological oscillatory activity in the magnetoencephalogram of patients with cortical brain lesions. *Neurosci. Lett.* 355 (1–2), 93–96.

Conn, H.O., Lieberthal, M.M., 1979. Hepatic Coma; Lactulose; Disaccharides; Chemotherapy; Therapeutic Use; Drug Therapy. Williams & Wilkins, Baltimore.

Davies, M.G., Rowan, M.J., Feely, J., 1991. EEG and event related potentials in hepatic encephalopathy. *Metab. Brain Dis.* 6 (4), 175–186.

de Jongh, A., Baayen, J.C., de Munck, J.C., Heethaar, R.M., Vandertop, W.P., Stam, C.J., 2003. The influence of brain tumor treatment on pathological delta activity in MEG. *Neuroimage* 20 (4), 2291–2301.

Eberhardt, G., 1994. Flimmerfrequenz-Analysator. Automatische Messmethode. Version 3.00. Dr. G. Schuhfried GmbH, Mödling, Austria.

Engel, A.K., Fries, P., 2010. Beta-band oscillations – signalling the status quo? *Curr. Opin. Neurobiol.* 20 (2), 156–165.

Fries, P., Reynolds, J.H., Rorie, A.E., Desimone, R., 2001. Modulation of oscillatory neuronal synchronization by selective visual attention. *Science* 291 (5508), 1560–1563.

Fries, P., Scheeringa, R., Oostenveld, R., 2008. Finding gamma. *Neuron* 58 (3), 303–305.

Gaetz, W., Edgar, J.C., Wang, D.J., Roberts, T.P.L., 2011a. Relating MEG measured motor cortical oscillations to resting γ -Aminobutyric acid (GABA) concentration. *Neuroimage* 55 (2), 616–621.

Gaetz, W., Roberts, T.P.L., Singh, K.D., Muthukumaraswamy, S.D., 2011b. Functional and structural correlates of the aging brain: relating visual cortex (V1) gamma band responses to age-related structural change. *Hum. Brain Mapp.*

Gray, C.M., König, P., Engel, A.K., Singer, W., 1989. Oscillatory responses in cat visual cortex exhibit inter-columnar synchronization which reflects global stimulus properties. *Nature* 338 (6213), 334–337.

Green, M.F., 1996. What are the functional consequences of neurocognitive deficits in schizophrenia? *Am. J. Psychiatry* 153 (3), 321–330.

Green, M.F., Mintz, J., Salveson, D., Nuechterlein, K.H., Breitmeyer, B., Light, G.A., Braff, D.L., 2003. Visual masking as a probe for abnormal gamma range activity in schizophrenia. *Biol. Psychiatry* 53 (12), 1113–1119.

Gross, J., Kujala, J., Hämäläinen, M., Timmermann, L., Schnitzler, A., Salmelin, R., 2001. Dynamic imaging of coherent sources: studying neural interactions in the human brain. *Proc. Natl. Acad. Sci. U. S. A.* 98 (2), 694–699.

Gruber, T., Müller, M.M., Keil, A., Elbert, T., 1999. Selective visual-spatial attention alters induced gamma band responses in the human EEG. *Clin. Neurophysiol.* 110 (12), 2074–2085.

Guérit, J.-M., Amantini, A., Fischer, C., Kaplan, P.W., Mecarelli, O., Schnitzler, A., Ubiali, E., Amodio, P., 2009. Neurophysiological investigations of hepatic encephalopathy: ISHEN practice guidelines. *Liver Int.* 29 (6), 789–796.

Häussinger, D., Schliess, F., 2008. Pathogenetic mechanisms of hepatic encephalopathy. *Gut* 57 (8), 1156–1165.

Häussinger, D., Kircheis, G., Schliess, F., 2006. Hepatic Encephalopathy and Nitrogen Metabolism, 1st ed. Springer, Netherlands.

Herrmann, C.S., 2001. Human EEG responses to 1–100 Hz flicker: resonance phenomena in visual cortex and their potential correlation to cognitive phenomena. *Exp. Brain Res.* 137 (3–4), 346–353.

Holm, S., 1979. A simple sequentially rejective multiple test procedure. *Scand. J. Stat.* 6 (2), 65–70.

Hoogenboom, N., Schoffelen, J.M., Oostenveld, R., Parkes, L.M., Fries, P., 2006. Localizing human visual gamma-band activity in frequency, time and space. *Neuroimage* 29 (3), 764–773.

Hoogenboom, N., Schoffelen, J.M., Oostenveld, R., Fries, P., 2010. Visually induced gamma-band activity predicts speed of change detection in humans. *Neuroimage* 51 (3), 1162–1167.

Jones, E.A., Schäfer, D.F., Ferenci, P., Pappas, S.C., 1984. The GABA hypothesis of the pathogenesis of hepatic encephalopathy: current status. *Yale J. Biol. Med.* 57 (3), 301–316.

Kahlbrock, N., Butz, M., May, E.S., Schnitzler, A., 2012. Sustained gamma band synchronization in early visual areas reflects the level of selective attention. *Neuroimage* 59 (1), 673–681.

Kaiser, J., Hertrich, I., Ackermann, H., Lutzenberger, W., 2006. Gamma-band activity over early sensory areas predicts detection of changes in audiovisual speech stimuli. *Neuroimage* 30 (4), 1376–1382.

Kircheis, G., Wettstein, M., Timmermann, L., Schnitzler, A., Häussinger, D., 2002. Critical flicker frequency for quantification of low-grade hepatic encephalopathy. *Hepatology* 35 (2), 357–366.

Kircheis, G., Fleig, W.E., Görtelmeyer, R., Grafe, S., Häussinger, D., 2007. Assessment of low-grade hepatic encephalopathy: a critical analysis. *J. Hepatol.* 47 (5), 642–650.

Kircheis, G., Knoche, A., Hilger, N., Manhart, F., Schnitzler, A., Schulze, H., Häussinger, D., 2009. Hepatic encephalopathy and fitness to drive. *Gastroenterology* 137 (5), 1706–1715. [e1-9](#).

Koenig, T., Prichep, L., Dierks, T., Hubl, D., Wahlund, L.O., John, E.R., Jelic, V., 2005. Decreased EEG synchronization in Alzheimer's disease and mild cognitive impairment. *Neurobiol. Aging* 26 (2), 165–171.

Kullmann, F., Hollerbach, S., Lock, G., Holstege, A., Dierks, T., Schölmerich, J., 2001. Brain electrical activity mapping of EEG for the diagnosis of (sub)clinical hepatic encephalopathy in chronic liver disease. *Eur. J. Gastroenterol. Hepatol.* 13 (5), 513–522.

Lachaux, J.P., George, N., Tallon-Baudry, C., Martinerie, J., Hugueville, L., Minotti, L., Kahane, P., Renault, B., 2005. The many faces of the gamma band response to complex visual stimuli. *Neuroimage* 25 (2), 491–501.

Marchetti, P., D'Avanzo, C., Orsato, R., Montagnese, S., Schiff, S., Kaplan, P.W., Piccione, F., Merkel, C., Gatta, A., Sparacino, G., Toffolo, G.M., Amodio, P., 2011. Electroencephalography in patients with cirrhosis. *Gastroenterology* 141 (5), 1680–1689. [e1-2](#).

Maris, E., Oostenveld, R., 2007. Nonparametric statistical testing of EEG- and MEG-data. *J. Neurosci. Methods* 164 (1), 177–190.

Mattarozzi, K., Campi, C., Guarino, M., Stracciari, A., 2005. Distinguishing between clinical and minimal hepatic encephalopathy on the basis of specific cognitive impairment. *Metab. Brain Dis.* 20 (3), 243–249.

Montagnese, S., Jackson, C., Morgan, M.Y., 2007. Spatio-temporal decomposition of the electroencephalogram in patients with cirrhosis. *J. Hepatol.* 46 (3), 447–458.

Montagnese, S., Biancardi, A., Schiff, S., Carraro, P., Carlà, V., Mannaioni, G., Moroni, F., Tono, N., Angeli, P., Gatta, A., Amodio, P., 2011. Different biochemical correlates for different neuropsychiatric abnormalities in patients with cirrhosis. *Hepatology* 53 (2), 558–566.

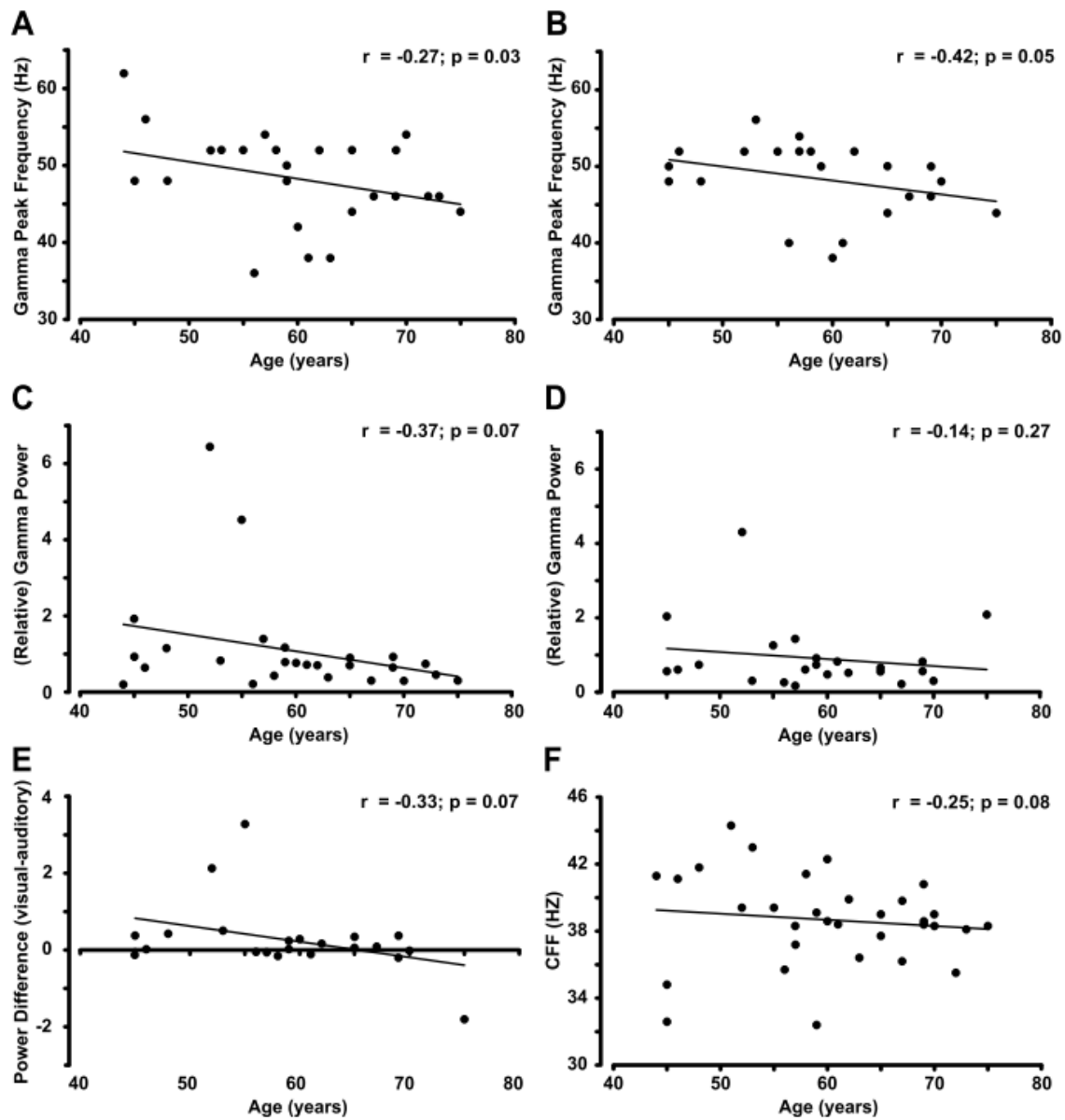
Muthukumaraswamy, S.D., Edden, R.A.E., Jones, D.K., Swettenham, J.B., Singh, K.D., 2009. Resting GABA concentration predicts peak gamma frequency and fMRI amplitude in response to visual stimulation in humans. *Proc. Natl. Acad. Sci. U. S. A.* 106 (20), 8356–8361.

Muthukumaraswamy, S.D., Singh, K.D., Swettenham, J.B., Jones, D.K., 2010. Visual gamma oscillations and evoked responses: variability, repeatability and structural MRI correlates. *Neuroimage* 49 (4), 3349–3357.

Nichols, T.E., Holmes, A.P., 2002. Nonparametric permutation tests for functional neuroimaging: a primer with examples. *Hum. Brain Mapp.* 15 (1), 1–25.

- Nolte, G., 2003. The magnetic lead field theorem in the quasi-static approximation and its use for magnetoencephalography forward calculation in realistic volume conductors. *Phys. Med. Biol.* 48 (22), 3637–3652.
- Olesen, S.S., Graversen, C., Hansen, T.M., Blauenfeldt, R.A., Hansen, J.B., Steimle, K., Drewes, A.M., 2011. Spectral and dynamic electroencephalogram abnormalities are correlated to psychometric test performance in hepatic encephalopathy. *Scand. J. Gastroenterol.* 46 (7–8), 988–996.
- Oostenfeld, R., Fries, P., Maris, E., Schoffelen, J.-M., 2011. FieldTrip: open source software for advanced analysis of MEG, EEG, and invasive electrophysiological data. *Comput. Intell. Neurosci.* 2011, 156869.
- Pantiga, C., Rodrigo, L.R., Cuesta, M., Lopez, L., Arias, J.L., 2003. Cognitive deficits in patients with hepatic cirrhosis and in liver transplant recipients. *J. Neuropsychiatry Clin. Neurosci.* 15 (1), 84–89.
- Parson-Smith, B.G., Summerskill, W.H., Dawson, A.M., Sherlock, S., 1957. The electroencephalograph in liver disease. *Lancet* 273 (7001), 867–871.
- Prakash, R., Mullen, K.D., 2010. Mechanisms, diagnosis and management of hepatic encephalopathy. *Nat. Rev. Gastroenterol. Hepatol.* 7 (9), 515–525.
- Pugh, R.N.H., Murray-Lyon, I.M., Dawson, J.L., Pietroni, M.C., Williams, R., 1973. Transection of the oesophagus for bleeding oesophageal varices. *Br. J. Surg.* 60 (8), 646–649.
- Rihs, T.A., Michel, C.M., Thut, G., 2009. A bias for posterior α -band power suppression versus enhancement during shifting versus maintenance of spatial attention. *Neuroimage* 44 (1), 190–199.
- Roelfsema, P.R., Engel, A.K., König, P., Singer, W., 1997. Visuomotor integration is associated with zero time-lag synchronization among cortical areas. *Nature* 385 (6612), 157–161.
- Romero-Gómez, M., Córdoba, J., Jover, R., del Olmo, J.A., Ramírez, M., Rey, R., de Madaria, E., Montoliu, C., Nuñez, D., Flavia, M., Compañy, L., Rodrigo, J.M., Felipo, V., 2007. Value of the critical flicker frequency in patients with minimal hepatic encephalopathy. *Hepatology* 45 (4), 879–885.
- Schnitzler, A., Gross, J., 2005. Normal and pathological oscillatory communication in the brain. *Nat. Rev. Neurosci.* 6 (4), 285–296.
- Sharma, P., Sharma, B.C., Puri, V., Sarin, S.K., 2007. Critical flicker frequency: diagnostic tool for minimal hepatic encephalopathy. *J. Hepatol.* 47 (1), 67–73.
- Siegel, M., Donner, T.H., Oostenfeld, R., Fries, P., Engel, A.K., 2008. Neuronal synchronization along the dorsal visual pathway reflects the focus of spatial attention. *Neuron* 60 (4), 709–719.
- Spencer, K.M., Nestor, P.G., Perlmutter, R., Niznikiewicz, M.A., Klump, M.C., Frumin, M., Shenton, M.E., McCarley, R.W., 2004. Neural synchrony indexes disordered perception and cognition in schizophrenia. *Proc. Natl. Acad. Sci. U. S. A.* 101 (49), 17288–17293.
- Starns, J.J., Ratcliff, R., 2010. The effects of aging on the speed–accuracy compromise: boundary optimality in the diffusion model. *Psychol. Aging* 25 (2), 377–390.
- Steinmetz, P.N., Roy, A., Fitzgerald, P.J., Hsiao, S.S., Johnson, K.O., Niebur, E., 2000. Attention modulates synchronized neuronal firing in primate somatosensory cortex. *Nature* 404 (6774), 187–190.
- Tallon-Baudry, C., Bertrand, O., Peronnet, F., Pernier, J., 1998. Induced gamma-band activity during the delay of a visual short-term memory task in humans. *J. Neurosci.* 18 (11), 4244–4254.
- Tallon-Baudry, C., Bertrand, O., Henaff, M.A., Isnard, J., Fischer, C., 2005. Attention modulates gamma-band oscillations differently in the human lateral occipital cortex and fusiform gyrus. *Cereb. Cortex* 15 (5), 654–662.
- Thut, G., Nietzel, A., Brandt, S.A., Pascual-Leone, A., 2006. α -band electroencephalographic activity over occipital cortex indexes visuospatial attention bias and predicts visual target detection. *J. Neurosci.* 26 (37), 9494–9502.
- Timmermann, L., Gross, J., Kircheis, G., Häussinger, D., Schnitzler, A., 2002. Cortical origin of mini-asterixis in hepatic encephalopathy. *Neurology* 58 (2), 295–298.
- Timmermann, L., Gross, J., Butz, M., Kircheis, G., Häussinger, D., Schnitzler, A., 2003. Mini-asterixis in hepatic encephalopathy induced by pathologic thalamo-motor-cortical coupling. *Neurology* 61 (5), 689–692.
- Timmermann, L., Butz, M., Gross, J., Kircheis, G., Häussinger, D., Schnitzler, A., 2005. Neural synchronization in hepatic encephalopathy. *Metab. Brain Dis.* 20 (4), 337–346.
- Timmermann, L., Butz, M., Gross, J., Ploner, M., Südmeyer, M., Kircheis, G., Häussinger, D., Schnitzler, A., 2008. Impaired cerebral oscillatory processing in hepatic encephalopathy. *Clin. Neurophysiol.* 119 (2), 265–272.
- Uhlhaas, P.J., Singer, W., 2006. Neural synchrony in brain disorders: relevance for cognitive dysfunctions and pathophysiology. *Neuron* 52 (1), 155–168.
- Van der Rijt, C.C., Schalm, S.W., De Groot, G.H., De Vlieger, M., 1984. Objective measurement of hepatic encephalopathy by means of automated EEG analysis. *Electroencephalogr. Clin. Neurophysiol.* 57 (5), 423–426.
- Vidal, J.R., Chaumon, M., O'Regan, J.K., Tallon-Baudry, C., 2006. Visual grouping and the focusing of attention induce gamma-band oscillations at different frequencies in human magnetoencephalogram signals. *J. Cogn. Neurosci.* 18 (11), 1850–1862.
- Vienna test system, WINWTS, Version 4.50, 1999. Dr. G. Schuhfried GmbH, Mödling, Austria.
- Weissenborn, K., Heidenreich, S., Ennen, J., Rückert, N., Hecker, H., 2001. Attention deficits in minimal hepatic encephalopathy. *Metab. Brain Dis.* 16 (1–2), 13–19.
- Weissenborn, K., Heidenreich, S., Giewekemeyer, K., Rückert, N., Hecker, H., 2003. Memory function in early hepatic encephalopathy. *J. Hepatol.* 39 (3), 320–325.
- Weissenborn, K., Giewekemeyer, K., Heidenreich, S., Bokemeyer, M., Berding, G., Ahl, B., 2005. Attention, memory, and cognitive function in hepatic encephalopathy. *Metab. Brain Dis.* 20 (4), 359–367.
- Wyart, V., Tallon-Baudry, C., 2008. Neural dissociation between visual awareness and spatial attention. *J. Neurosci.* 28 (10), 2667–2679.

Supplementary Figure



Supplementary Fig. 1:

One-sided Spearman's rank correlation coefficients were calculated between age and

- A) gamma band frequency in the visual condition
- B) gamma band frequency in the auditory condition
- C) gamma band power relative to baseline in the visual condition
- D) gamma band power relative to baseline in the auditory condition

- E) differences in gamma band power between visual and auditory condition
- F) CFF.

Resulting p-values were corrected for multiple comparisons, using Bonferroni–Holm correction. The results were:

- A) age - visual gamma band frequency ($r = -0.27$, $p = 0.03$, $df = 25$).
- B) age - auditory gamma band frequency ($r = -0.42$, $p = 0.05$, $df = 22$).
- C) age - visual gamma band power ($r = -0.37$, $p = 0.07$, $df = 25$). In order to explore, whether the here found correlations could be influenced by apparent outliers, the data were corrected by visual inspection. Thereby, the two upper most outliers were excluded (with power values > 2). Thereafter, the analysis yields the following results ($r = -0.29$, $p = 0.164$, $df = 23$).
- D) age - auditory gamma band power ($r = -0.14$, $p = 0.27$, $df = 22$). When excluding the three upper most outliers (with power values > 2), the analysis yields the following results ($r = -0.06$, $p = 0.34$, $df = 20$).
- E) age - differences in gamma band power (visual–auditory condition; $r = -0.33$, $p = 0.07$, $df = 21$). When excluding the three upper most outliers (with power changes $> \pm 1.7$), the analysis yields the following results ($r = -0.09$, $p = 0.36$, $df = 19$).
- F) age - CFF ($r = -0.25$, $p = 0.08$, $df = 32$).

Supplementary Table

		Reaction Times				Correctness of Responses			
		Visual	Auditory	Divided Visual	Divided Auditory	Visual	Auditory	Divided Visual	Divided Auditory
Low CFF - All Participants	N	12	12	11	11	12	12	11	11
	Median	975	753	780	684	91.03	93.91	82.05	84.62
	Std	237	198	223	160	2.58	5.95	10.77	8.50
High CFF - All Participants	N	14	14	14	14	14	14	14	14
	Median	690	562	682	598	92.95	94.55	89.74	91.03
	Std	181	142	133	130	2.46	2.53	5.26	3.29
Low CFF - Patients Only	N	10	10	9	9	10	10	9	9
	Median	928	753	771	645	91.03	94.54	83.33	88.46
	Std	251	207	120	145	2.84	6.54	9.13	6.06
High CFF - Patients Only	N	10	10	10	10	10	10	10	10
	Median	690	547	649	587	91.67	94.55	89.74	91.03
	Std	200	150	71	112	2.67	1.62	6.10	2.57

Supplementary Table: Behavioral Data of Low and High CFF Groups

For the high (≥ 39 Hz) and the low CFF groups (< 39 Hz), including all participants (two upper rows) and patients only (two lower rows), numbers of participants (N), median values, and standard deviations (Std) are displayed for reaction times and correctness of responses for each of the conditions. Please note that only those subjects showing significant gamma band activity in response to the visual stimulus in condition *visual* were included in the low and high CFF groups.